Renewable Energy Focus 56 (2026) 100781

Contents lists available at ScienceDirect

Renewable Energy Focus

journal homepage: www.elsevier.com/locate/ref

Research Review

Artificial Intelligence in Deep Geothermal Energy: Trends, Insights, and Future Perspectives

Danial Sheini Dashtgoli [a,b,c,*], Michela Giustiniani [b], Martina Busetti [b], Claudia Cherubini [a,b], Giulia Alessandrini [b], Guillermo A. Narsilio [c]

[a] Department of Mathematics, Informatics, and Geosciences, University of Trieste, Italy
[b] National Institute of Oceanography and Applied Geophysics - OGS, Sgonico, Trieste, Italy
[c] Department of Infrastructure Engineering, The University of Melbourne, Parkville, Australia

A B S T R A C T

Deep geothermal energy, known for its stable base load power and resilience to environmental fluctuations, is increasingly recognized as an important renewable energy source. Yet, its development is constrained by subsurface variability, high exploration costs, and operational inefficiencies. Artificial intelligence (AI) can analyze complex data, reveal patterns, and support predictive modeling to lower costs, shorten timelines, and improve efficiency. This review aims to evaluate how AI can address these barriers by systematically synthesizing its applications in deep geothermal research. A structured Web of Science search and multi-stage screening yielded 183 peer-reviewed journal papers, classified across eight research areas: reservoir characterization, exploration and resource identification, system optimization, seismic monitoring and risk assessment, drilling optimization, hybrid energy systems, environmental impact and sustainability, and techno-economic analysis. Our analysis shows that since 2020, AI applications in geothermal energy have expanded exponentially, surpassing overall AI growth rates. China and the United States dominate research output, followed by Germany, Turkey, Canada, and India. Advanced algorithms are increasingly preferred: convolutional neural networks for spatial modeling and image interpretation, recurrent neural networks for time-series forecasting, physics-informed AI, Bayesian frameworks, and autoencoders advance uncertainty quantification and data reconstruction. The novelty of this review lies in its comprehensive cross-domain synthesis of AI applications in deep geothermal energy, using a unified algorithm–input–output–performance lens. This structured mapping enables comparisons not possible in earlier overviews, reveals methodological strengths, identifies effective approaches for different geothermal tasks, and uncovers underexplored areas such as environmental assessment and techno-economic analysis.

Introduction

The global transition towards renewable energy is motivated by the need to address climate change and reduce dependency on fossil fuels. Among the renewable options, geothermal energy offers a unique advantage: it provides a stable, continuous source of energy that does not rely on external conditions like sunlight or wind, making it particularly valuable for base-load power and long-term grid stability[1]. However, despite its potential, geothermal energy has yet to achieve the same growth and scalability as solar and wind, largely due to higher initial costs, geographical limitations, and technical complexities. As shown in Fig. 1, the global installed capacity of renewable electricity has experienced remarkable growth since 2000, with the total capacity reaching approximately 4,000 thousand MW by 2023. This surge reflects advancements in renewable energy technologies and increasing global efforts to transition to low-carbon energy systems. Among these technologies, wind, solar, and hydropower have dominated the expansion. However, geothermal energy represents a relatively small share, with its installed capacity increasing from around 8 thousand MW in 2000 to approximately 15 thousand MW in 2023, as highlighted in the inset of Fig. 1. This growth corresponds to an average annual increase of about 300 MW, underscoring its stable but modest contribution to the renewable energy mix. The disparity between geothermal and other renewable energy sources reflects persistent challenges. High up-front costs, site-specific limitations, and the slow pace of technological innovation have constrained geothermal energy's scalability. Despite these hurdles, geothermal energy's stable output makes it an attractive complement to intermittent renewables, such as wind and solar, reinforcing the case for innovations to overcome its existing limitations [2]. This quantitative context highlights the critical need for advanced solutions to accelerate geothermal energy development. The integration of artificial iIntelligence (AI) presents a promising pathway to address geothermal energy's unique challenges. AI-driven approaches can enhance site identification, optimize reservoir management, and improve operational efficiency, ultimately reducing costs and boosting scalability. These advancements could bridge the gap between geothermal energy and other renewables, unlocking its untapped

* Corresponding author.
E-mail address: dsheinidashtgoli@ogs.it (D. Sheini Dashtgoli).

https://doi.org/10.1016/j.ref.2025.100781
Received 21 May 2025; Received in revised form 17 September 2025; Accepted 30 October 2025
Available online 4 November 2025

Nomenclature

AI	Artificial intelligence
ANFIS	Adaptive neuro-fuzzy inference system
ANN	Artificial neural network
AOSMA	Adaptive opposition slime mould algorithm
AdaBoost	Adaptive boosting
CART	Classification and regression trees
CNN	Convolutional neural network
CatBoost	Categorical boosting
DDPG	Deep deterministic policy gradient
DNN	Deep neural network
DPMM	Dirichlet process mixture model
DL	Deep learning
DNLS-MFA	Deep neural least squares with modified firefly algorithm
DRL	Deep reinforcement learning
DT	Decision tree
DBSCAN	Density-based spatial clustering
EGS	Enhanced geothermal systems
ELM	Extreme learning machine
ERT	Extremely randomized trees
ESOM	Emergent self-organizing maps
GAN	Generative adversarial network
ML	Machine learning
MLR	Multiple linear regression
MW	Megawatt
NNMF	Non-negative matrix factorization
ORCs	Organic rankine cycles
PCA	Principal component analysis
PGSSNet	Progressive global–semantic segmentation network
PIML	Physics-informed machine learning
PINNs	Physics-informed neural networks
PNN	Probabilistic neural network
RBFNN	Radial basis function neural network
ROM	Reduced order modeling
GBM	Gradient boosting machine
GEP	Gene expression programming
GLM	Generalized linear model
GHP	Geothermal heat pump
GMDH	Group method of data handling
GMM	Gaussian mixture model
GPR	Gaussian process regression
GRNN	Generalized regression neural network
GRU	Gated recurrent unit
GTM	Generative topographic mapping
HCA	Hierarchical clustering analysis
INN	Inversion neural network
IoU	Intersection over Union
KNN	K-nearest neighbors
KSOM	Kohonen’s self-organizing map
LDA	Linear discriminant analysis
LSTM	Long short-term memory
LightGBM	Light gradient boosting machine
LR	Linear regression
LST	Land surface temperature
MARS	Multivariate adaptive regression splines
MAXENT	Maximum entropy classifier
RF	Random forest
RL	Reinforcement learning
RMSE	Root mean squared error
RNN	Recurrent neural network
SLLES	Surrogate-assisted level-based learning Evolutionary Search
SLR	Single linear regression
STL-LSTM	LSTM with seasonal-trend decomposition
SVM	Support vector machine
TIRS	Thermal infrared sensor
TFT	Temporal fusion transformer
XGBoost	Extreme gradient boosting

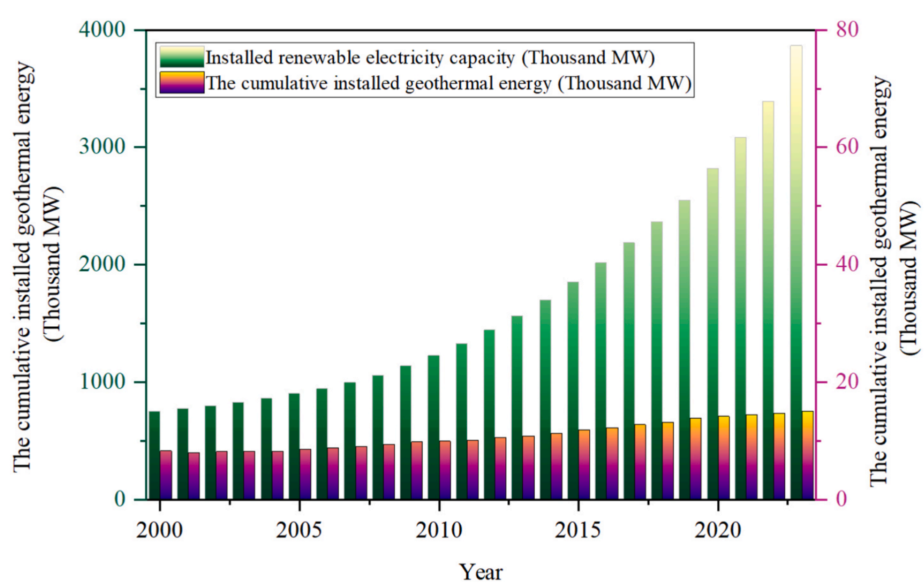

Fig. 1. Growth of global renewable electricity capacity, including the cumulative installed geothermal capacity International Renewable Energy Agency (IRENA) [4]

potential as a reliable and sustainable energy source [3].

The Role of AI in advancing geothermal energy

The rapid growth in AI research across diverse fields highlights its expanding role and potential in addressing complex challenges. The number of AI-related publications worldwide has increased sharply from 2010 to 2022, and increasing at an accelerated rate of between 15% and 25% in the last few years indicating the widespread adoption of AI technologies across various sectors, including healthcare, finance, transportation, and energy [5]. This surge underscores the versatility and relevance of AI in solving intricate problems, including those encountered in renewable energy systems.

In the context of geothermal energy, AI offers tools that can significantly enhance exploration, operational efficiency, and sustainability. Geothermal systems face unique challenges such as site-specific variability, high initial costs, and complex geological conditions. AI can address these issues by enabling advanced data analysis, predictive modeling, and real-time optimization, which are crucial for improving efficiency and reducing costs [6]. The substantial growth in AI publications across all fields, as shown in Fig. 4, reflects AI's expanding influence and applicability. This general trend supports the case for integrating AI into geothermal energy operations, where its advanced capabilities can help overcome specific operational and economic barriers [5]. The application of AI represents a transformative shift in managing the complexities of geothermal energy systems. AI can improve every phase of geothermal energy development, from exploration and resource assessment to operational efficiency and

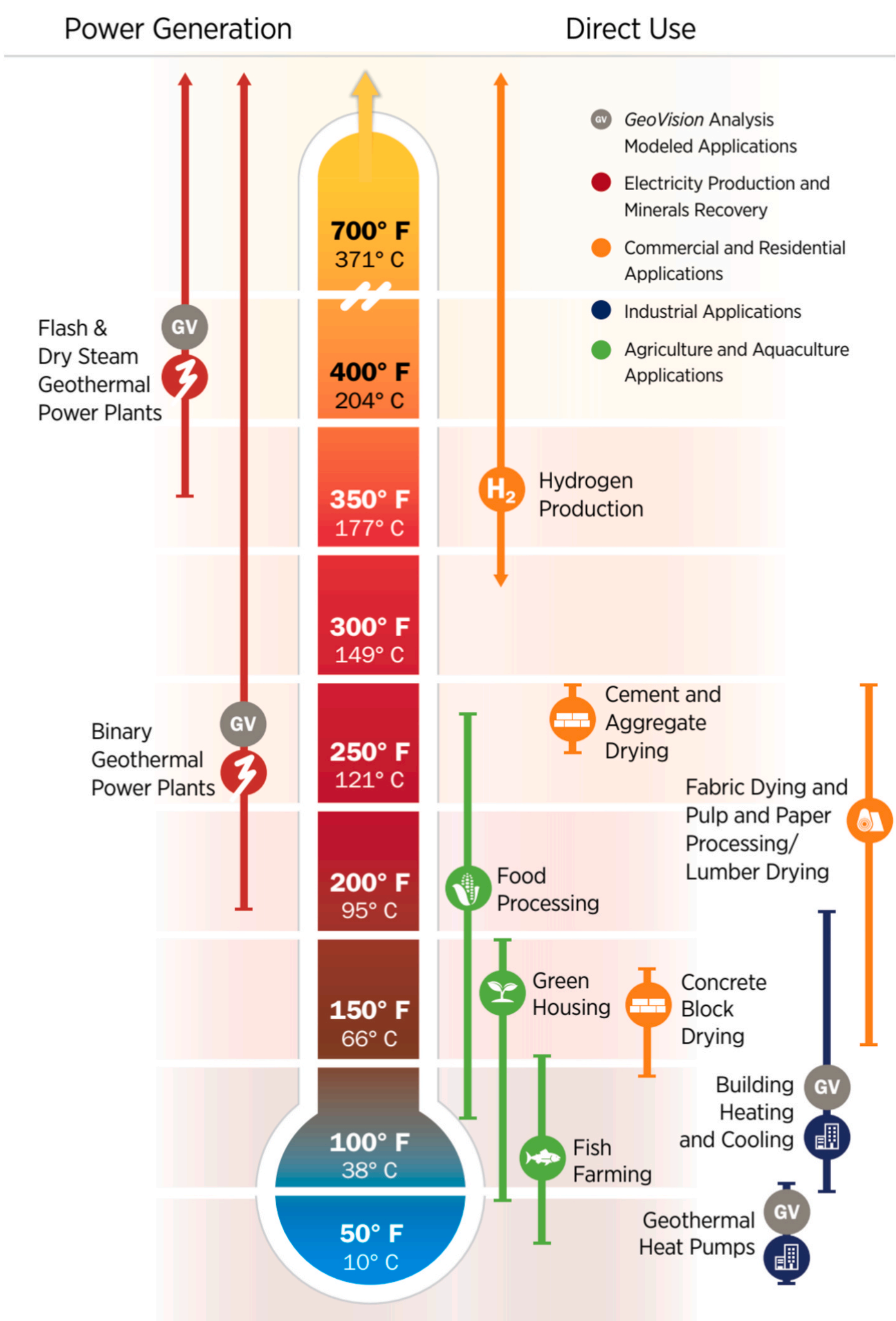

Fig. 2. The diverse range of geothermal energy applications GeoVision: Harnessing the Heat beneath Our Feet [8]

maintenance. By leveraging AI, geothermal projects can overcome many of the traditional barriers associated with this energy source, enhancing both performance and economic viability. AI-driven models allow for real-time data analysis and predictive insights, making it possible to optimize system performance in dynamic and unpredictable environments. AI's potential to enhance geothermal energy is further underscored by the diversity of geothermal applications illustrated in Fig. 2. Geothermal resources span a wide temperature range, supporting not only high-temperature power generation but also direct uses such as heating, industrial processes, and agriculture. Each application has specific operational requirements that AI can help optimize. For instance, machine learning (ML) algorithms can adaptively control temperature and pressure levels across applications, enhancing efficiency and reducing waste. This versatility highlights the potential of the geothermal energy to support various industries, further reinforcing the importance of advanced AI solutions to maximize its utilization and adaptability [7].

The necessity of AI in optimizing geothermal systems

In geothermal systems, traditional methods often struggle with the complexity of resource variability and unpredictable geological conditions. However, AI-based models offer predictive capabilities that are essential for efficient resource management. For instance, AI can accurately forecast production and injection well flow rates, which are critical for maintaining operational efficiency and ensuring the longevity of geothermal reservoirs. This predictive ability is particularly beneficial in hybrid geothermal systems that integrate multiple energy sources, allowing for optimized energy generation and load balancing [9]. By transforming geothermal operations with real-time data analysis, AI can also enable the development of digital twins, geospatially enabled virtual models of geothermal plants that mirror real-world components, associated information of various types, operations. These digital twins allow for continuous monitoring and adjustments, ensuring that geothermal systems remain efficient and cost-effective over time. As geothermal projects grow in complexity, AI's role becomes indispensable in helping to address the technical, logistical, and economic challenges associated with scaling geothermal energy [10]. While geothermal energy presents a reliable and versatile option within the renewable energy landscape, it faces unique challenges that have limited its growth and scalability. The integration of AI offers a promising path to overcome these barriers, providing tools for enhanced exploration, efficient resource management, and optimized operations as detailed later in this article. By addressing the challenges inherent to geothermal systems, artificial intelligence not only enhances geothermal energy's viability as a renewable energy source, but also positions it as a key contributor to a sustainable and resilient energy future by enabling optimized resource utilization, improved system efficiency, and reduced environmental impact.

Objective of the review

The significance of this review is rooted in the rapid progress and widespread adoption of AI technologies, especially in fields requiring complex data analysis and predictive modeling, such as geothermal energy. Due to the swift progress and evolving trends in AI, a comprehensive, up-to-date review of AI applications in geothermal systems is essential. To achieve this, a structured search and screening process was conducted, leading to a curated dataset of 183 peer-reviewed studies that form the analytical basis of this review. Given the potential of AI to reduce costs, improve operational efficiency, and address environmental challenges in geothermal energy, this review provides a timely synthesis of recent literature, trends, and regional advancements. It highlights emerging AI techniques like ML and deep learning (DL), mapping their integration into geothermal research and identifying areas where AI has significantly impacted efficiency and scalability. The main objective of this review is to provide a comprehensive and structured synthesis of AI applications in deep geothermal energy by categorizing 183 peer-reviewed studies across eight major research domains and subgroups, systematically mapping algorithms to their inputs, outputs, and performance in order to identify prevailing trends, highlight methodological strengths and weaknesses, and expose critical research gaps that must be addressed to advance geothermal science and practice. In contrast to previous reviews that have mainly focused on specific domains (e.g., exploration, reservoir characterization, or HDR systems) ([11–13],), this study provides a comprehensive categorization across eight domains using a structured framework. Accordingly, the literature gaps identified in prior studies directly motivate the five research questions (RQ1–RQ5) that structure this review.

Methodology

This section outlines the search strategy and classification framework used in this review. The study aims to address the following key questions:

RQ1: What are the key global and reginal trends in AI applications for geothermal energy?

RQ2: How has the adoption of AI evolved over time across different geothermal research areas?

RQ3: Which AI algorithms are most commonly used, and what are their strengths and limitations in handling geothermal datasets?

RQ4: Which regions and geothermal fields have been most studied using AI, and where are the research gaps?

RQ5: What emerging AI techniques show the greatest potential for advancing geothermal exploration, system optimization, and sustainability? By systematically analyzing AI applications across different geothermal research areas, this review provides a comprehensive perspective on current advancements and future directions in the field

Search strategy

To evaluate the integration of AI techniques into deep geothermal energy research, a structured and transparent screening process was applied to literature from the Web of Science Core Collection. An initial keyword-based query combining geothermal and AI-related terms yielded 437 records (as of September 9, 2024). The selection process involved several levels of refinement to ensure technical relevance and methodological consistency. First, title-based filtering was performed to eliminate duplicate entries, non-research articles (e.g. editorials, book chapters) and gray literature, reducing the set to 312 articles. Next, an abstract-level screening was performed to exclude studies in which AI or geothermal topics were mentioned only superficially, leaving 226 articles. In the final phase, the assessment of the full texts focused on identifying studies that explicitly applied AI methods in the context of deep geothermal systems. This rigorous process resulted in a curated dataset of 183 peer-reviewed journal articles, which formed the analytical basis for this review.

Classification framework

In this study, we categorized the application of AI in deep geothermal energy into key areas, including reservoir characterization, exploration and resource identification, geothermal energy system optimization, seismic monitoring and risk assessment, drilling optimization, hybrid energy systems, environmental impact and sustainability, and techno-economic analysis (Fig. 3).

Reservoir characterization focuses on methods, such as geophysical methods, that describe the subsurface properties that affect geothermal reservoirs, while seismic monitoring also assesses the risks associated with induced seismicity (i.e., Giustiniani et al. [14]). Geothermal energy system optimization covers AI-driven methods to enhance energy output and resource management. Exploration and resource identification

Fig. 3. Research areas in AI applications for geothermal energy

include AI techniques for predicting geothermal potential, and drilling optimization applies AI to improve drilling efficiency and reduce costs. Hybrid energy systems involve integrating geothermal energy with other renewable sources, and environmental impact and sustainability examine how AI helps mitigate environmental risks. Finally, techno-economic analysis evaluates the economic viability of geothermal projects using AI tools. This categorization allowed for a detailed analysis of the current state of AI applications in geothermal energy research. In summary, while prior studies have demonstrated the value of AI for specific geothermal challenges, the literature remains fragmented, with

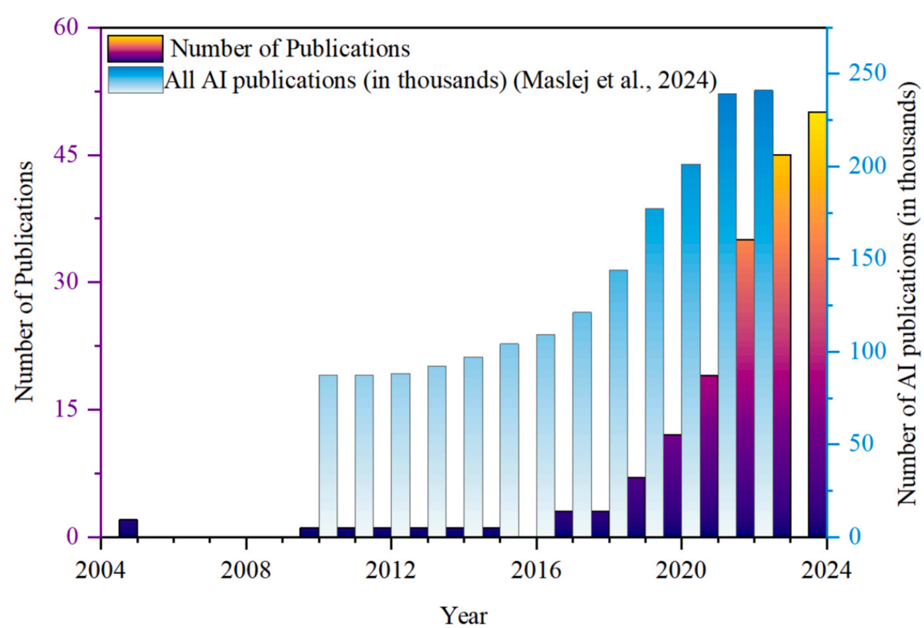

Fig. 4. Trends in AI applications in geothermal energy (2005–2024) alongside global AI publication trends (2010–2022)

limited cross-domain synthesis, uneven regional focus, and insufficient comparative evaluation of methods. These observations directly shape our guiding research questions (RQ1–RQ5), which ask where and how AI has been applied, which algorithms perform best for different geothermal data, which regions remain underexplored, and what emerging methods hold the greatest promise for advancing geothermal science and practice.

Results and discussions on AI applications in geothermal energy

This section presents a comprehensive analysis of the application of AI in geothermal energy research. Based on the reviewed literature, we examine overarching trends, regional variations, and cumulative patterns in AI applications within the field of geothermal energy. Furthermore, a detailed exploration of publication trends by research areas and commonly used AI algorithms provides insights into the evolution and potential future directions of AI-driven geothermal energy studies.

Trends in AI publications

The application of AI in geothermal energy research has experienced substantial growth in recent years, as depicted in Fig. 4. Between 2005 and 2017, publications in this domain remained minimal, with only sporadic contributions. A noticeable shift occurred between 2018 and 2020, as geothermal AI research began gaining traction, rising from 3 publications in 2018 to 12 in 2020. This period marks the initial phase of AI adoption, aligning with a broader increase in global AI research, which saw an expansion from approximately 144,000 to 201,000 publications within the same timeframe. A sharp surge followed from 2021 onward, with publications more than doubling from 19 in 2021 to 45 in 2023, reflecting the sector's increasing reliance on AI-driven approaches for reservoir characterization, geothermal system optimization, and predictive maintenance. As of 2024, the number of geothermal AI publications has already reached 50, underscoring its sustained momentum. When compared to global AI trends, geothermal energy applications initially lagged behind, with minimal research activity until 2018, whereas AI publications across all domains had already exceeded 100,000 annually by 2015. However, geothermal AI research has since grown at an average annual rate of nearly 75% from 2019 onward, significantly outpacing the general AI field's 20% growth rate. This delayed but rapid expansion highlights the geothermal sector's increasing recognition of AI's potential, demonstrating how advancements in ML, DL, and predictive modeling are now pivotal in overcoming geothermal exploration and operational challenges.

The global distribution in AI applications

The global distribution of publications on AI applications in geothermal energy, as shown in Fig. 5, highlights concentrated research efforts in key countries. China 49 and the USA 43 lead the field, demonstrating their strong role in AI-driven geothermal advancements. Germany 13, Turkey 12, Canada 11, and India 11 follow, reflecting significant contributions. Saudi Arabia 10, Iran 8, and Italy 8 also show notable research activity. European contributions are led by Switzerland 6, France 6, and the UK 5, alongside efforts from Iceland 5, Denmark 5, and the Netherlands 4. In Asia, South Korea 6, Japan 6, Pakistan 4, and Indonesia 2 have engaged in AI-based geothermal research. Mexico 6 represents key contribution from the Americas, while Australia 5 and New Zealand 3 highlight research in the Pacific region. Scandinavian countries such as Norway 2, Sweden 2, and Finland 2 show interest aligned with their geothermal potential. Additional contributions come from Austria 3, Iraq 2, Egypt 2, and Oman 2. Although some nations, including UAE, Poland, and Qatar 1 each, have fewer publications, their involvement indicates expanding global participation. This distribution underscores a diverse international effort, spanning both economically advanced and developing countries, to advance geothermal energy with AI technologies.

Fig. 6 illustrates the global distribution of research publications by the region of geothermal energy research. The USA 44 publications and China 32 publications continue to lead the field, highlighting their strong research focus on geothermal energy. Turkey follows with 13 publications, demonstrating significant engagement. Japan 8 and Germany 7 also contribute notably, indicating active research participation. Other countries, including Italy 6, India 6, and Iran 5, maintain steady contributions, while Switzerland 4, New Zealand 4, South Korea 4, Canada 4, Iceland 4, and Denmark 4 also show research activity in this

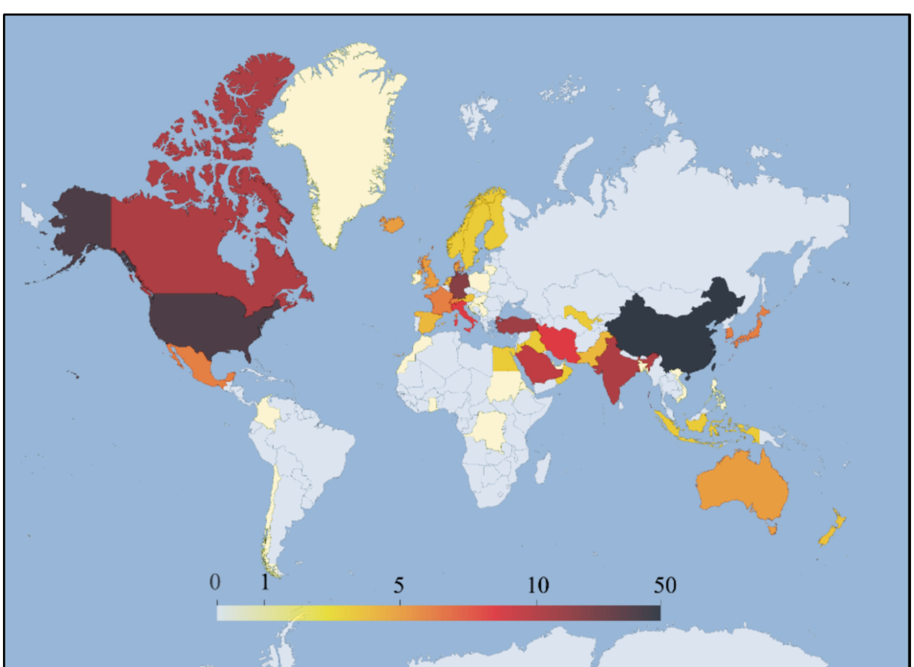

Fig. 5. Global distribution of publications on AI applications in geothermal energy based on affiliation of authors

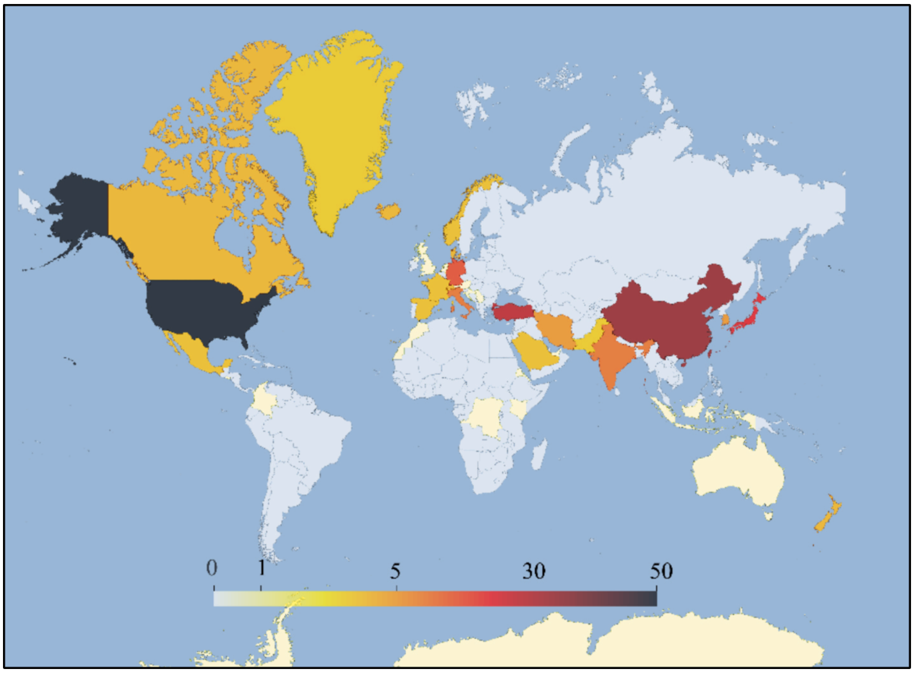

Fig. 6. Global distribution of publications on AI applications in geothermal energy based on region of interest

domain. Scandinavian countries, such as Norway 3, continue to contribute to the field, reflecting their geothermal resource potential. France 3, Mexico 3, Spain 3, and Saudi Arabia 3 also contribute to the global research landscape. Although contributions from some countries, including Greenland 2 and Pakistan 2, are lower, they still signify a broadening international interest. A few nations, such as the UAE 1, Morocco 1, Kenya 1, and Indonesia 1, have emerging research activities. The presence of publications from Antarctica 1 suggests ongoing explorations and modeling efforts. While the level of engagement varies across countries, the data underscores a diverse international commitment to geothermal energy research, fostering a more comprehensive understanding of its potential and challenges worldwide.

AI applications in geothermal energy: Publication trends by research area

Understanding the cumulative trends in AI applications across different geothermal research areas is essential for assessing how AI has evolved to address key challenges in the sector. Fig. 7 illustrates the cumulative publication trends from 2005 to September 2024, revealing a clear acceleration in AI adoption across multiple domains. Tracking these trends is crucial as it provides insights into how AI-driven innovations have matured over time, enabling more efficient geothermal exploration, resource management, and operational optimization.

Early phase (2005-2019): Limited growth

Between 2005 and 2019, AI applications in geothermal energy were limited, with only gradual growth. The primary focus during this period was reservoir characterization, which accumulated seven studies by 2019, reflecting the early use of AI in subsurface modeling and resource estimation. Another key research area was geothermal energy system optimization, which saw a steady rise, reaching five studies by 2019. This phase marked an initial exploration of AI's potential in geothermal applications, but adoption remained relatively slow due to limited computational resources and geothermal-specific datasets.

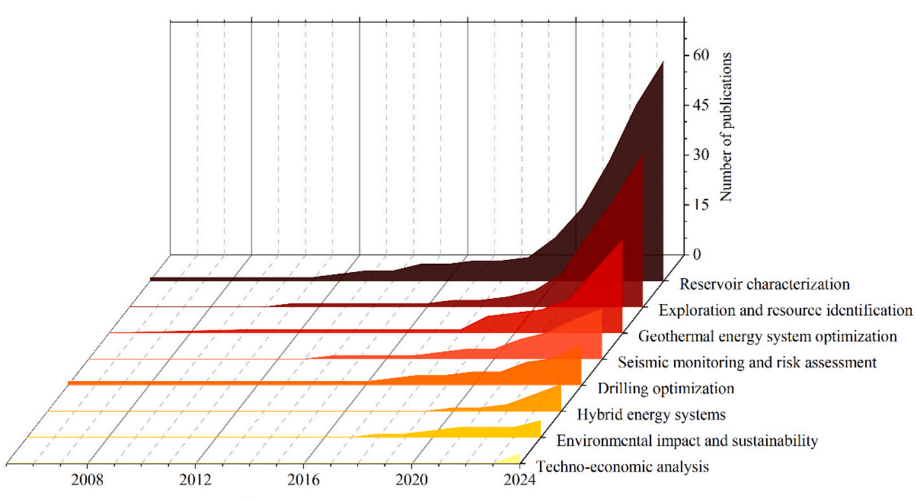

Fig. 7. Cumulative trends in AI fields of application within geothermal energy

Breakthrough period (2019-2020): AI adoption expands rapidly

A significant turning point occurred between 2019 and 2020, when AI applications in geothermal energy doubled across multiple research areas. For instance, the cumulative number of publications jumped from 7 to 13 in reservoir characterization. This surge coincided with advancements in ML methodologies, increased availability of geothermal datasets, and a broader global push toward renewable energy technologies. AI tools became more accessible, enabling researchers to apply predictive models to optimize geothermal resource management.

Rapid growth phase (2020-2024): AI becomes integral to geothermal research

Since 2020, AI applications have expanded across all geothermal research domains at an unprecedented rate. The most significant growth is observed in reservoir characterization, which has grown from 13 studies in 2020 to 66 in 2024, highlighting its critical role in reducing exploration risks and improving subsurface analysis. Similarly, exploration and resource identification has seen exponential growth, rising from 5 studies in 2020 to 46 in 2024. AI's ability to analyze geological, geophysical, and geochemical data has significantly improved site selection accuracy and reduced exploration costs. Geothermal energy system optimization has followed a similar trajectory, reaching 28 studies in 2024, demonstrating the increasing reliance on AI-driven models for improving power plant efficiency, predictive maintenance, and operational stability.

AI's application in drilling optimization has expanded from 4 studies in 2020 to 12 in 2024, reflecting its role in enhancing precision drilling, optimizing the rate of penetration (ROP), and minimizing risks associated with wellbore instability. Similarly, seismic monitoring and risk assessment has become a critical area, growing from 3 studies in 2020 to 15 in 2024. AI-driven seismic data analysis now plays a key role in mitigating induced seismicity risks, ensuring compliance, and improving real-time event detection. While AI's impact has been most pronounced in geothermal energy production and subsurface characterization, hybrid energy systems have also gained momentum, rising from one study in 2020 to eight in 2024. AI is now being applied to optimize hybrid geothermal-solar and geothermal-hydrogen systems, improving their integration and energy efficiency. Additionally, environmental impact and sustainability applications have experienced moderate but steady growth, increasing from two studies in 2020 to five in 2024. AI is now being used to assess geothermal emissions, manage water quality, and enhance sustainable resource management. The rise of techno-economic analysis in 2024, with three reported studies, indicates the increasing role of AI in economic feasibility assessments, financial risk modeling, and investment planning.

A shift toward AI-driven geothermal optimization

The cumulative trends in AI applications for geothermal energy underscore a paradigm shift toward data-driven decision-making across the industry. The rapid growth observed since 2020 highlights AI's increasing role in optimizing geothermal resource utilization, improving energy efficiency, and reducing environmental impacts. Reservoir characterization and exploration have led the adoption curve, followed closely by energy system optimization and drilling advancements.

Trends in AI algorithms for geothermal energy

Understanding trends in AI algorithms for geothermal energy is crucial for identifying emerging methodologies, optimizing resource exploration, and improving predictive accuracy in geothermal systems. As geothermal datasets grow in complexity and availability, analyzing algorithmic trends provides insights into the most effective AI approaches, guiding future research and industry applications. The integration of AI in geothermal energy research has undergone a significant transformation, evolving from early ML models to more sophisticated DL architectures (Fig. 8). This transition is driven by increasing data availability, computational advancements, and the need for more precise predictive modeling. Early studies predominantly relied on artificial neural networks (ANNs), which continue to be the most widely applied AI approach, appearing in 71 publications since 2005. ANNs have played a fundamental role in temperature prediction, reservoir characterization, and geothermal system optimization. However, as geothermal datasets have expanded, more advanced AI techniques have gained traction. Since 2018, algorithmic diversity has significantly increased, with a notable rise in ensemble-based methods such as random forests (RF), gradient boosting models (GBMs), extreme gradient boosting (XGBoost), and AdaBoost. Collectively, these tree-based approaches have been applied in 66 studies, demonstrating

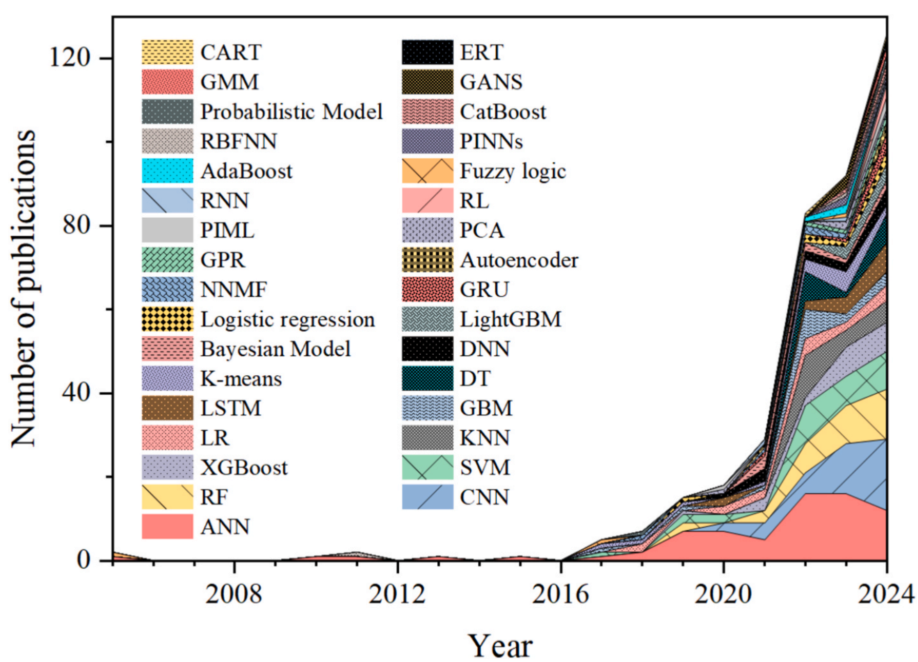

Fig. 8. Annual trend in publications by AI algorithm in geothermal energy research (2005–2024)

their effectiveness in handling complex, nonlinear geothermal data. Convolutional neural networks (CNNs) have also seen remarkable growth, increasing sharply from 2020 onward, reaching 40 occurrences in 2024. Their ability to extract spatial patterns has made them particularly effective for subsurface imaging, seismic interpretation, and geothermal anomaly detection. Support vector machines (SVMs) have maintained a steady presence with 30 applications, primarily in classification and regression tasks, highlighting their continued relevance in geothermal research. Meanwhile, long short-term memory networks (LSTMs) have gained traction in recent years, with 15 occurrences, indicating a growing emphasis on time-series forecasting in geothermal system monitoring, heat flow modeling, and production optimization. The adoption of physics-informed neural networks (PINNs) remains in its early stages, with three reported applications, but represents a promising direction where domain-specific knowledge is integrated into AI models to enhance physical consistency. The increasing use of Bayesian models (eight applications) underscores a shift toward probabilistic modeling and uncertainty quantification, particularly in cases of sparse geothermal data. Autoencoders (four applications) have also been applied for missing data reconstruction and feature extraction. The growing presence of reinforcement learning (RL), generative adversarial networks (GANs), and hybrid models suggests an expanding research landscape focused on improving AI-driven geothermal exploration and operational efficiency.

A striking trend in the graph is the exponential increase in AI-based geothermal studies from 2018 onward, with a sharp surge in publications after 2020. This reflects the accelerated adoption of AI techniques in geothermal research, driven by advancements in computational power, increased data availability, and the demand for more accurate and interpretable models. As geothermal AI research continues to evolve, future studies are expected to integrate DL, hybrid learning, and physics-informed frameworks, further enhancing predictive capabilities and advancing sustainable geothermal energy utilization on a global scale.

AI algorithm trends by research area

AI applications in geothermal energy differ by research area, with specific algorithms excelling in distinct domains. This section examines the most utilized AI techniques by research area, highlighting their impact and adoption trends.

Reservoir characterization

Reservoir characterization is crucial for optimizing geothermal energy extraction, as it provides insights into subsurface properties such as temperature, permeability, and porosity, which directly impact resource sustainability and production efficiency. AI applications in geothermal reservoir characterization have increasingly incorporated DL and ensemble methods for temperature prediction, permeability estimation, and reservoir characterization (Fig. 9). ANN remains the most widely used approach, with 25 studies leveraging its capabilities for nonlinear regression tasks, such as geothermal temperature estimation and permeability modeling. CNN usage has expanded, increasing from a single publication in 2020 to seven in 2023, reflecting its role in spatial data processing and geophysical imaging. Ensemble models, including RF (13 publications) and XGBoost (6 publications), have gained traction, particularly in geothermal temperature prediction based on geochemical and petrophysical inputs. Traditional ML models like SVM (13 publications) and k-nearest neighbors (KNN) (9 publications) maintain steady usage, demonstrating their reliability in classification tasks such as geothermal temperature categorization and permeability clustering. Bayesian models (4 publications) and clustering techniques like K-means (3 publications) are emerging in uncertainty quantification and unsupervised geothermal resource classification. PINNs and physics-informed machine learning (PIML) have recently been applied to integrate domain knowledge with AI models, as seen in geothermal temperature and permeability field predictions. Transfer learning (2 publications) suggests an emerging trend of adapting pre-trained models to geothermal applications, reducing the need for extensive labeled datasets. The increasing use of Autoencoders, U-Net, and generative models in structural and geomechanical characterization highlights AI's evolving role in data-driven geothermal exploration. These developments indicate a shift toward hybrid approaches, combining data-driven ML, DL, and physics-based modeling to enhance geothermal resource assessment and energy production forecasting.

Evaluating studies on AI applications in geothermal reservoir

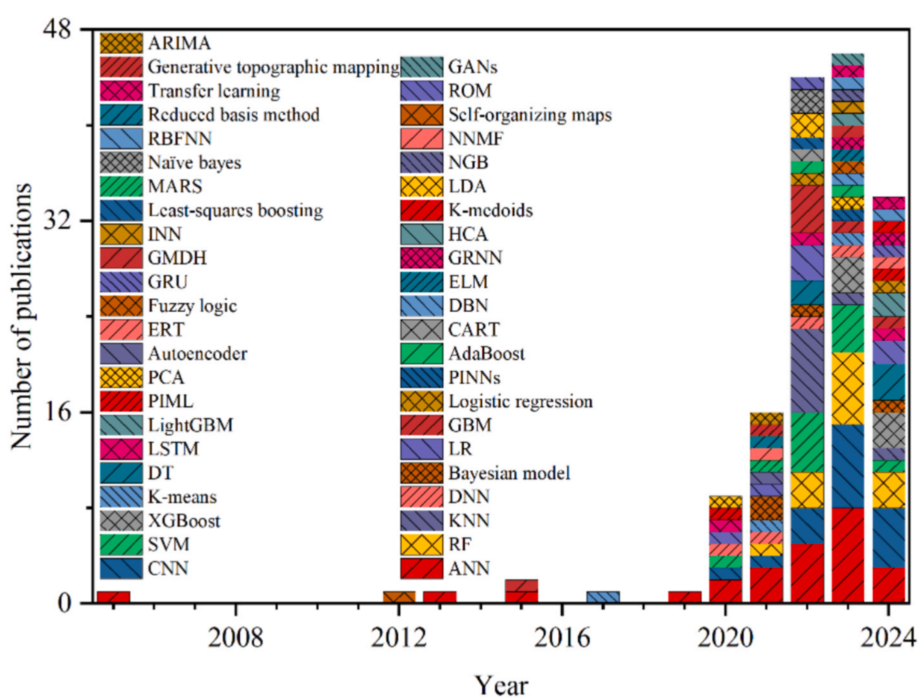

Fig. 9. Annual trend in publications by AI algorithm in geothermal reservoir characterization

Table 1
Summary of application of AI in geothermal reservoir characterization

Application area	Reference	AI Algorithms	Input	Output
Temperature prediction in geothermal reservoirs	Porkhial et al. [15]	GMDH	Northing, Easting, Depth, Angle, Azimuth	Geothermal reservoir temperature prediction at different depths in Sabalan geothermal, NW Iran (prediction error ±2–3 °C; dataset: 947 training and 469 testing samples)
	Ishitsuka & Lin [16]	PINNs	Spatial coordinates, electrical resistivity, temperature, pressure, permeability	Geothermal reservoir temperature, pressure, and permeability distribution using PINNs (temperature error 1.9 °C interpolation and 5.8 °C extrapolation in 1 km × 1 km model; reduced extrapolation error by ∼50% vs NN in 6 km × 3 km model; permeability error reduced to 1.5% with resistivity model)
	Degen et al. [17]	Physics-based ML (Reduced basis method)	Thermal conductivities, radiogenic heat production, boundary conditions	Optimization and calibration of a basin-scale conductive heat flow model for geothermal reservoir temperature prediction using Reduced Basis surrogate ML (forward runs accelerated 44 min → 3 ms; calibration reduced to ≤7 evaluations; temperature misfit improved 29 °C → 17 °C)
	Haklidir & Haklidir [18]	DNN, SVM, LR	pH, electrical conductivity, Cl^-, potassium K^+, B, Na^+, SiO_2	Prediction of geothermal reservoir temperature in Western Anatolia, Turkey (DNN outperformed SVM and LR with RMSE = 8.29 °C, MAE = 6.45 °C on test set)
	Yan et al. [19]	PIML, CNN	Fracture permeability field, injection mass rate, injected water temperature, production well bottom-hole pressure, time step	Prediction of geothermal reservoir temperature distribution and produced fluid temperature in EGS using PIML (forward model error 0.53 ± 0.46% for Tprod, 0.60 ± 0.74% for energy; surrogate $2.0\times10^4\times$ faster than simulation; optimization improved total energy +53.7% and ran 5465× faster than DE)
	Sheini Dashtgoli et al. [20]	XGBoost, DT, GRNN, RBFNN, ERT, Elastic Net	Depth, pH, electrical conductivity, total dissolved solids, bicarbonate, magnesium, calcium, sodium, chloride, sulfate, ammonium, nitrate, iron	Prediction of geothermal reservoir temperature in a carbonate geothermal system (lower Friulian Plain, NE Italy) using multiple ML models; XGBoost performed best (R^2 = 0.993, RMSE = 0.788, MAE = 0.587 on test set), with sensitivity analysis highlighting HCO_3^-, Mg, EC, and depth, and Monte Carlo uncertainty showing P10 = 25.4 °C, P50 = 33.6 °C, P90 = 38.4 °C
	Ibrahim et al. [21]	NGB, ELM, GMDH, GRNN, BPNN	Electrical conductivity, pH, Cl^-, K^+, B, Na^+, SiO_2	Prediction of geothermal reservoir temperature in Western Anatolia, Turkey using hydrogeochemical data with NGB (R^2 = 0.996, RMSE = 4.59 °C, MAE = 3.97 °C on test set); SHAP analysis highlighted SiO_2 as dominant predictor, with K, B, and Na also influencing reservoir temperature
	Shi et al. [22]	XGBoost, Bayesian Ridge Regression, DT, Light gradient-boosting machine (LightGBM)	Hydrogeochemical parameters including pH, EC, K^+, Na^+, B, SiO_2, and Cl^-	Prediction of reservoir temperature in geothermal systems in Western Anatolia, Turkey; XGBoost performed best (R^2 = 0.973, RMSE ≈ 9–10 °C, MAE ≈ 6–7 °C; external validation R^2 = 0.997, RMSE = 0.328 °C), outperforming traditional geothermometers (MAE > 30 °C)
	Acevedo-Anicasio et al. [23]	ANN	Gas-phase compositions (CO_2, H_2S, CH_4, H_2) from geothermal wells	Prediction of geothermal reservoir temperatures for liquid-dominated and vapor-dominated reservoirs. ANNs achieved RMSE ≈ 7–10 °C, MAE ≈ 5–8 °C, r = 0.97–0.99, consistently outperforming 25 classical geothermometers
	Al-Fakih & Kaka [24]	ANN- Fuzzy logic, KNN, RF	Bottomhole temperature, mud inlet temperature, mud outlet temperature, shut-in time	Prediction of static formation temperature in geothermal and petroleum wells; RF performed best (R^2 = 0.996–0.999, RMSE ≈ 0.98 °C, MAE = 0.78 °C, AAPE < 1%), with KNN and Fuzzy logic also accurate, while ANN showed lower accuracy (R^2 ≈ 0.95)
	Yang et al. [25]	ANN	Chemical geothermometers (Na-K, Na-K-Ca, K-Mg, SiO2), Water-rock interaction data	Reservoir temperature prediction, Lindian geothermal field, China, (avg. error ≈ 9 °C; 55% of predictions within 5 °C, outperforming chalcedony and IMG geothermometers)
	Gurgenc et al. [26]	AOSMA-ANN	pH, EC, Cl^-, K^+, B, Na^+, SiO_2	Prediction of geothermal reservoir temperature in Anatolia using AOSMA-ANN (R^2 = 0.851, RMSE = 26.8 °C, MAE = 21.5 °C), outperforming ANN (RMSE = 36.9 °C) and other metaheuristic ANNs (RMSE ≈ 30–33 °C)
	Altay et al. [27]	Naïve Bayes, ANN, KNN, LDA, DT, SVM	EC, pH, Cl^-, K^+, B, Na^+, SiO_2	Classification of geothermal reservoir temperature in Anatolia into <100 °C (direct use) and ≥100 °C (electricity generation) using hydrogeochemical data; hybrid GWO-MLP

(continued on next page)

Table 1 (*continued*)

Application area	Reference	AI Algorithms	Input	Output
				achieved highest accuracy (91.8%, sensitivity 84.2%, specificity 96.7%), outperforming ANN (79.6%) and other ML classifiers (71–82%)
Permeability and porosity prediction	Jiang et al. [28]	3D Autoencoder neural network combined with Bayesian inversion using Markov chain Monte Carlo	Borehole temperature, flow rate from single-well injection-withdrawal tests	Estimation of heterogeneous permeability distribution in enhanced geothermal reservoirs, autoencoder compressed 262,144 parameters into 20 features with negligible reconstruction error (MSE $<$ 0.001, SSIM $>$ 0.9). Bayesian inversion on this reduced space matched data error (RMSE = 0.1) and predicted permeability with mean error $<$0.2 mD and maximum error ≈0.9 mD
	Yan et al. [29]	INN, CNN, Transfer learning	Transient pressure derivative data from well tests, spatial distance to extraction well	Prediction of heterogeneous permeability fields in geothermal reservoirs; INN achieved high accuracy (RMSE ≈ 1.1 mD, R^2 = 1.0) for simple reservoirs and up to R^2 = 0.991 (RMSE = 18 mD) for complex heterogeneous cases; transfer learning improved sparse 5×5 grids (R^2 = 0.749)
	Fathi et al. [30]	KNN, GBM	Travel time, rate of penetration, revolutions per minute, vibration in x-direction, shock in x-direction, gamma ray.	Prediction of natural fracture intensity in geothermal and unconventional reservoirs using AutoML; KNN achieved CV score = 0.9225 (MSE = 0.0017) for regression and $>$98% accuracy (precision/recall ≈ 99%) for classification, reducing image log interpretation time by ~10× with only 10–15% labeled data
	Ntibahanana et al. [31]	DNN, RF, DT, KNN, SVM, GBM	Acoustic impedance, lithofacies	Prediction of reservoir porosity using weighted ensemble DNN; achieved MAE = 0.80, MSE = 1.10, R = 0.935, outperforming RF (MAE = 1.25, MSE = 2.57, R = 0.845) and GBM/KNN/SVM, with porosity maps closely matching historical data
	Suzuki et al. [32]	RF, SVM, ANN, GBM, KNN, Ridge regression, Lasso regression	Pressure measurements, spatial coordinates, permeability field from reservoir simulation	Prediction of permeability distribution in geothermal reservoirs; RF performed best (Train R^2 = 0.979, Test R^2 = 0.789), generalizing across different flow rates (R^2 ≈ 0.72–0.77) and partially under source/sink shifts, outperforming linear and SVR/MLP models
	Zhang & Wu [33]	DBN optimized with Improved Quantum-Behaved Particle Swarm Optimization (IQPSO)	Acoustic, spontaneous potential, gamma ray, compensated neutron log, caliper, density, medium induction logging resistivity, deep induction logging resistivity	Prediction of permeability in the Lizhai Geothermal Field, Zhangye Basin (Northern China); using DBN optimized with IQPSO; achieved RMSE = 0.05–0.08, outperforming QPSO–DBN (≈0.25) and XGBoost (≈0.12), with faster runtime (~30–59 s)
	Song et al. [34]	RF, DNN	Seismic attributes derived from well-log and seismic data, including acoustic impedance, density, P-wave velocity, and frequency components	Prediction of porosity distribution for subsurface reservoir characterization; DNN achieved R^2 = 0.943 and r = 0.973, with field test in North Sea showing r = 0.9743 and porosity 27–35% (close to reference 20–33%), outperforming single and standard ensemble models
	Pal et al. [35]	ANN with backpropagation	Fine-scale permeability realizations	Upscaling permeability in porous media using ANN; achieved R ≈ 0.98–0.99, matched analytical solutions in layered cases, and reproduced numerical upscaling in heterogeneous media with error $<10^{-3}$
	Zou et al. [36]	RF	Selected seismic attributes (variance, Vp/Vs, P-impedance, first peak amplitude, arc length, skewness, energy half-time, instant weighted frequency, first peak frequency)	Predicted porosity distribution with quantified uncertainty; achieved test RMSE = 0.018–0.024 and R^2 ≈ 0.71–0.81
	Yasin et al. [37]	XGBoost, MLP, RF, SVR	Well-log data including gamma-ray, density, neutron porosity, P-wave sonic, deep resistivity, shallow resistivity, uranium, and caliper	Prediction of fracture density in geothermal carbonate reservoirs; XGBoost with Q-learning optimization performed best (R^2 = 0.93, RMSE = 0.02, ≈95% accuracy)
	Hawkins et al. [38]	PCA, Genetic Algorithm	Inert tracer breakthrough curves, interwell frictional pressure loss, permeability field	Prediction of fracture aperture/permeability distribution and advective heat transfer; dimensionality reduced 7,196 → 200 parameters, with GA inversion predicting breakthrough in 26–40 h (measured 7 h) and production T = 23–26 °C (measured 29 °C)
Reservoir flow and pressure distribution	Li et al. [39]	K-Means	Production rate, drawdown, tank capacitance, conductance between tanks	Geothermal reservoir drawdown clustering under different production conditions; best 6-cluster model gave validation error = 3.97 m and training error = 5.71 m, outperforming models with more clusters (e.g., 8 clusters, error 4.40 m)
	Starikov et al. [40]	Similarity-based unsupervised classification	Pressure transient responses, Bourdet derivatives, flow regime characteristics	Flow regime recognition in geothermal reservoirs using similarity-based unsupervised classification of pressure transient responses and Bourdet

(*continued on next page*)

Table 1 (*continued*)

Application area	Reference	AI Algorithms	Input	Output
				derivatives; model reached weighted F1 = 0.91 on synthetic and field data
	Yan et al. [41]	Physics-constrained DL model (U-Net)	Permeability, porosity, injection well controls, time step	Prediction of pressure, saturation, and water production in 3D reservoirs using physics-constrained U-Net; achieved 1460× speedup, with temporal errors ≈0.27% (pressure) and 0.099% (saturation), and water rate predicted within 4.2% error
	Maldonado-Cruz & Pyrcz [42]	U-Net (CNN)	Porosity, permeability, well position, non-dimensional time	Prediction of pressure, saturation, and recovery factor using U-Net surrogate; achieved test MSE = 0.0011 and MSSIM = 0.848, with uncertainty model goodness = 0.95 and Pearson r = 0.98, while reducing runtime to 13–42% of numerical simulation
	Dashti et al. [43]	DT, RF, GBM	Fracture geometry parameters (position, depth, dip angle), reservoir structural variations.	Tracer breakthrough prediction under structural uncertainty in EGS using DT, RF, and chain GBR; chain GBR performed best (test RMSE = 0.05 ppm), balancing accuracy and robustness, while reducing runtime by six orders of magnitude to allow 2,000 structural scenarios
	Bassam et al. [44]	ANN using Levenberg-Marquardt optimization	Wellbore depth, inclination angle, wellbore diameter, mass flow rate, bottom-hole temperature, bottom-hole pressure	Prediction of flowing pressure gradients in geothermal wells; ANN achieved $R^2 = 0.987$ with <2.3% error (RMSE = 0.5–3.8 bar), outperforming ANN1 and GEOWELLS simulator, with bottom-hole pressure/temperature as key inputs
	Gudala & Govindarajan [45]	DNN, ARIMA	Injection rate, initial fracture aperture, reservoir temperature, fracture length, matrix porosity, matrix permeability, Biot-Willis coefficient, coefficient of thermal expansion, injection temperature.	Prediction of geothermal reservoir production temperature under coupled thermo-hydro-geomechanical conditions; DNN achieved $R^2 =$ 0.994 with RMSE ≈ 2.7–3.8 °C, while ARIMA provided long-term forecasts with $R^2 = 0.9989$ and RMSE ≈ 0.31 °C
	Yang et al. [46]	1D-CNN	Injection temperature, reservoir temperature, reservoir permeability, injection rate, well spacing.	Prediction of geothermal reservoir production temperature over time in a three-well system; achieved MAE = 0.36–0.43, RMSE = 0.34–0.40, max error 1.82 °C
	Duplyakin et al. [47]	Curve-based Neural Networks	Time-series geothermal well production data, injection rates, enthalpy, pressure, temperature, steam fraction, and flow rates	Prediction of long-term geothermal well performance and production sustainability; NN achieved errors of 0.13–3.7% (pressure), 0.17–4.8% (temperature), and <4.1% (cumulative energy), delivering 20-year forecasts in 0.9 s versus 4 h for full simulations
	Ullah et al. [48]	LSTM, GRU	Injection flow rates at injectors, tracer concentration data at producers	Prediction of thermal breakthrough and reservoir behavior for sustainable geothermal energy management; GRU performed best (R^2 up to 0.98 with target feedback, 0.95 for unified model), outperforming LSTM ($R^2 = 0.83$–0.93) with shorter training time and better generalization
	Jiang et al. [49]	CNN, recurrent neural network (RNN)	Historical well control parameters (e.g., motor speed of well pumps, injection rates, production rates, bottom-hole pressure, enthalpy) and their corresponding production response data from geothermal fields	Short- and long-term prediction of geothermal reservoir performance using CNN–RNN with data gap labeling; achieved accurate short-term enthalpy/BHP forecasts, and long-term BHP stability, with 20-year enthalpy predictions improved by adding simulated data (RMSE convergence with ~5–10 training sequences)
Structural and geological characterization	Singh et al. [50]	ANN	Apparent resistivity values from Vertical Electrical Sounding data	Geothermal subsurface resistivity structure prediction; ANN with LMA achieved $R^2 \approx 0.995$ in synthetic tests (SSE = 0.00035 in 24 epochs), outperforming ABP (SSE = 0.0019), and resolved conductive layers (2–12 Ω·m) with <1% borehole error
	Singh et al. [51]	ANN	Apparent resistivity values from vertical electrical sounding data	Subsurface resistivity and reservoir thickness prediction in Puga Valley from VES data; ANN with Levenberg–Marquardt achieved best results, converging in 4 epochs and resolving 24–80 m conductive layers (3–28 Ω·m) consistent with boreholes, outperforming Backpropagation and Adaptive Backpropagation
	Zhou et al. [52]	U-Net (CNN)	Gravity anomaly data, spatial coordinates, geological model labels	3D density model inversion for geothermal reservoir characterization in Gonghe Basin, Qinghai Province; U-Net achieved ~25–35% lower RMSE than standard DL (e.g., Model I Em reduced 10.27→7.25, Ed 98.9→34.1) and delineated 3–10 km geothermal reservoirs consistent with geophysical surveys

(*continued on next page*)

Table 1 (*continued*)

Application area	Reference	AI Algorithms	Input	Output
	Liu & Misra [53]	Adaboost, KNN, GBM, SVM, RF, Bayesian ridge regression	Full-waveform data from compressional and shear wave transmission measurements	Detection and localization of fractures from full-waveform data; AdaBoost with KNN base learner achieved best performance ($R^2 \approx 0.96$), outperforming KNN and SVR ($R^2 = 0.93$–0.95) and showing robustness to noise with >0.9 accuracy under reduced sensor setups
	Siler et al. [54]	NNMF, K-means	3D geologic factors including faults, fracture density, dilation tendency, stratigraphic thickness, and temperature	Identification of geological factors controlling geothermal fluid flow and production potential in the Brady geothermal field, Nevada; NMFk 4-cluster solution grouped 6/9 production wells with high fault density and dilation, confirming faults and step-over zone as main controls
	Jiao et al. [55]	U-Net (CNN)	Gravity and magnetic anomaly data from geophysical surveys	Prediction of density and magnetic susceptibility distribution in Gonghe Basin using U-Net; model achieved sharper boundary recovery and remained robust under 6% noise, consistent with drilling validation
Rock and mineralogical properties	Collard et al. [56]	ANN, RF, GBM, Adaboost, SVM	Temperature, pH, NaCl, Ca, Mg, C concentrations	Prediction of dolomite and calcite precipitation/dissolution under hydrothermal dolomitization; ANN achieved best accuracy ($R^2 > 0.997$, RMSE ≈ 0.007–0.008 mol, APE $< 0.3\%$), ~1000× faster than geochemical simulator, outperforming GBM, SVM, RF, and AdaBoost
	Pang et al. [57]	CNN, RF, SVM	Primary-wave velocity, density, shallow lateral resistivity, compensated neutron log, density, gamma rays, spontaneous potential, acoustic transit time.	Prediction of rock thermal conductivity in geothermal reservoirs; RF achieved best accuracy ($R^2 > 0.86$, RMSE $\approx 8\%$), outperforming CNN ($R^2 = 0.79$) and SVR ($R^2 = 0.69$), with strong robustness across lithologies
	Ullah et al. [58]	SVM, BPNN, RBFNN, PCA, LDA	Gamma-ray, heat production, thermal conductivity, heat flow, spectral gamma-ray, potassium, uranium, thorium , resistivity logs, compensated neutron log, bulk density, photoelectric absorption capture, P-wave velocit, spontaneous potential	Mineral classification and geothermal anomaly detection in the Yingxiu-Beichuan fault zone (Sichuan Basin); BPNN with LDA achieved best accuracy (86.3%), outperforming SVM (78%) and RBFNN (77%), and identified anomalies at 1550 m (GR 350 API, HP 5.5 $\mu W/m^3$, TC 0.28 W/mK)
	Boiger et al. [59]	CNN with Transfer Learning	Drill core images from borehole samples	Mineral content and lithology prediction from drill core images using CNN with transfer learning (ResNet152); achieved 96.7% lithology classification accuracy and mineral regression with $R^2 = 0.81$ (clay), 0.71 (silicate), and 0.61 (carbonate), validated against XRD
	Hu et al. [60]	CNN, XGBoost	Gamma ray, sonic transit time, deep resistivity, bulk density, neutron porosity, photoelectric factor, mineralogical data from X-ray diffraction analysis and geochemical logging tool, and well data from the Horn River Basin	Mineralogical composition prediction in Horn River Basin using CNN + XGBoost (ConvXGB); six-log model achieved R^2 up to 0.93 (carbonate, clay, QFM) and 0.75 (pyrite), validated against XRD and GLT, enabling spatial mineralogical mapping for geothermal reservoir evaluation
	Bauer et al. [61]	Self-Organizing Maps	Seismic P-wave velocity, vertical P-wave velocity gradient, electrical resistivity	Lithological classification for geothermal reservoir characterization in the Groß Schönebeck geothermal site; identified 8 classes down to 5 km depth, resolving Jurassic shales (0.1–10 Ω·m, low P-gradient) and Zechstein evaporites (0.01–1 Ω·m, 4.6–5 km/s), consistent with borehole and seismic horizons
	Feng [62]	Hybrid ANN - Hidden Markov Model	Gamma ray, resistivity, neutron-density porosity difference, average neutron-density porosity , photoelectric effect, Acoustic Impedance, P-wave to S-wave velocity ratio	Lithofacies classification for geothermal and hydrocarbon reservoirs; ANN–HMM; achieved best accuracy with MCC up to 0.62 in a Danish geothermal well, outperforming standalone ANN (0.56), HMM (0.43), and SVM (0.41)
	Chopra et al. [63]	Generative topographic mapping, Bayesian model	Well-log data, prestack seismic data, geological information	Facies classification, reservoir property predictions, enhanced spatial subdivision
	Ullah et al. [64]	RF, SVM, ANN, XGBoost, MLP	Gamma ray, resistivity, density, neutron porosity, acoustic, and photoelectric factor logs.	Facies classification in the Sawan field (Lower Indus Basin) using well logs; MLP achieved best accuracy, classifying sand facies at 87–94%, shale 70–85%, and siltstone 65–79%, outperforming RF, SVM, ANN, and XGB
	Buono et al. [65]	U-Net, GANs	Low-resolution and high-resolution X-ray, microtomography scans of microporous volcanic tuff. Corresponding paired volumes of real low resolution and hight resolution images. 3D microstructural images of volcanic rocks.	Super-resolution of Campanian Ignimbrite tuff micro-CT scans using U-Net and pix2pix; achieved Peak Signal-to-Noise Ratio (PSNR) up to 28.8 dB and Structural Similarity Index Measure (SSIM) of 0.82, with porosity/permeability estimates consistent with lab measurements, improving digital rock physics for geothermal application.

(*continued on next page*)

Table 1 (*continued*)

Application area	Reference	AI Algorithms	Input	Output
Geomechanical and elastic properties	Chen & Zhang [66]	Physics-constrained LSTM	Gamma ray, deep resistivity, bulk density, neutron porosity, sonic logs (if available), well depth, and geological formation data from the North Dakota Williston Basin.	Prediction of geomechanical logs in the Williston Basin using physics-constrained LSTM; achieved 12.5% lower MSE than standard LSTM with MAE ≈ 3.7% across 10 parameters, enabling accurate 3D geomechanical field modeling
	Ali et al. [67]	RF, K-means	Standard well logs (gamma ray, neutron porosity, bulk density, deep resistivity) and elastic logs (compressional and shear velocity) from wells in the Lower Indus Basin, Pakistan	Predicted elastic logs (compressional and shear velocity) for subsurface reservoir characterization; achieved $R^2 = 0.92–0.98$ in blind wells with RMSE ≈ 0.95, demonstrating robust sonic log prediction for subsurface reservoir characterization
	Li & Misra [68]	MARS, ANN, Ordinary least squares	Conventional well logs (gamma ray, density porosity, neutron porosity, photoelectric factor, bulk density, lithology type, and laterolog resistivity logs) from two wells	Predicted compressional and shear travel time logs (DTC and DTS) for subsurface geomechanical characterization; MARS achieved best accuracy with R^2 up to 0.80 (DTC) and 0.77 (DTS) in well #1, and 0.63 (DTC) and 0.59 (DTS) in cross-well testing, with relative errors mostly <5%
	Feng [69]	Unsupervised CNN	Pre-stack seismic gathers, wavelets, prior low-frequency models (Acoustic Impedance, Vp/Vs), smoothed density model	Elastic property prediction (acoustic impedance and Vp/Vs ratio) for geothermal reservoir characterization in the Copenhagen area; accurately recovered acoustic impedance and Vp/Vs in synthetic tests, with field application showing reasonable but lower accuracy due to well–seismic offset (~600 m)
	Gao et al. [70]	CNN, XGboost	Seismic data from clastic reservoirs with class-imbalanced lithofluid distributions	Predicted lithofluid classifications; BalanceCascade improved gas-sandstone F1 by ~15% and outperformed ResNet and XGBoost in blind tests
Simulation and model optimization	Suzuki et al. [71]	LightGBM, Logestic regression, RF, KNN	Reservoir temperature, pressure, permeability, heat source/sink conditions (position, size, flow rate, enthalpy)	Automated estimation of geothermal reservoir parameters (permeability, heat source/sink conditions) using LightGBM; achieved near-perfect classification of source/sink positions (Accuracy, F1, MCC ≈ 1.0) and regression with $R^2 = 0.998$ (enthalpy), 0.968 (flow rate), and 0.868 (permeability), enabling accurate 3D reservoir simulations
	Degen et al. [72]	Physics-based ML (Reduced basis method)	Crustal-scale geothermal model parameters including thermal conductivity, heat production rate, boundary conditions	Prediction of temperature distribution and sensitivity analysis of boundary conditions in geothermal simulations; achieved orders-of-magnitude faster simulations with FEM-level accuracy, showing boundary condition errors up to ±50 °C at 6 km depth
	Wang et al. [73]	CNN	Porous media geometry, Euclidean Distance Transform, flow boundary conditions.	Prediction of steady-state velocity fields and permeability in porous media using CNN; permeability estimated with >90% accuracy in most cases
Additional geothermal processes	Taherdangkoo et al. [74]	Least-squares boosting ensemble combined with Bayesian optimization	Young's modulus, Poisson's ratio, overburden thickness, maximum swelling pressure, initial volumetric water content	Prediction of swelling-induced heave in clay-sulfate rocks using LSBoost with Bayesian optimization; model achieved R2 = 0.98 and RMSE = 0.239 on synthetic hydro-mechanical datasets, ranking maximum swelling pressure and Young's modulus as the most influential parameters
	Yin et al. [75]	SVM, LDA, KNN, Naïve Bayes, CART, Logestic regression	Groundwater chemistry (ion concentrations: NO_3^-, Cl^-, K^+, Mg^{2+}, Na^+, Ca^{2+}, SO_4^{2-}), spatial location, geological setting	Groundwater source discrimination and geothermal evolution mechanism in the Xiluodu high-arch dam impoundment area; the bagging-based ensemble achieved the best performance with F1 = 0.979, reliably separating limestone vs. basalt groundwater contributions to explain temperature rise phenomena
	Jin et al. [76]	Sequential threshold ridge regression	Temperature values at different spatial and temporal points.	Coefficients and terms of partial differential equations describing transient heat transfer; achieved correct recovery of governing terms with coefficient errors <0.15%, robust to sparse and noisy data
	Bruss et al. [77]	ANN, KNN	Temperature sensor readings from a wellbore to detect and localize thermal defects.	Predicted location and orientation of thermal defects in the wellbore; ANN achieved 100% correct classification of defect orientation, while centroid-guided kNN localization reached an average RMS error of 1.49 in. in lab-scale tests

characterization, we identified seven key areas, including temperature prediction, permeability and porosity modeling, flow and pressure forecasting, structural characterization, mineralogical assessments, geomechanical modeling, and AI-driven simulation and optimization, as summarized in Table 1.

Exploration and resource identification

Geothermal exploration and resource identification are critical for assessing subsurface thermal potential and optimizing site selection for drilling (Fig. 10). Since 2021, the application of AI techniques in this domain has increased significantly, reflecting a growing reliance on ML and DL for geothermal heat flow estimation, temperature prediction, and resource favorability mapping. ANN (11 publications) is the most frequently used method, particularly in geothermal potential classification and subsurface temperature prediction. CNN applications have also increased, with five studies utilizing its spatial feature extraction capabilities for geothermal site identification and structural mapping. Ensemble learning models such as RF (8 publications) and XGBoost (7 publications) are widely applied for heat flow modeling and geothermal gradient estimation, leveraging multiple geological and geophysical parameters. Clustering approaches, including K-means (7 publications) and non-negative matrix factorization (NNMF) (3 publications), have gained traction in unsupervised geothermal prospectivity classification. Bayesian models (4 publications) and logistic regression (3 publications) remain relevant for geothermal favorability assessments, particularly in probabilistic modeling of geothermal site potential. Emerging trends include the use of PINNs and generalized linear models (GLMs), reflecting a shift toward integrating physical laws into AI-driven geothermal exploration. The adoption of advanced AI techniques underscores the transition from conventional mapping approaches to data-driven, physics-aware methodologies, improving geothermal resource identification and reducing exploration uncertainties. A detailed overview of AI applications in this category is presented in Table 2.

Geothermal energy system optimization

Geothermal energy system optimization has seen a growing integration of AI techniques, particularly since 2019, with ML and DL models being applied to improve power generation efficiency, reservoir heat extraction, and system integration (Fig. 11). ANN (17 publications) remains the most frequently used approach, playing a key role in optimizing geothermal power plant performance and thermodynamic cycle efficiency. The adoption of LSTM (7 publications) and gated recurrent unit (GRU) with 3 publications have grown, particularly in time-series forecasting for geothermal energy management and predictive maintenance. Ensemble models, including XGBoost (4 publications) and RF (3 publications), have been utilized in predictive modeling for energy output estimation and fault detection in geothermal systems. RL and probabilistic models are emerging for real-time decision-making and uncertainty quantification in geothermal operations. The introduction of PIML and PINNs suggests an increasing interest in integrating physics-based constraints for more accurate geothermal system modeling. Generative models, such as GANs, and advanced architectures like Transformers indicate early exploration into AI-driven energy system simulations. The expanding role of AI in geothermal optimization highlights a shift from traditional control strategies to data-driven, adaptive methodologies, enhancing operational efficiency and long-term sustainability. Table 3 presents a comprehensive overview of AI applications in this category .

Seismic monitoring and risk assessment

Seismic monitoring and risk assessment are critical for ensuring the safe and sustainable operation of geothermal energy projects, particularly in regions prone to induced seismicity. AI applications in this field have expanded significantly, with increasing adoption of DL and probabilistic models for event detection, hazard assessment, and subsurface imaging. Since 2018, CNN-based approaches (11 publications) have gained traction, particularly in seismic waveform analysis and fault detection, growing from a single occurrence in 2020 to five in 2024 (Fig. 12). ANN (3 publications) has been used in seismic hazard prediction and ground motion estimation, while SVM and logistic regression (1 publication each) remain relevant for traditional classification tasks. Probabilistic models and clustering techniques, including GMM and K-means, have been applied for seismic event clustering and spectral analysis. The emergence of autoregressive models, GANs, and RNN-based approaches indicates growing interest in leveraging sequential and generative models for seismic forecasting and microseismic event

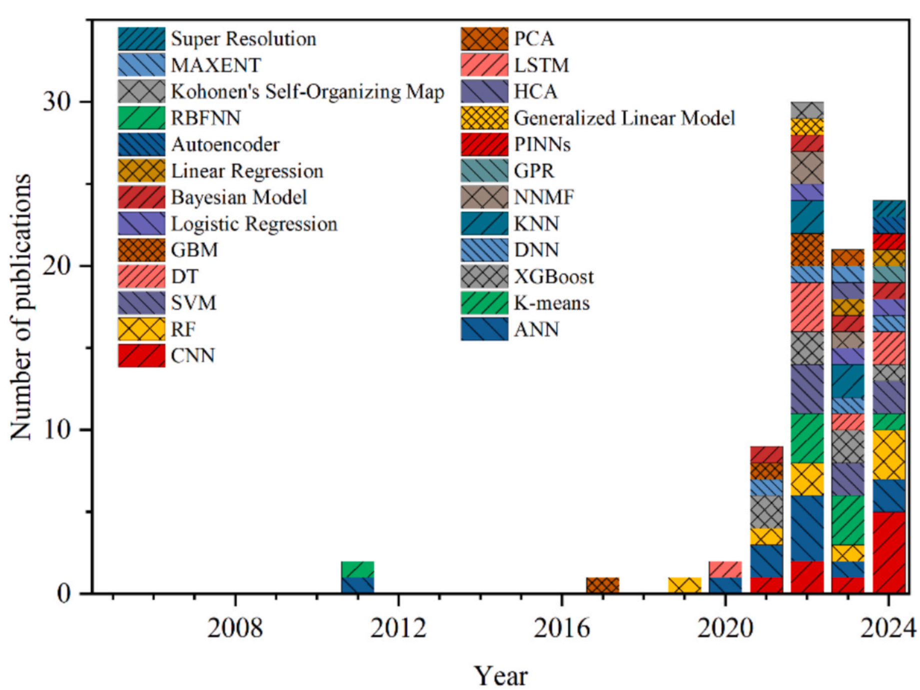

Fig. 10. Annual trend in publications by AI algorithm in exploration and resource identification

Table 2
Summary of application of AI in geothermal exploration and resource identification

Application area	Reference	AI Algorithms	Input	Output
Geothermal heat flow and temperature prediction	Chen et al. [78]	HCA, K-Means	Ground Surface Temperature (GST) data from temperature loggers	Geothermal heat flux, geothermal anomalies; K-Means best highlighted subsurface regimes, detecting anomalies of 0.27–0.63 °C above background with 11–25 fewer snow-curtain days
	Rezaei et al. [79]	RF	Geothermal gradient data (107 deep oil, gas, and water wells), hot spring geothermometry, geological attributes (fault zones, hot spots, lithology), thermal conductivity values	Heat flow map; RF with 100 trees achieved R2 = 0.91 and MSE = 0.004, providing the most accurate gradient predictions for constructing Iran's heat flow map
	Mejia-Fragoso [80]	XGBoost	Geological, geophysical, thermal, and geothermal gradient data	Geothermal gradient prediction; achieved R^2 = 0.83 (train) and 0.55 (test) with RMSE = 2.14 and 3.58, giving ~12% accuracy against independent datasets
	Colgan et al. [81]	XGBoost	419 geothermal heat flow measurements, Moho depth, Curie depth, lithospheric thickness, magnetic anomaly, gravity data, topographic correction factors	Modeled geothermal heat flow across Greenland; achieved residuals generally <20 mW/m^2 for continental areas, predicting mean onshore heat flow of 44–48 mW/m^2
	Zhang & Ritzwoller [82]	RF, DT, LR	Seismic structural variables (uppermost mantle shear wave speed, crustal shear wave speed, Moho depth), direct heat flow observations from the United States and Europe, global heat flow database, geophysical proxies (magnetic Curie depth, surface topography)	Geothermal heat flow extrapolation; DT achieved $R^2 \approx 0.62$ (US) and 0.50 (Europe) with RMSE ≈ 8 and 13 mW/m^2, while RF showed higher training fit ($R^2 \approx 0.95$) but poorer validation ($R^2 \approx 0.67$), highlighting DT as the most balanced model
	He et al. [83]	DNN, GBM, SVM, GLM	Geological features, geothermal heat flow data	Geothermal heat flow prediction in the Bohai Bay Basin, China; the hybrid SVM–DNN achieved the best results with $R^2 = 0.62$, N-RMSE = 0.122, and MAE = 5.58, surpassing DNN ($R^2 = 0.57$) and SVM ($R^2 = 0.55$)
	Ishitsuka et al. [84]	Bayesian Estimation, ANN	Electrical resistivity data, geological boundaries, microseismic observations	Deep subsurface temperature estimation; Bayesian achieved ~11–14% error (RMSE ≈ 49–57 °C) at 3000–3700 m, while ANN performed better at shallow depths but less reliable for deep targets
	Chen et al. [85]	Cross-scale (CS) diffusion model, Super resolution, CNN	Land surface temperature retrieval images from satellite remote sensing	Super-resolution geothermal anomaly images; CS-Diffusion with attention achieved PSNR = 33.02 and SSIM = 0.889 (4×), outperforming CNN- and GAN-based baselines
	Shahdi et al. [86]	XGBoost, RF, DNN	Bottom-hole temperature, stratigraphic information	Subsurface temperature prediction, geothermal gradient estimation; XGBoost achieved the best performance with MAE = 3.21 °C, RMSE = 4.94 °C, and MAPE = 9.22%, slightly outperforming RF (MAE = 3.25 °C, RMSE = 5.01 °C) and DNN (MAE = 3.39 °C, RMSE = 5.08 °C)
	Loesing & Ebbing [87]	GBM	Geothermal heat flow measurements, geological and tectonic features	Geothermal heat flow map for Antarctica; the GBM model achieved $R^2 = 0.44$ on the test set with normalized RMSE ≈ 29%, producing a continental map with values 35–156 mW/m^2 and improved reliability compared to previous models
	Mirfallah Lialestani et al. [88]	Hybrid adaptive multitask Deep Neural Least Squares with Modified Firefly Algorithm (DNLS-MFA)	Geolocation data, Geothermal borehole temperature data	3D geothermal subsurface temperature mapping; DNLS-MFA achieved $R^2 = 0.92$ (50 m) / 0.91 (150 m) with RMSE = 0.37 / 0.79 and CCR = 86.5–90.7%, outperforming base DNLS
	Bai et al. [89]	DNN	heat flow data points, geological and geophysical parameters	Terrestrial heat flow map; the DNN predicted values in the Songliao Basin ranged 38–85 mW/m^2 with an average of 67.1 mW/m^2, achieving ~10.6% error against 20 in-situ measurements, showing reliable regional heat flow reconstruction
	Alqahtani et al. [90]	XGBoost, RF	Borehole temperature, magnetic data, land surface temperature	Bottom hole temperature, Geothermal gradient maps; XGBoost achieved the best BHT performance with $R^2 = 0.999$ (train) and 0.997 (test), MAE = 0.007–0.015 and RMSE = 0.012–0.031, then used to generate reliable gradient maps
	Aljubran & Horne [91]	Interpolative physics-informed graph neural network	Bottomhole temperature, depth, elevation, sediment thickness, magnetic anomaly, gravity anomaly, seismicity, electrical conductivity	Subsurface temperature, surface heat flow, rock thermal conductivity; The model achieved MAE = 6.4 °C for temperature, 6.9 mW/m^2 for heat flow, and 0.04 W/m·K for conductivity

(*continued on next page*)

Table 2 (*continued*)

Application area	Reference	AI Algorithms	Input	Output
Geothermal resource potential and favorability mapping	Previati & Crosta [92]	ANN, gaussian process regression (GPR), SVM	Aquifer thickness, saturation, porosity, groundwater flow velocity	Geothermal potential estimation; ANN achieved the best potential prediction with $R^2 > 0.999$ and RMSE ≈ 0.002, outperforming GPR (RMSE = 0.017–0.0035) and SVM (RMSE ≈ 0.13)
	Moraga et al. [93]	CNN, KSOM, K-mean	Mineral markers, surface temperature, faults, deformation	Geothermal potential estimation; the CNN-based Geothermal AI achieved 95.5% accuracy at Brady and 92.3% at Desert Peak, with cross-site tests yielding 72–76% accuracy, showing robustness even at blind sites
	Cheng et al. [94]	Bayesian model, SVM, ANN, DT, Bagging, Logistic regression	Geothermal gradient, Curie depth, Moho depth, lithospheric thickness, heat flow measurements, gravity anomalies, magnetic field data, crustal age, tectonic setting	Geothermal potential classification maps; Bagging (ensemble) achieved the best performance with ACC = 92.6%, F1 = 0.93, and AUC = 0.95, outperforming BPNN, DT, LR, SVM, and Bayes
	Yalcin et al. [95]	Maximum Entropy (MaxEnt) Method	Land Surface Temperature anomaly, proximity to fault lines, drainage density, slope, geological indicators, remote sensing (Landsat thermal infrared bands).	Geothermal favorability mapping; MaxEnt achieved AUC = 0.916 (train) and 0.852 (test), showing higher sensitivity to geological factors than AHP and more precise targeting of geothermal areas in the Büyük Menderes Graben
	Mordensky et al. [96]	Logistic Regression, XGBoost, SVM, ANN	Heat flow, distance to Quaternary fault, seismic event density, maximum horizontal stress, distance to magmatic activity, geological resource assessment data from the 2008 USGS geothermal resource assessment.	Geothermal favorability mapping; all models showed very low predictive skill (median F1 < 0.04), with logistic regression performing slightly better than XGBoost, SVM, and ANN, underscoring the limitations of the input features
	Smith et al. [97]	BNN, PCA, K-means	Geologic and geophysical features (fault density, earthquake density, heat flow, strain rate, gravity gradient, permeability indicators), remote sensing data, geothermal well data (temperature, flow rate), structural setting classification	Geothermal potential mapping; the Bayesian Neural Network achieved the best results with ACC = 0.91, AUC = 0.94, and PR-AUC = 0.95 on the test set, outperforming deterministic ANN designs, while PCA–K-means clustering highlighted structural and geophysical controls
	Holmes & Fournier [98]	Logistic regression, DT, XGBoost, ANN, Bayesian neural network	25 geothermal attributes, including heat flow, fault density, geodetic strain rate, gravity anomaly, magnetic anomaly, geothermometry data, precipitation, and water-table depth.	Geothermal site favorability assessment; the weighted ensemble of ML models achieved the best performance with ACC = 0.955 and AUC = 0.997, outperforming individual models (ANN AUC = 0.992, XGB AUC = 0.993, LR AUC = 0.890)
	Assouline et al. [99]	RF	Topographic, weather, and surface layer/soil data	Geothermal potential mapping; RF achieved RMSE = 0.07–0.08 (cm^3/cm^3) and NRMSE = 19–27% for soil moisture prediction, with OOB scores ≈ 0.82–0.87, enabling accurate mapping of ground temperature, conductivity, and diffusivity at 200 × 200 m resolution
	Demir et al. [100]	CNN, K-means	Geothermal indicators (mineral markers, LST, faults, subsurface structural data)	Geothermal site prediction and transferability; CNN-based geothermal AI achieved up to 92% accuracy and AUC = 0.953 at Desert Peak, 82% accuracy and AUC = 0.914 at Coso, and 75% accuracy and AUC = 0.828 at Brady, demonstrating strong cross-site transferability between Coso and Desert Peak but limited generalization to Brady
	Yadav et al. [101]	ANN	Gravity data, magnetic susceptibility, magnetotelluric resistivity data, seismic refraction survey results, geological attributes from six profile lines in Gandhar, Gujarat, India.	Geothermal sweet spots; a feedforward ANN joint inversion identified subsurface anomalies with hybrid training errors of 0.1 (gravity), 0.0055 (magnetic), and 0.15 (MT), delineating geothermal targets at 200–300 m depth
	Sang et al. [102]	CNN	Geological observation data, gravity anomalies, remote sensing (Landsat 8), digital elevation model, fault structures, river network, Bouguer gravity, lithology maps, hot spring locations.	Hot spring locations and geothermal potential; CNN with full preprocessing achieved 95.4% accuracy and AUC = 0.882, improving by +11.9 p.p. and +0.086 over unprocessed data
	Ahmmed & Vesselinov [103]	NNMF, K-means	Shallow groundwater chemistry (14,341 sites, 18 attributes: major cations/anions, trace elements, isotopes, geothermometers, pH, TDS)	Geothermal prospectivity classification and geochemical reconstructions; NMFk with K-means extracted five hidden geothermal signatures distinguishing low- vs. medium-temperature systems, with optimal k = 5 based on silhouette scores and minimized reconstruction error, enabling robust probability and prospectivity maps.

(*continued on next page*)

Table 2 (*continued*)

Application area	Reference	AI Algorithms	Input	Output
Structural and geological modeling for exploration	Martin-Martin et al. [104]	KNN	Borehole grain-size data, geological and hydrogeological datasets, seismic reflection survey results	3D geological model, spatial distribution of grain-size classes, syn-sedimentary fault detection; KNN achieved up to 90% confidence near dense boreholes, with K = 1 best for heterogeneity and K ≈ 25 for basement geometry
	Hu et al. [105]	U-Net (CNN)	Airborne magnetic data, gravity gradient data, susceptibility models, density models, geophysical structure classifications	Enhanced subsurface geological inversion; U-Net achieved RMSE (data) = 0.012, RMSE (model) = 0.025, and SSIM = 0.92, outperforming conventional inversions
	Kaftan et al. [106]	MLP, RNFNN	Bouguer gravity data from the Seferihisar geothermal area, synthetic gravity models, noise-added gravity anomalies, structural parameters (depth, density contrast, location)	Depth, density contrast, structure location; both models retrieved parameters close to true values, with RBFNN slightly more accurate and faster (e.g., density contrast ≈0.27 g/cm^3, depth ≈1.8 km) and robust up to 10% noise
	Yao et al. [107]	RF	High-precision magnetic data	3D basin basement relief model; RF achieved misfit = 0.0186 (model) and 0.0084 (data) in synthetic tests, staying robust under noise, and reduced misfit to 0.0485 in the Datong Basin case vs. 0.0564 for conventional inversion
	Xiong et al. [108]	GoogLeNet (CNN-based DL model), SVM, DT, KNN	Geothermal surface manifestation images	Recognition of geothermal surface features; GoogLeNet with transfer learning achieved OA = 93.5% (validation) and 88.8% (test) with F1 ≈ 0.89–0.94, clearly outperforming SVM (OA ≈ 49–54%), DT (26%), and KNN (20%)
	Engle et al. [109]	Emergent Self-Organizing Maps (ESOM)	Geothermal and produced water chemistry	Rare earth element potential prediction; ESOM reproduced rare earth element concentrations within an order of magnitude, with slight underestimation for some elements
	Tamburello et al. [110]	RF	Global geothermal spring dataset (temperature, flow rate, dissolved solids)	Global geothermal spring distribution maps; RF identified heat flow, topography, volcanism, and tectonics as key controls, validated through 500-run variable importance tests
Geophysical and resistivity-based exploration	Jevinani et al. [111]	Variational Autoencoder, ResNet, U-Net	Magnetotelluric data	1-D geothermal resistivity inversion; U-Net performed best with validation loss ≈ 0.0022 and R up to 0.99, achieving lower RMSE ranges
	Xu et al. [112]	CNN with self-attention mechanism	Magnetotelluric survey data, resistivity models, geoelectric structure samples	2D resistivity inversion; the self-attention CNN achieved lower MSE and faster convergence than conventional CNNs.
	Rezvanbehbahani et al. [113]	GBM	Global geothermal heat flux measurements, geological and tectonic features	Predicted GHF map for Greenland; GBM achieved normalized RMSE ≈ 0.15 (~15% relative error) with R2 ≈ 0.75 in cross-validation, clearly outperforming linear regression (RMSE = 0.21, R2 = 0.40)
	He et al. [114]	Progressive Global–Semantic Segmentation Network (PGSSNet, CNN-based)	Landsat-8 Thermal Infrared Sensor (TIRS) images, Land Surface Temperature (LST) retrieval, geological/climatic data	Geothermal radiation source segmentation and reservoir mapping; PGSSNet achieved Intersection over Union (IoU) = 89.1, Dice = 89.9, and Pixel Accuracy = 94.5, outperforming U-Net (IoU = 72.8)
	Ouzzaouit et al. [115]	ANN, SVM, KNN, DT	Geothermal flow, geothermal gradient, Bouguer gravity, aero-magnetic field, tectonic fracture density, proximity to faults, thermal spring data, earthquake data	Geothermal flow prediction; ANN performed best with MAE = 5.97, MSE = 75.6, RMSE = 8.69, outperforming KNN, SVM, and DT, and was used to map geothermal flow in northern Morocco
Geochemical and remote sensing approaches	Vesselinov et al. [116]	NNMF, K-means	18 geothermal attributes, including geochemical (Boron, Lithium), geophysical (gravity anomaly, magnetic intensity), geological (fault density, crustal thickness), and hydrogeological (hydraulic gradient, precipitation) data from 44 locations in Southwest New Mexico	Hidden geothermal resource signatures; NMFk extracted five hydrothermal signatures distinguishing low (<90 °C) and medium (90–150 °C) systems, with optimal k = 5 determined by reconstruction error and silhouette width (S > 0.5), enabling mapping of favorable zones
	Santamaría-Bonfil et al. [117]	KNN, DT, SVM, RF	Geochemical data (fluid chemistry from geothermal wells)	Reconstructed missing geochemical data; KNN and DT performed best with minimum equivalence interval≤ 0.2–0.3 and up to 17% charge balance error improvement
	Li et al. [118]	Bidirectional LSTM	Hourly weather data (temperature, dew point, relative humidity, wind speed, solar radiation), soil temperature at 5, 10, 20, 50, and 100 cm depth, time-based parameters (month, day, hour)	Hourly soil temperature prediction; integrated BiLSTM achieved accuracy with RMSE = 1.53 °C, MAE = 1.22 °C, R^2 = 0.923

(*continued on next page*)

Table 2 (*continued*)

Application area	Reference	AI Algorithms	Input	Output
	Mudunuru et al. [119]	NNMF, K-means	Temperature at 2m depth, heat flow, NaK-Giggenbach geothermometer, K-Mg geothermometer, NaK-Fournier geothermometer, silica geothermometer, gravity, fault distance, Quaternary fault density, lithium concentration	Geothermal resource signatures; NMFk identified four signatures, with A and B showing strong prospectivity, validated by low reconstruction error and silhouette width > 0.25, consistent with Tularosa Basin play fairway analysis

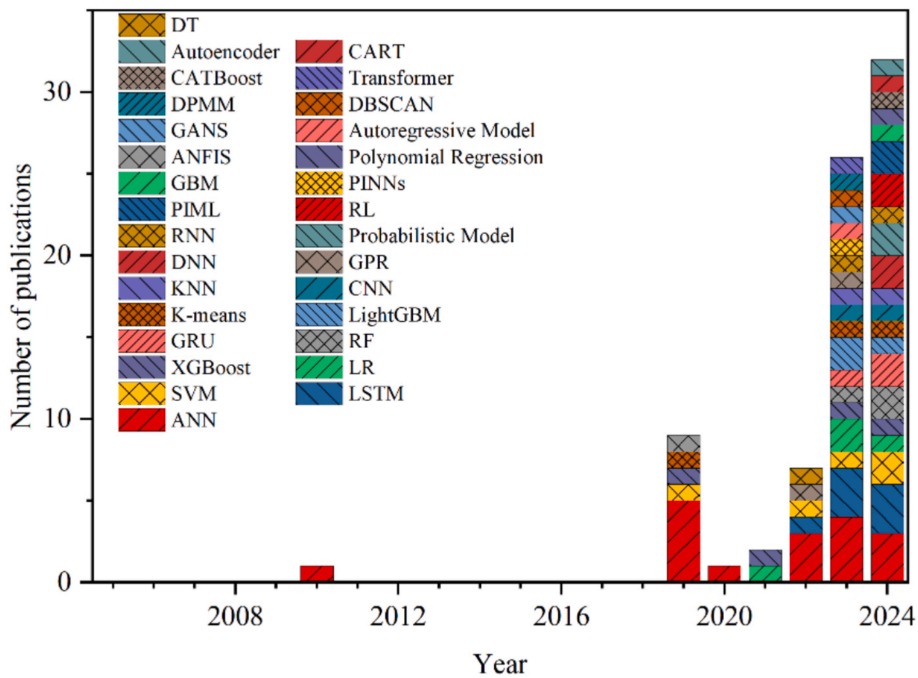

Fig. 11. Annual trend in publications by AI algorithm in geothermal energy system optimization

characterization. The integration of AI into seismic risk assessment highlights a shift toward real-time monitoring, automated classification, and physics-informed modeling, improving the accuracy of hazard predictions and subsurface fault characterization in geothermal environments. A thorough summary of AI applications in this category is shown in Table 4.

Drilling optimization

While drilling optimization has seen relatively limited AI adoption, recent years have brought increased algorithmic diversification (Fig. 13). ANNs have appeared intermittently, while RF and gradient boosting have gained traction since 2022, highlighting their predictive capabilities in drilling efficiency and parameter optimization. The re-emergence of fuzzy logic suggests its continued relevance in handling uncertain and nonlinear drilling conditions. More recently, ensemble techniques such as XGBoost, LightGBM, and AdaBoost have been incorporated, emphasizing the role of robust decision-making models in real-time drilling performance assessment. The appearance of extreme randomized tree (ERT) and LSTM networks in 2024 signals a shift toward time-series forecasting for drill bit wear prediction and adaptive drilling control. Drilling optimization in geothermal energy has increasingly integrated AI methodologies to enhance ROP prediction, wellbore stability, and drilling automation. As shown in (Fig. 14), since 2017, the use of AI models has gained momentum, with ANN (7 publications) being the most applied approach for predicting ROP and optimizing drilling performance. The adoption of ensemble learning techniques, including RF (6 publications), XGBoost (3 publications), and LightGBM (2 publications), has grown, particularly for real-time drilling parameter optimization. Fuzzy logic (2 publications) remains relevant for expert-driven wellbore stability assessments, while LSTM (1 publication) and GRU (1 publication) have been introduced for time-series forecasting of drilling conditions. The increasing use of principal component analysis (PCA) and logistic regression (1 publication each) highlights ongoing efforts to improve feature selection and classification in wellbore integrity assessments. Recent applications of CNN-based models for cement isolation evaluation signal a shift toward automated well integrity analysis. As AI-driven approaches continue to evolve, a growing emphasis on hybrid models combining ML with physics-based constraints is emerging, aiming to enhance drilling efficiency while mitigating risks in geothermal well construction.

Table 5 highlights key AI advancements in geothermal drilling optimization, covering predictive modeling for rate of penetration (ROP), wellbore stability, drilling automation and fault detection.

Hybrid energy systems

Hybrid energy systems integrating geothermal energy with other renewable sources have seen a gradual increase in AI applications, with a notable rise in publications since 2020. As shown in (Fig. 14), ANN (5 publications) has been the dominant approach, widely applied for optimizing geothermal-based power generation, heating, and hydrogen production systems. The introduction of DNN, GPR, and gene expression profiling (GEP) (1 publication each) in 2024 suggests growing interest in advanced machine learning techniques for system performance forecasting and energy efficiency improvements. While SVM and linear regression (LR) have not yet gained traction in this domain, emerging AI-driven methodologies indicate a shift towards predictive modeling for hybrid system design, including geothermal-solar and geothermal-hydrogen integrations. The optimization of thermal energy storage,

Table 3
Summary of application of AI in geothermal energy system optimization

Application area	Reference	AI Algorithms	Input	Output
Geothermal power generation and efficiency optimization	Xue et al. [120]	KNN, SVM, XGBoost, ANN	Injection rate, injection temperature, hydraulic fracture number, hydraulic fracture half-length, well spacing	Predicted geothermal electricity production; ; ANN performed best with $R^2 = 0.998$ and RMSE ≈ 62–86 kW, clearly outperforming XGBoost ($R^2 = 0.996$, RMSE ≈ 95–128 kW), SVM ($R^2 = 0.996$, RMSE ≈ 84–146 kW), and KNN ($R^2 = 0.948$, RMSE ≈ 630 kW)
	Podlasek et al. [121]	ANN, RL, LSTM	Solar irradiance, geothermal temperature, ambient temperature, mass flow rate, working fluid pressure, turbine inlet temperature	Predicted optimal operational parameters and electricity generation; RL achieved the best result with 4993.4 MWh annually, 10–17% higher than baseline sequential quadratic programming models
	Buster et al. [6]	Multi-linear regression, ANN	Geothermal fluid temperature, pressure, mass flow rate, separator/flasher pressures, condenser pressure, power efficiency, heat sink temperature, turbine performance data, plant sensor data	Predicted steam mass flow and power outputs in geothermal plants; regression models achieved relative MAE ≈ 5% and mean bias error≈ −4% for system power, outperforming simplified Willans Line models (MAE 8.6%)
	Langiu et al. [122]	ANN	Brine temperature, pressure, enthalpy, mass flow rate, turbine parameters, heat exchanger properties, ambient temperature	Surrogate predictions of turbine efficiency and heat exchanger effectiveness for geothermal ORC optimization; ANN-based surrogate models enabled tractable global optimization, achieving improved net power and total annualized return across multiple operating scenarios
	Hai et al. [123]	ANN	Geothermal brine temperature, mass flow rate, turbine inlet pressure, ammonia–water ratio, ORC working fluid properties, Kalina cycle evaporator temperature, condenser pressure, economic parameters	Predicted net power output, Kalina cycle and ORC efficiencies, exergy destruction, and thermoeconomic performance; ANN–GA optimization achieved hybrid cycle efficiency of 48.57% vs. 44.21% for Kalina alone, with levelized cost of electricity reduced to $0.04898/kWh
	Khanmohammadi et al. [124]	ANN, SVM, GPR, DT	Operational parameters including injection rate, injection temperature, hydraulic fracture half-length, hydraulic fracture number, and well spacing	Predicted geothermal power generation and thermal energy output for enhanced geothermal system (EGS) optimization; ANN with Bayesian regularization achieved the best performance with $R^2 = 0.9999$, RMSE ≈ 0.0001, and MAE ≈ 0.0001, followed by GPR ($R^2 = 0.99$, RMSE ≈ 0.30, MAE ≈ 0.15)
	Abrasaldo et al. [125]	RF, LightGBM	Wellhead pressure, header pressure, steam flow data from real-time sensors	Predicted probability of low discharge pressure events in geothermal wells; LightGBM achieved the best performance with matthews correlation coefficient = 0.66 on validation, correctly predicting 28 of 33 events
Energy system integration and optimization	Khosravi et al. [9]	ANN, ANFIS	Solar irradiance, geothermal temperature, working fluid mass flow rate, turbine outlet pressure, surface area of the solar collector, preheater inlet pressure	Predicted net power output, energy and exergy efficiencies, and levelized cost of energy (LCOE) for a geothermal–solar ORC; ANFIS-PSO performed best with R^2 up to 0.9999 and RMSE ≈ 12 kW (power), 3.6×10^{-4} (energy efficiency), 3.3×10^{-4} (exergy efficiency), and 1.3×10^{-4} ($/kWh for LCOE), surpassing ANN-PSO accuracy
	Huster et al. [126]	ANN	Working fluid composition, temperature, pressure, enthalpy, vapor fraction	Predicted optimal working fluid mixture for geothermal Organic ORC and Kalina cycles; ANN–hybrid optimization identified globally optimal isobutane–isopentane mixtures increasing net power output by 17% and ammonia–water mixtures boosting Kalina cycle output by 6%
	Ding et al. [127]	LSTM with Seasonal-Trend Decomposition (STL-LSTM)	Monthly electricity generation data, decomposed trend, seasonal, and remainder components from renewable sources	Predicted monthly electricity generation for geothermal and other renewable energy sources; STL-LSTM clearly outperformed benchmarks with MAPE as low as 2.02% (Canada hydropower case) and generally below 9% for geothermal and other renewables, versus >16% for pure LSTM and >30% for SVR
	Yilmaz et al. [128]	ANN	Geothermal fluid temperature, geothermal fluid mass flow rate, electricity consumption, system thermodynamic parameters	Predicted net electricity, hydrogen production rate, exergy efficiency, and hydrogen cost; ANN modeling achieved RMSE as low as 3.4×10^{-6} (electricity) and 4.4×10^{-4} (hydrogen), with hydrogen cost ≈ $1.09/kg and payback period ≈ 4.1 years, confirming high predictive accuracy

(continued on next page)

Table 3 (*continued*)

Application area	Reference	AI Algorithms	Input	Output
	Li et al. [129]	LR, polynomial regression	Rankine pressure ratio, mass flow rate, geothermal temperature, turbine pressure ratio.	Predicted freshwater production, power generation capacity, heating capacity, and overall system efficiency for geothermal tri-generation systems; regression models achieved $R^2 > 0.96$ overall, with freshwater, heating, and efficiency predictions exceeding $R^2 = 0.99$, yielding outputs of 7.88 kg/s freshwater, 1283 kW power, 30.8 kg/s heating, and 24.98% efficiency under optimal conditions
Reservoir and heat extraction optimization	Yang et al. [130]	Coupled generative adversarial network (Co-GAN)	Permeability distribution, injection rate, well spacing, fracture geometry, thermal and pressure properties	Predicted reservoir temperature and pressure distributions for enhanced geothermal systems; Co-GAN proxy model achieved high accuracy in reproducing thermo-hydro-mechanical-chemical (THMC) simulation results, enabling optimized injection–production strategies with ~50% higher energy extraction and 8 MPa lower pressure differentials compared to baseline
	Zhang & Li [131]	PINNs	Wellhead pressure, reservoir temperature, geothermal gradient, heat transfer coefficient, porous media properties	Predicted reservoir temperature and heat extraction in closed-loop geothermal systems; PINNs converged closely to exact partial differential equation solutions with relative L^2 error <0.06 and interface loss <0.005, demonstrating stable accuracy in multi-physics
	Chen et al. [132]	Probabilistic Neural Network (PNN) surrogate combined with Surrogate-assisted Level-based Learning Evolutionary Search (SLLES)	Well control variables (injection/production rates), fracture network characteristics, temperature, pressure, and permeability	Optimized well-control for EGS; PNN–SLLES outperformed Differential Evolution (DE), Level-based Search (LS), and other surrogates, achieving higher cumulative heat extraction and Net Present Value with faster convergence
	Akin et al. [133]	ANN	Injection flow rate, injection temperature, injection location (X, Y, Z coordinates), reservoir pressure, reservoir temperature.	Predicted reservoir pressure and temperature distributions for reinjection optimization; the best ANN design achieved correlation coefficients of $R^2 = 0.91$ (temperature) and 0.89 (pressure) against simulator outputs, supporting identification of optimal well placement in Kizildere field
	Yang et al. [134]	DBN + LSTM	Reservoir thickness, reservoir temperature, reservoir permeability, exploitation time.	Predicted flow rate, outlet temperature, heat generation power, and thermal breakthrough distance for regional geothermal production potential assessment; DBN + LSTM achieved $R^2 > 0.99$ with absolute errors <15 m^3/d (flow), <2.2 °C (temperature), <0.03 MW (power), and <20 m (breakthrough)
	Wang et al. [135]	LSTM, CNN	Permeability field, well control sequences (injection rate, bottom-hole pressure), time-series production data	Predicted production rate, production temperature, bottom-hole pressure for geothermal reservoir optimization; ; surrogate predictions closely matched simulator results ($R^2 \approx 0.98$ for rate, 0.97 for temperature, 0.96 for pressure), enabling closed-loop optimization with higher Net Present Value than random well-control strategies
	Jiang et al. [136]	Auto-regressive, RNN, LSTM	Wellhead pressure, production flow rate, injection flow rate, brine enthalpy, reservoir temperature, and control parameters (pumping speed and reinjection temperature)	Predicted production enthalpy decline, reservoir pressure response, , and energy output; the proposed multiscale RNN (with LSTM + FCNN) outperformed AR and standard RNN, achieving lowest RMSE and robust long-term forecasts under noisy field data.
Fault detection and condition monitoring	Zulkarnain et al. [137]	ANN, SVM, XGBoost, K-means	Electrical currents, electrical resistance, pressure, and heat from geothermal power plant cooling systems	Predicted machine condition state (normal or alert) for fault detection in geothermal power plant cooling systems; SVM achieved the best accuracy at 96.28% with RMSE = 21.04%, slightly outperforming ANN (95.45%, RMSE = 21.12%), while XGBoost overfit with only 78.51% test accuracy
	Abrasaldo et al. [138]	GBM, SVM, RF	Pump power, pump speed, system pressure, temperature, vibration, and fluid level data from real-time sensors	Predicted abnormal feed pump operation in geothermal binary plants; GBM performed best with MCC = 0.733, outperforming RF (0.656) and SVM (0.616) in detecting cavitation-related anomalies

(*continued on next page*)

Table 3 (*continued*)

Application area	Reference	AI Algorithms	Input	Output
	Matsuzaki et al. [139]	Temporal fusion transformer (TFT)	Wellhead valve operations, wellhead pressure, steam enthalpy, turbine inlet pressure, weather data	Predicted steam enthalpy response to valve operations and detection of subsurface instability before sudden pressure drops; TFT successfully anticipated sudden enthalpy drops up to 25 h in advance, supporting valve control strategies to prevent well pressure collapse
Thermal performance and borehole heat exchange	Yan et al. [19]	PIML, Deep reinforcement learning, DNN	Rock thermal conductivity, fracture aperture, initial reservoir T/P, interwell distance, injection T/flow, production wellbottom-hole pressure	Predicted produced geothermal fluid temperature over time; PIML achieved error ≈0.53 ± 0.46% for temperature and 0.60 ± 0.74% for energy, while delivering ~5465× faster optimization than differential evolution with comparable recovery gains
	Cetin et al. [140]	SVM, KNN, CART, RF, XGBoost, LightGBM, Catboost	Tank and pipe temperature/pressure data from geothermal–thermoelectric hybrid setup	Predicted hot and cold water flow rates; LightGBM achieved the best accuracy with $R^2 = 0.987$, RMSE ≈ 29.9, and MAE ≈ 6194, clearly outperforming other models
	Bourhis et al. [141]	XGBoost	Borehole location, depth, diameter, rock type, lithology, hydrogeological characteristics	Predicted undisturbed ground temperature, predicted ground effective thermal conductivity, predicted undisturbed ground temperature, effective thermal conductivity, and borehole thermal resistance from 174 TRTs; achieved site-specific MAE ≈ 0.66 °C (temperature), 0.19 W/m·K (conductivity), 0.016 m·K/W (resistance), with slightly higher errors at regional scale (MAE 0.78 °C, 0.26 W/m·K)
	Sias et al. [142]	Single linear regression (SLR), Multiple linear regression (MLR)	Daily energy production data (geothermal, coal, wind, hydro, biomass, oil, gas, etc.)	Predicted daily electricity consumption; MLR performed better with RMSE = 13,043 MWh and MAE = 10,662 MWh, slightly improving over SLR (RMSE = 13,459 MWh, MAE = 10,887 MWh)
	Xiao et al. [143]	LSTM-based Recurrent Autoencode	Injection rates, well control sequences, history production data (oil/water/gas rate, bottom-hole pressure)	Predicted net present value for geothermal reservoir optimization; achieved $R^2 \approx 0.95$ with median relative error reduced to 4–7% across synthetic 2D/3D reservoir benchmarks

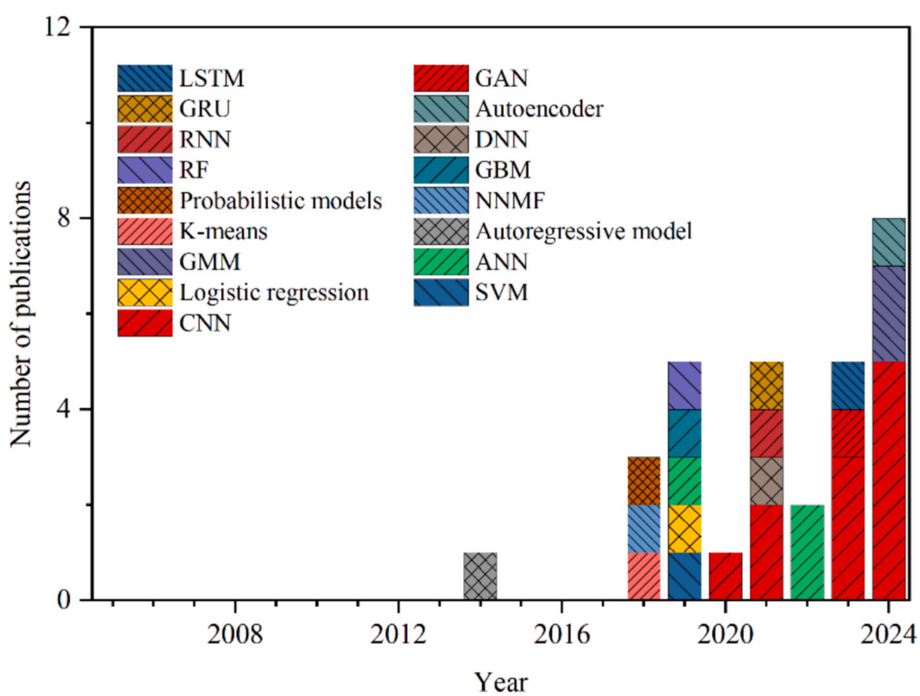

Fig. 12. Annual trend in publications by AI algorithm in seismic monitoring and risk assessment

Table 4
Summary of application of AI in seismic monitoring and risk assessment

Application area	Reference	AI Algorithms	Input	Output
Seismic event detection and classification	Picozzi & Iaccarino [144]	RNN, GRU	Seismic event catalogs from The Geysers geothermal field	Forecasting preparatory phase of M∼4 induced earthquakes; RNN1 achieved MCC up to 0.74 in identifying preparatory sequences, while GRU-based RNNs consistently detected several hours–days of precursory activity, demonstrating reliable discrimination of preparatory vs. aftershock phases
	Chien et al. [145]	Convolutional Autoencoder, GMM	Spectrograms of seismic signals (FORGE EGS site)	Seismic event classification; GMM clustering produced 7 classes with silhouette coefficients up to 0.35 and average SNR ≈ 7.7 (classes 4 & 6), showing reliable separation of signal types though with weak correlation to injection activity
	Herrmann et al. [146]	SVM, RF, ANN, logestic regression, GBM	Seismic waveforms	High-resolution seismic event catalog for induced seismicity monitoring in the Basel EGS project; classifier ensemble achieved >97% accuracy with reservoir event classification yielding precision = 0.987, recall = 0.993, and F1 ≈ 0.99
	Gauntlett et al. [147]	CNN (transfer learning) with uncertainty-aware generalized phase detection (U-GPD)	Seismic waveforms, event metadata, phase arrivals.	3D seismic velocity models for Nabro volcano, Eritrea, identifying magma storage regions and geothermal potential ; U-GPD phase picker achieved RMS residuals of 0.038 s (P) and 0.053 s (S), reducing inversion residuals by ∼30–37% and variance by ∼50–60%, enabling robust identification of magma storage zones and geothermal potential
	Cheng et al. [148]	Dilated convolution net (DCNet), CNN based	Seismic ambient noise data, time-frequency representations, surface wave dispersion curves	3D S-wave velocity structure estimation in geothermal reservoir imaging; DCNet achieved 95.3% agreement with manual dispersion picks, enabling reliable inversion and identification of low-velocity anomalies (−1% to −4%) linked to fractured, fluid-saturated zones
Seismic hazard and risk assessment	Yin et al. [149]	PhaseNet (CNN), GMM	Seismic event data, hydraulic fracturing parameters, fault parameters	Maximum induced earthquake magnitude forecasting (Seismic risk assessment in EGS); the best hybrid model achieved ≈95% classification rate with MAE ≈0.78
	Prezioso et al. [150]	ANN	Seismic waveform data from 212 earthquakes in The Geysers geothermal field	Predicted ground motion parameters (PGA, PGV, spectral acceleration) for seismic hazard assessment in The Geysers geothermal field; ANN outperformed empirical models with R^2 up to 0.88 and ∼2–5% lower total deviation, giving ∼3% better accuracy in seismic hazard prediction
	Holtzman et al. [151]	NNMF, Hidden Markov models (Probabilistic models), K-means	Seismic waveform data	Clustered seismic events by spectral properties; revealed cyclic annual patterns correlated with reservoir fluid injection, showing changes in faulting processes without clear spatial clustering.
	Tary et al. [152]	Autoregressive Model	Seismic waveforms, injection parameters (slurry flow, nitrogen rate), resonance signal properties	Peak frequencies, quality factors, amplitude variations, resonance classification in geothermal reservoir monitoring; identified resonance frequencies (17–51 Hz) with Q factors ranging from ∼40 to 650, showing strong correlation with slurry flow and nitrogen injection rate
Subsurface imaging and fault characterization	Jreij et al. [153]	U-Net (CNN)	Migrated seismic profies (from distributed acoustic sensing (DAS) and geophones)	Fault detection and subsurface imaging for geothermal reservoir characterization at Brady Hot Springs; U-Net achieved F1 ≈ 0.919 with DAS and ≈ 0.877 with geophones, confirming DAS provided higher fault detection accuracy
	Lou et al. [154]	Multiscale attention-based CNN	Seismic reflection data, synthetic seismic images, fault attributes	Seismic fault probability maps and fault segmentation in geothermal fault detection for induced seismicity analysis; Multiscale attention-based CNN outperformed coherence, holistically-sested edge detection, and U-Net with lower MSE, higher peak signal-to-noise ratio, and higher structural similarity index measure on synthetic and field data
	Gao et al. [155]	GAN	Seismic waveforms, denoised seismic data, velocity models, anisotropic parameters, and seismic images.	Fault detection and seismic velocity models for geothermal reservoir characterization at the Blue Mountain geothermal field; GAN-based denoising reduced inversion misfits and produced clearer seismic images, improving fault continuity and anisotropy estimation compared to conventional processing
Deformation monitoring and seismic source parameter estimation	Yazbeck & Rundle [156]	CNN, LSTM	InSAR images, geothermal injection rates, seismic activity data	Predicted future deformation maps for geothermal subsidence forecasting at The Geysers; CNN–LSTM with geothermal data outperformed linear baseline with lower MSE
	Nooshiri et al. [157]	CNN	Seismic waveforms	Full seismic moment tensor and hypocenter spatial location for microseismic events in Hengill geothermal field; predictions matched manual inversions with location errors of only a few hundred meters and 95%

(*continued on next page*)

Table 4 (*continued*)

Application area	Reference	AI Algorithms	Input	Output
				of moment-tensor distances below 0.1, enabling near real-time inversion
	Okamoto et al. [158]	CNN	Continuous microseismic waveform data from geothermal fields (P- and S-wave arrivals, noise records).	Microseismic event detection and hypocenter relocation; the fine-tuned CNN achieved 74% accuracy for P-waves and 78% for S-waves with precision ≈100% and recall up to 86%, yielding 482 located events with RMS residual ≈0.07 s, comparable to manual picks.

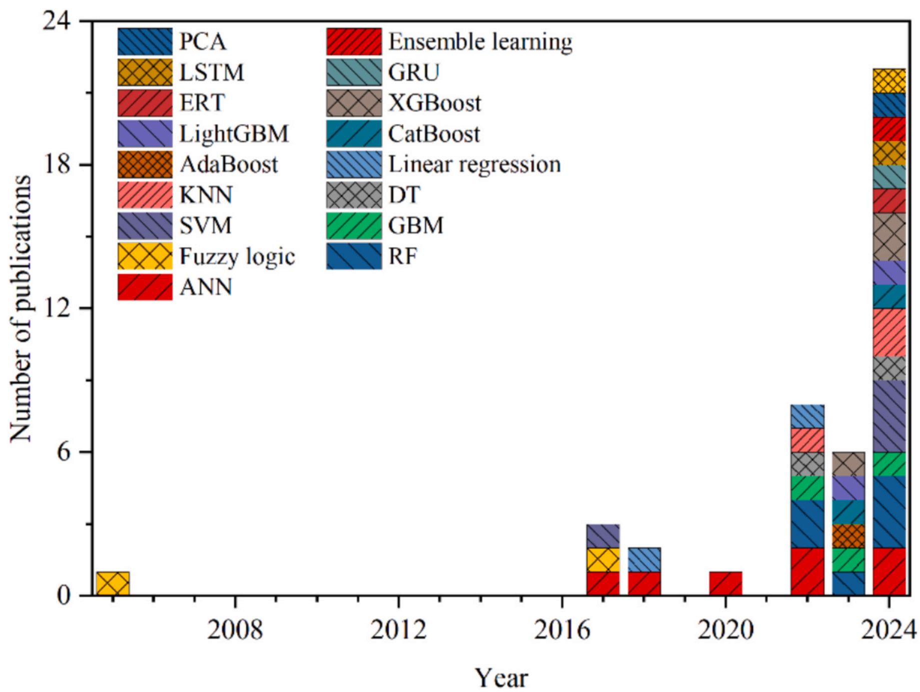

Fig. 13. Annual trend in publications by AI algorithm in drilling optimization

exergy efficiency, and operational constraints highlights AI's role in maximizing the economic and technical feasibility of hybrid geothermal energy systems. Future trends point toward expanding AI applications in multi-energy system coordination and real-time optimization to enhance sustainability and resource utilization.

Table 6 summerizes recent advancements in hybrid energy systems demonstrate promising innovations, integrating geothermal energy with various renewable sources to enhance sustainability and efficiency.

Environmental impact and sustainability

AI applications in environmental impact and sustainability within geothermal energy have gradually emerged, with an increase in studies since 2018 (Fig. 15) . ANN (2 publications) has been the primary method for predicting geothermal water quality and contamination, particularly for scale deposition and boron contamination assessments. The integration of RF (2 publications) and LSTM (1 publication) in recent years highlights the growing role of machine learning in climate impact modeling and geothermal heat flow analysis. The use of DT, SVM, and KNN (1 publication each in 2024) for infrastructure durability and corrosion mitigation suggests expanding AI-driven approaches for long-term geothermal system sustainability. While early research focused on water chemistry and contamination, more recent applications are incorporating AI for predictive monitoring of geothermal heat loss, subsurface temperature variations, and material degradation. The trend indicates an increasing reliance on AI to enhance geothermal system resilience, optimize resource management, and mitigate environmental risks associated with geothermal energy production. Table 7 provides a detailed summary of AI applications in this category .

Techno-Economic analysis

The category shows limited activity, with a couple of publications appearing only in 2024 (Fig. 8). This reflects that AI-driven techno-economic analysis is still a nascent field in geothermal energy, but its emergence suggests an increasing recognition of the importance of economic modeling to make geothermal projects more feasible and profitable.

Starting from 2024, studies in the realm of techno-economic analysis have increasingly employed AI-driven methodologies to assess and optimize geothermal systems, highlighting their potential for both cost efficiency and energy integration. Clemens et al. [182] applied RL to optimize geothermal field development planning. Using geothermal reservoir parameters (porosity, permeability, temperature, pressure), economic factors, and data acquisition strategies as inputs, the study generated an optimized geothermal field development plan. This included data acquisition strategies, well placement, and decision-making under uncertainty, showcasing AI's ability to enhance strategic planning and investment decisions in geothermal energy projects. In the realm of techno-economic analysis, recent studies have employed AI-driven methodologies to assess and optimize geothermal systems, highlighting their potential for both cost efficiency and energy integration. Zeng et al. [183] analyzed the extreme linkages and time-frequency co-movements between AI and clean energy indices, including geothermal. By applying frequency-domain and Granger causality analyses, the study found that the NASDAQ OMX Geothermal

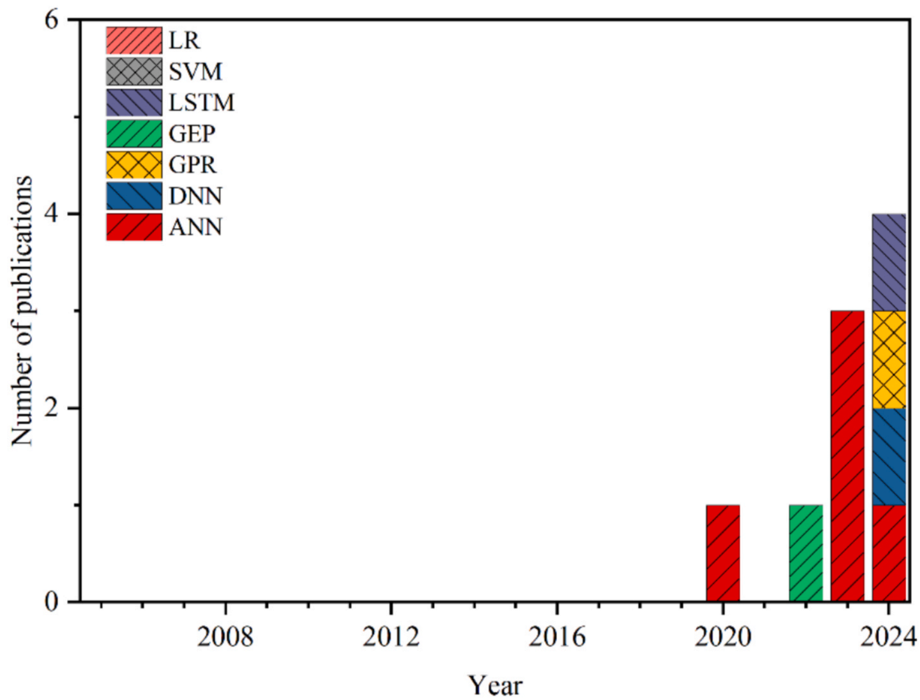

Fig. 14. Annual trend in publications by AI algorithm in hybrid energy systems

Index acted as a key sender of shocks under extreme market conditions, revealing significant co-movements with AI across various frequency domains. This study emphasized AI's predictive power in identifying market interdependencies, which is crucial for informed investment in clean energy sectors. Ramachandran et al. [184] conducted a techno-economic analysis and optimization of a binary geothermal combined district heating and power plant in Puga Valley, India. Using a neural network-assisted optimization approach, the study achieved optimal system efficiencies by identifying design parameters that maximized exergy and minimized cost. This analysis provided a practical framework for enhancing the viability of geothermal systems, particularly in regions with high geothermal potential such as Puga Valley.

AI algorithm trends in geothermal energy research reveal evolving preferences (Fig. 16). ANNs dominate with 797 citations, reinforcing their role in regression and prediction. RF (228) and CNNs (215) follow, with CNNs excelling in spatial data interpretation for geothermal mapping. Gradient boosting (192) and XGBoost (120) highlight a shift toward models optimized for complex data patterns. K-means clustering (141) and LSTM (138) are gaining traction, reflecting the industry's embrace of time-series forecasting and unsupervised learning. SVM (199) remains essential in classification tasks, while Bayesian models (42) and probabilistic approaches signal a growing interest in uncertainty quantification. DNN (109), NNMF (90), and KNN (75) are emerging for specialized applications. Meanwhile, traditional models like LR (124) and GPR (72) persist but are increasingly supplemented by data-driven AI. The trend suggests a future focused on high-performance, adaptable AI for geothermal exploration and optimization. While these pioneering studies demonstrate the potential of AI for techno-economic assessments, most research still emphasizes technical optimization, with limited integration of full economic viability or energy balance analyses. Expanding this dimension would provide a more holistic understanding of the practical feasibility and long-term sustainability of geothermal systems.

Limitations and Future Directions

While this review provides a comprehensive and structured synthesis of AI applications in deep geothermal energy, its scope is naturally defined by several boundaries. The analysis is limited to peer-reviewed journal articles, which ensures quality and reliability but may not capture the very latest insights available in preprints, conference proceedings, or industry reports. In addition, the categorization into eight domains, although broad and inclusive, reflects the structure of current research and will need refinement as the field evolves and new interdisciplinary directions emerge. The algorithm–input–output–performance framework offers a useful lens for comparison, but future work could complement this approach by incorporating additional dimensions such as computational cost, interpretability, and practical deployment challenges.

Looking ahead, further studies should expand the dataset to include grey literature and open repositories, allowing a more diverse representation of ongoing work. Developing benchmark geothermal datasets for cross-comparison of AI models would also strengthen the reliability of performance assessments. Particular opportunities exist in the underexplored areas of environmental impact assessment and techno-economic analysis, where AI applications remain sparse. Finally, as interpretability and physics-informed AI methods continue to advance, future research should explore their integration to enhance both scientific insight and trust in real-world geothermal deployment.

Conclusion

This review provides a comprehensive assessment of AI applications in deep geothermal energy analyzing research methods, publication trends, global distribution, and algorithmic advances. A systematic search of the Web of Science Core Collection identified 183 journal articles categorized under eight major research areas: Reservoir characterization, exploration and resource identification, geothermal system optimization, seismic monitoring and risk assessment, drilling optimization, hybrid energy systems, environmental impact and sustainability, and techno-economic analysis. These classifications provide valuable insights into the role of AI in advancing geothermal research. The key findings of this study are summarized below:

Table 5
Summary of application of AI in drilling optimization for geothermal energy

Application area	Reference	AI Algorithms	Input	Output
ROP prediction and drilling performance	Diaz et al. [159]	ANN, Multiple regression	Drilling parameters, including depth, pore pressure gradient, mud density, weight on bit, rotary speed, tooth wear, Reynolds number	ROP prediction for geothermal drilling optimization at the Pohang EGS site in South Korea; ANN achieved the lowest prediction error of 39.7% using adjacent well data arrangements, outperforming other setups with errors up to 85.3%.
	Yehia et al. [160]	ERT, LightGBM, RF, GBM, ANN, SVM, KNN	Drilling parameters (ROP, depth, torque, weight on bit (WOB))	ROP prediction for geothermal drilling optimization at the FORGE site in Utah, USA; ERT, LightGBM, RF, and GBM performed best with MAE ≈ 3.5–4.5 and R^2 = 0.90–0.95, while ANN and SVM lagged with higher errors (MAE 4.7–6.3, R^2 = 0.85–0.91)
	Feng et al. [161]	CatBoost, RF, GBM, ADAboost, XGBoost, LightGBM	Drilling parameters (Temperature, pressure, flow rate, RPM, WOB, Surface torque)	ROP prediction for geothermal drilling optimization at the UTAH FORGE site, USA; CatBoost gave the best results with R^2 = 0.98, RMSE = 0.14, and MAE = 0.11, clearly outperforming RF and other ensemble methods
	Ben Aoun & Madarasz [162]	RF, ANN	Drilling parameters (ROP, WOB, rotary speed, pump pressure, flow rate, temperature)	ROP prediction for geothermal drilling optimization at the Utah FORGE site, USA; RF performed best with MAE = 2.46 and R^2 = 0.84, while ANN gave MAE = 3.98 and R^2 = 0.73
	Seo et al. [163]	GRU	Drilling parameters (previous and current ROP values)	ROP prediction for geothermal drilling optimization in the Pohang EGS, South Korea; the GRU achieved MAPE < 3% immediately below training data and 5–10% when trained on adjacent-well data, while errors rose above 20% for multi-step forecasts
Wellbore stability and temperature estimation	Laureano-Cruces & Espinosa-Paredes [164]	Fuzzy Logic	Logged temperatures, expert decisions, wellbore geometry, drilling fluid properties, flow rate, geothermal gradient	Estimated static formation temperature for geothermal well; fuzzy model achieved convergence within ±5 °C of logged values
	Wang et al. [165]	Multiple linear regression	Wellbore depth, geothermal gradient, casing size, hole size, flow rate	Predicted hot spot temperature and corresponding well depth for geothermal well cementing; model matched CFD with errors of 1.6–9.3% for temperature and 1.2–15.9% for depth
	Khaled et al. [166]	LSTM, DNN, SVR, RF, XGBoost, Stacked Ensemble	Drilling parameters, thermo-hydraulic data	Bottom-hole circulating temperature prediction for geothermal drilling optimization at the Utah FORGE site, USA; LSTM achieved the best performance with MAE = 0.9–1.3 °C and RMSE ≈ 4.2–4.3
	Abdollahian et al. [167]	Pre-trained CNN models (Xception, VGG16, MobileNetV2, ResNet50), PCA, KNN, Logestic regression, SVM, DT, RF	Variable density log converted into images using continuous wavelet transform	Cement isolation classification (good, medium, bad) for wellbore integrity evaluation in geothermal well; ; Xception + RF achieved the best accuracy at 97.5%.
Drilling automation and fault detection	Kiran et al. [168]	KNN, RF, DT, GBM, ANN	Surface drilling parameters ROP , WOB, pump pressure, torque, rotary speed)	Lost circulation classification for geothermal drilling risk mitigation at FORGE site in Utah, USA; RF performed best with accuracy up to 87.3%, outperforming GBM (82.7%) and ANN (80.1%)
	Chhantyal et al. [169]	Fuzzy Logic, ANN, SVM	Ultrasonic level measurements (LT-1, LT-2, LT-3)	Drilling fluid flow rate estimation for geothermal drilling fluid monitoring; ANN achieved best performance with R^2 ≈ 0.99 and RMSE ≈ 0.002 m^3/s, outperforming fuzzy logic and SVM

- Publication growth: AI research in the field of geothermal energy has increased significantly since 2018, with an average annual growth rate of 75%, well above the 20% growth rate of global AI publications. This underlines the increasing importance of AI for geothermal exploration, modeling and optimization.
- Geographic distribution: Output is dominated by China and the United States, followed by Germany, Turkey, Canada, and India, with new contributions from Saudi Arabia, Iran, Mexico, and Scandinavia indicating a widening global engagement.
- Domain coverage: Strong progress has been made in reservoir characterization and resource identification, while hybrid systems, environmental assessment, and techno-economic analysis remain comparatively underexplored.
- Algorithm usage: ANNs remain the most widely applied for prediction, reservoir modeling, and system optimization, while tree-boosting methods (RF, GBM, XGBoost) have gained popularity for nonlinear geothermal datasets.
- Advanced modeling: CNNs are increasingly employed for spatial modeling and seismic interpretation, whereas LSTMs are applied to time-series forecasting in monitoring and heat flow prediction.
- Recent advances: Physics-informed AI, Bayesian approaches, and autoencoders are expanding capabilities in uncertainty quantification, data reconstruction, and integration of physics-based constraints.
- Emerging trends: Self-supervised learning and reinforcement learning are beginning to provide novel opportunities for leveraging limited datasets and enabling real-time decision-making in geothermal operations.

The increasing use of AI in various research areas of geothermal energy underscores its transformative potential in improving resource exploration, system optimization and sustainable energy production. Continued advances in AI methodologies will play a critical role in addressing geothermal challenges and accelerating the global shift towards AI-driven energy solutions. The novelty of this review lies in its

Table 6
Summary of application of AI for hybrid energy systems in geothermal energy

Application area	Reference	AI Algorithms	Input	Output
Geothermal-based power and heating systems	Ling et al. [170]	ANN	Geothermal system parameters (temperature, pressure, mass flow), Organic rankine cycle (ORC) working fluid properties, operational variables for combined cooling, heating, and power (CCHP) system	Optimized geothermal CCHP system efficiency, reduced payback period, maximized net power output; ANN reduced payback by 21%, raised net power by 14%, improved cooling by 12%, with outputs of 655.8 kW (power), 578.3 kW (cooling), 3042 kW (heat), and LCOE ≈ 0.05 $/kWh
	Nourpour & Manesh [171]	ANN	Geothermal system parameters (temperature, pressure, mass flow), ORC working fluid properties, operational variables for CCHP	Optimized geothermal cogeneration system efficiency; ANN–GP optimization increased power output by ~60% and improved energy and exergy efficiencies by 12.8% and 10.8%, respectively, with availability reaching 87.3%
Geothermal-hydrogen and desalination integration	Almutairi [172]	ANN	Geothermal well parameters (mass flow rate, temperature, pressure), desalination process variables, hydrogen production efficiency	Optimized geothermal–hydrogen–desalination integration; ANN predictions achieved $R^2 = 0.9999$ with outputs of 5.15 MW power, 127.3 m^3/h freshwater, 91.4 kg/h hydrogen, cooling load 2.92 MW, LCOE ≈ 0.017 $/kWh, LCOW ≈ 0.25 $/$m^3$, and LCOH ≈ 1.77 $/kg
	Barogh & Moghimi [173]	ANN	Design parameters of the solar-geothermal energy system, including thermal energy storage, compressed air energy storage, and operational constraints.	Optimized system parameters (hydrogen production rate, net power output, round-trip efficiency, cost rate); ANN–GA optimization achieved 46% round-trip efficiency, 6.96 kg/day H_2 (+44%), with only +2.8% cost increase
Geothermal-solar hybrid systems	Khosravi & Syri [174]	ANN	Solar irradiance, cooling water temperature difference, ambient temperature, pinch-point temperature, evaporating and condensing temperatures	Predicted net power output, COP of absorption refrigeration system, heat exchanger area, and cycle thermal efficiency in a hybrid geothermal–solar system; ANN achieved R^2 train = 0.9965, R^2 test = 0.9944, RMSE train ≈ 1.58 kW, RMSE test ≈ 2.24 kW for power prediction, and COP prediction with RMSE ≤ 0.0023
	Jakhar et al. [175]	ANN, LR, SVM, DT	Nanofluid concentration, Reynolds number, time, PV/T inlet temperature, and environmental conditions related to geothermal cooling	Predicted PV panel temperature (32.1–36.5 °C), outlet temperature, thermal efficiency (72.1–75.7%), and electrical efficiency (10.51–10.66%); MLP achieved ~98% accuracy, outperforming LR, SVM, and DT
	Mun et al. [176]	Gene expression programming	Temperature, humidity, ventilation rate, ammonia concentration, CO2 concentration, heating load by pig's weight, and PM2.5 concentration in a geothermal-solar hybrid system	Predicted electricity consumption for geothermal-solar heating efficiency in livestock farming; achieving $R^2 = 0.97$, RMSE = 3.37, MAE = 0.28 (training) and $R^2 = 0.94$, RMSE = 3.89, MAE = 1.19 (testing), with 31.6% lower electricity use and reduced CO_2 emissions.

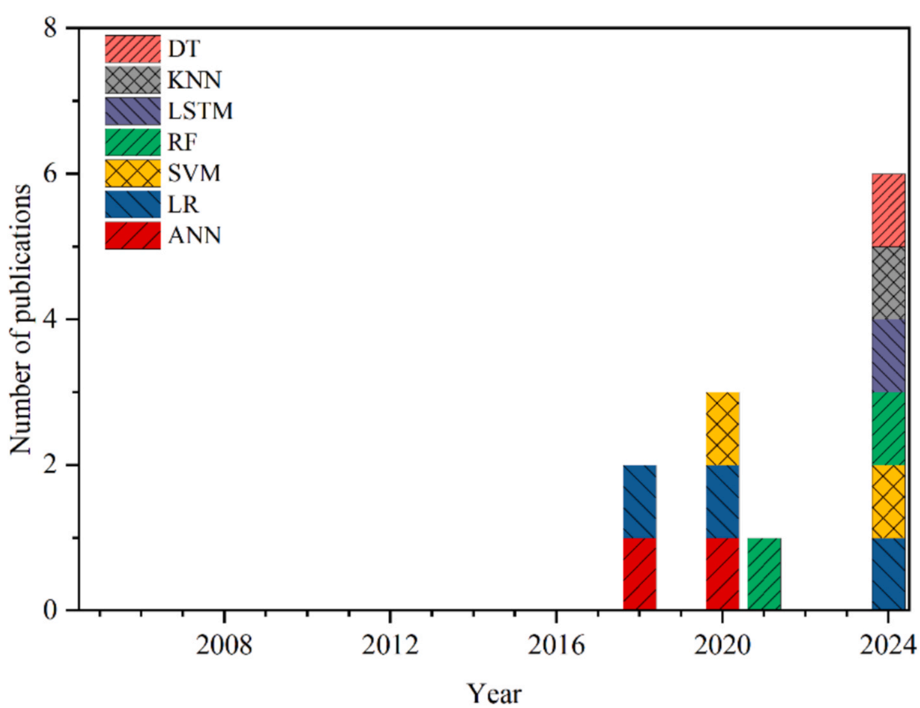

Fig. 15. Annual trend in publications by AI algorithm in environmental impact sustainability

Table 7
Summary of application of AI in environmental impact sustainability

Application area	Reference	AI Algorithms	Input	Output
Geothermal water quality and contamination	Milicevic et al. [177]	ANN, LR	Hydrochemical properties of geothermal water (temperature, pH, hardness, ion concentrations), hydromechanical parameters (flow rate, turbulence, pressure) from geothermal water sources	Predicted scale deposition rate and hardness reduction; ANN achieved R^2 up to 0.998 with MSE ≈ 10.8, outperforming linear regression (R^2 ≈ 0.997, MSE ≈ 14.2–18.9)
	Haklidir & Haklidir [178]	ANN, SVM, LR	Geothermal water chemistry (B, pH, Na, K, Ca, Mg, Cl, SO_4, HCO_3), geological/hydrogeological features (rock formations, faults, reservoir depth)	Predicted boron contamination; ANN achieved lowest error with RMSE = 5.13 and MAE = 3.95 on test data, outperforming linear regression (RMSE = 8.58) and SVM (RMSE = 6.98)
Geothermal heat flow and climate impact	Giannoulis et al. [179]	LSTM networks with attention mechanisms (DITAN)	Time-series surface temperature data from geothermal sites (Vulcano's Fossa crater), Meteorological data (air pressure, wind speed, rainfall, temperature)	Anomaly detection in geothermal surface temperature; DITAN identified 1,737 anomalies (~25% of 2020 records), mainly linked to low-pressure systems, with precision–recall validated against expert rules
	Li et al. [180]	RF	Geological and geophysical data (oceanic crust age, lithospheric density, crustal thickness, seismic wave velocities, gravity anomalies, Moho depth, LAB depth, distance to ridges and volcanoes).	Predicted global marine heat flow; best RF model achieved normalized RMSE = 0.13, normalized MAE = 0.07, and R^2 = 0.96, robustly mapping oceanic heat loss patterns
Geothermal infrastructure durability and corrosion mitigation	Bohane et al. [181]	DT, LR, SVM, KNN, RF	Geothermal corrosion factors, material properties, exposure conditions	Corrosion rate prediction for geothermal infrastructure; DT achieved best results with R^2 = 0.90/0.78 (uniform/pitting), improving to 0.96/0.83 after feature selection, outperforming RF (0.88/0.74) and KNN (0.58/0.69)

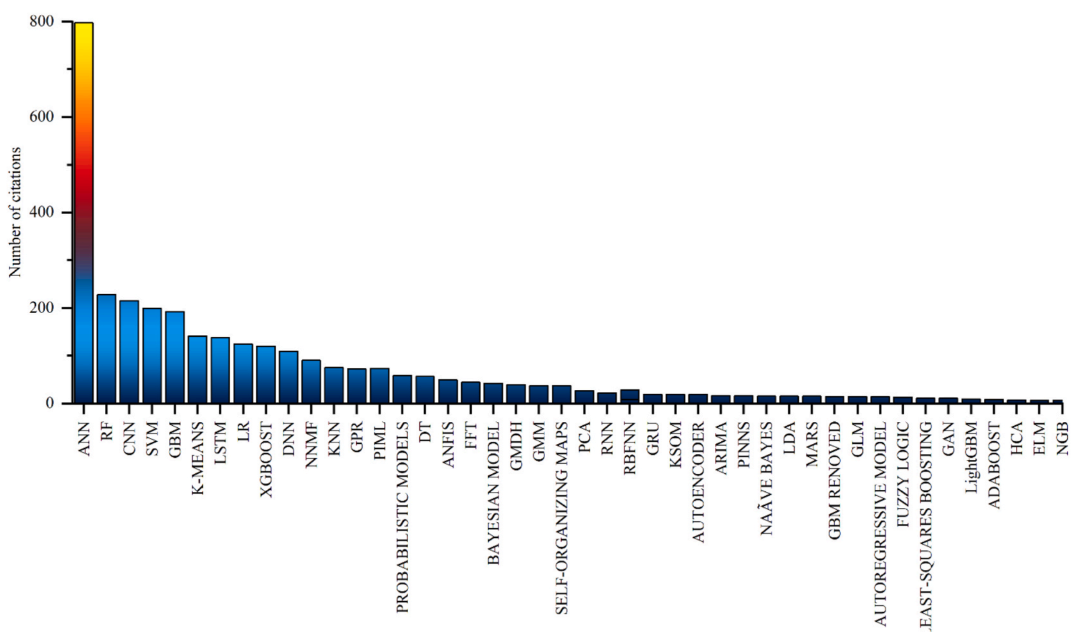

Fig. 16. Number of citations for different AI algorithms used in geothermal energy research.

comprehensive coverage of AI applications in deep geothermal energy, where 183 studies were systematically collected, categorized into eight domains and subgroups, and analyzed through a unified algorithm–input–output–performance framework. By combining this structured synthesis with trend and distribution analyses, the review not only benchmarks existing methods but also reveals critical gaps, particularly in environmental and techno-economic research.

CRediT authorship contribution statement

Danial Sheini Dashtgoli: Writing – review & editing, Writing – original draft, Visualization, Validation, Supervision, Software, Methodology, Investigation, Formal analysis, Data curation, Conceptualization. **Michela Giustiniani:** Writing – review & editing, Writing – original draft, Validation, Supervision, Methodology, Investigation, Funding acquisition. **Martina Busetti:** Writing – review & editing, Writing – original draft, Validation, Supervision, Software, Methodology, Investigation. **Claudia Cherubini:** Writing – review & editing, Writing – original draft, Validation, Supervision, Methodology, Investigation. **Giulia Alessandrini:** Writing – review & editing, Writing – original draft, Visualization, Software, Methodology, Investigation. **Guillermo Narsilio:** Writing – review & editing, Writing – original draft, Validation, Supervision, Methodology, Investigation.

Declaration of competing interest

The authors declare the following financial interests/personal relationships which may be considered as potential competing interests: Danial Sheini Dashtgoli reports financial support was provided by European Union. If there are other authors, they declare that they have no known competing financial interests or personal relationships that could have appeared to influence the work reported in this paper.

Acknowledgement

This study was carried out within the PNRR research activities of the consortium iNEST (Interconnected North-East Innovation Ecosystem) funded by the European Union Next-GenerationEU (Piano Nazionale di Ripresa e Resilienza (PNRR) – Missione 4 Componente 2, Investimento 1.5 – D.D. 1058 23/06/2022, ECS_00000043). This manuscript reflects only the Authors' views and opinions.

Data availability

No data was used for the research described in the article.

References

[1] M. Swarnkar, M. Chopra, V. Dhote, N. Nigam, K. Upadhyaya, M. Prajapati, Use of AI for development and generation of renewable energy, IEEE Renewable Energy and Sustainable E-Mobility Conference (RESEM) 2023 (2023) 1–5, https://doi.org/10.1109/RESEM57584.2023.10236136.
[2] D. Moya, C. Aldás, P. Kaparaju, Geothermal energy: Power plant technology and direct heat applications, Renew. Sustain. Energy Rev. 94 (2018) 889–901, https://doi.org/10.1016/j.rser.2018.06.047.
[3] Soltani, M., M. Kashkooli, F., Dehghani-Sanij, A. R., Kazemi, A. R., Bordbar, N., Farshchi, M. J., Elmi, M., Gharali, K., & B. Dusseault, M. (2019). A comprehensive study of geothermal heating and cooling systems. Sustainable Cities and Society, 44, 793–818. doi:10.1016/j.scs.2018.09.036.
[4] International Renewable Energy Agency (IRENA). (2024). Renewable Capacity Statistics 2024. International Renewable Energy Agency..
[5] Maslej, N., Fattorini, L., Perrault, R., Parli, V., Reuel, A., Brynjolfsson, E., Etchemendy, J., Ligett, K., Lyons, T., Manyika, J., Niebles, J. C., Shoham, Y., Wald, R., & Clark, J. (2024). Artificial Intelligence Index Report 2024 (Version 1). arXiv. doi:10.48550/ARXIV.2405.19522.
[6] G. Buster, P. Siratovich, N. Taverna, M. Rossol, J. Weers, A. Blair, J. Huggins, C. Siega, W. Mannington, A. Urgel, J. Cen, J. Quinao, R. Watt, J. Akerley, A New Modeling Framework for Geothermal Operational Optimization with Machine Learning (GOOML), In ENERGIES Vol. 14, Issue 20 (2021) MDPI, https://doi.org/10.3390/en14206852.
[7] Wardoyo, G. K., Pratama, H. B., Sutopo, Ashat, A., & Yudhistira, Y. (2021). Application of Artificial Intelligence in Forecasting Geothermal Production. IOP Conference Series: Earth and Environmental Science, 732(1), 012022. doi: 10.1088/1755-1315/732/1/012022.
[8] GeoVision: Harnessing the heat beneath our feet. (2023). U.S. Department of Energy, Geothermal Technologies Office..
[9] Khosravi, A., Syri, S., Zhao, X., & Assad, M. E. H. (2019). An artificial intelligence approach for thermodynamic modeling of geothermal based-organic Rankine cycle equipped with solar system. In GEOTHERMICS (Vol. 80, pp. 138–154). PERGAMON-ELSEVIER SCIENCE LTD. doi:10.1016/j.geothermics.2019.03.003.
[10] Ariturk, M. S. (2019). Optimizing the Production and Injection Wells Flow Rates in Geothermal Field Using Artificial Intelligence [MS, West Virginia University Libraries]. doi:10.33915/etd.3772.
[11] A. Al-Fakih, A. Abdulraheem, S. Kaka, Application of machine learning and deep learning in geothermal resource development: Trends and perspectives, Deep Underground Science and Engineering 3 (3) (2024) 286–301, https://doi.org/10.1002/dug2.12098.
[12] Ji, K., Li, H., Zhao, Y., Dai, K., Liu, S., & Tang, C. (2025). Review of artificial intelligence applications in geothermal energy extraction from hot dry rock. Deep Underground Science and Engineering, dug2.70018. doi:10.1002/dug2.70018.
[13] Okoroafor, E. R. S., Connor M. ;. Ochie, Karen Ifeoma; Nwosu, Chinedu Joseph; Gudmundsdottir, Halldora; Aljubran, Mohammad (Jabs). (2022). Machine learning in subsurface geothermal energy: Two decades in review. GEOTHERMICS. doi:10.1016/j.geothermics.2022.102401.
[14] M. Giustiniani, U. Tinivella, R. Nicolich, Reflection seismic sections across the Geothermal Province of Tuscany from reprocessing CROP profiles, Geothermics 53 (2015) 498–507, https://doi.org/10.1016/j.geothermics.2014.09.003.
[15] S. Porkhial, M. Salehpour, H. Ashraf, A. Jamali, Modeling and prediction of geothermal reservoir temperature behavior using evolutionary design of neural networks, Geothermics 53 (2015) 320–327, https://doi.org/10.1016/j.geothermics.2014.07.003.
[16] Ishitsuka, K., & Lin, W. (2023). Physics-informed neural network for inverse modeling of natural-state geothermal systems. In APPLIED ENERGY (Vol. 337). ELSEVIER SCI LTD. doi:10.1016/j.apenergy.2023.120855.
[17] Degen, D., Veroy, K., Freymark, J., Scheck-Wenderoth, M., Poulet, T., & Wellmann, F. (2021). Global sensitivity analysis to optimize basin-scale conductive model calibration-A case study from the Upper Rhine Graben. In GEOTHERMICS (Vol. 95). PERGAMON-ELSEVIER SCIENCE LTD. doi:10.1016/j.geothermics.2021.102143.
[18] F.S.T. Haklidir, M. Haklidir, Prediction of Reservoir Temperatures Using Hydrogeochemical Data, Western Anatolia Geothermal Systems (Turkey): A Machine Learning Approach, In NATURAL RESOURCES RESEARCH (Vol. 29 (4) (2020) 2333–2346.
[19] Yan, B., Gudala, M., Hoteit, H., Sun, S., Wang, W., & Jiang, L. (2024). Physics-informed machine learning for noniterative optimization in geothermal energy recovery. In APPLIED ENERGY (Vol. 365). ELSEVIER SCI LTD. doi:10.1016/j.apenergy.2024.123179.
[20] D. Sheini Dashtgoli, M. Giustiniani, M. Busetti, C. Cherubini, Artificial intelligence applications for accurate geothermal temperature prediction in the lower Friulian Plain (north-eastern Italy), J. Clean. Prod. 460 (2024) 142452, https://doi.org/10.1016/j.jclepro.2024.142452.
[21] B. Ibrahim, J.O. Konduah, I. Ahenkorah, Predicting reservoir temperature of geothermal systems in Western Anatolia, Turkey: A focus on predictive performance and explainability of machine learning models, Geothermics 112 (2023) 102727, https://doi.org/10.1016/j.geothermics.2023.102727.
[22] H. Shi, Y. Zhang, Z. Yu, Y. Yang, Reservoir temperature prediction based on characterization of water chemistry data-case study of western Anatolia, Turkey, In SCIENTIFIC REPORTS Vol. 14, Issue 1 (2024), https://doi.org/10.1038/s41598-024-59409-5.
[23] A. Acevedo-Anicasio, E. Santoyo, D. Perez-Zarate, K. Pandarinath, M. Guevara, L. Diaz-Gonzalez, GaS_GeoT: A computer program for an effective use of newly improved gas geothermometers in predicting reliable geothermal reservoir temperatures, In GEOTHERMAL ENERGY Vol. 9, Issue 1 (2021).
[24] Al-Fakih, A., & Kaka, S. (2023). Application of Artificial Intelligence in Static Formation Temperature Estimation. In ARABIAN JOURNAL FOR SCIENCE AND ENGINEERING (Vol. 48, Issue 12, pp. 16791–16804). SPRINGER HEIDELBERG. doi:10.1007/s13369-023-08096-x.
[25] F. Yang, R. Zhu, X. Zhou, T. Zhan, X. Wang, J. Dong, L. Liu, Y. Ma, Y. Su, Artificial neural network based prediction of reservoir temperature: A case study of Lindian geothermal field, Songliao Basin, NE China. Geothermics 106 (2022) 102547, https://doi.org/10.1016/j.geothermics.2022.102547.
[26] E. Gurgenc, O. Altay, E.V. Altay, AOSMA-MLP: A Novel Method for Hybrid Metaheuristics Artificial Neural Networks and a New Approach for Prediction of Geothermal Reservoir Temperature, In APPLIED SCIENCES-BASEL Vol. 14, Issue 8 (2024) MDPI, https://doi.org/10.3390/app14083534.
[27] Altay, E. V., Gurgenc, E., Altay, O., & Dikici, A. (2022). Hybrid artificial neural network based on a metaheuristic optimization algorithm for the prediction of reservoir temperature using hydrogeochemical data of different geothermal areas in Anatolia (Turkey). In GEOTHERMICS (Vol. 104). PERGAMON-ELSEVIER SCIENCE LTD. doi:10.1016/j.geothermics.2022.102476.
[28] Jiang, Z., Zhang, S., Turnadge, C., & Xu, T. (2021). Combining autoencoder neural network and Bayesian inversion to estimate heterogeneous permeability distributions in enhanced geothermal reservoir: Model development and verification. In GEOTHERMICS (Vol. 97). PERGAMON-ELSEVIER SCIENCE LTD. doi:10.1016/j.geothermics.2021.102262.
[29] B. Yan, C. Li, Z. Tariq, K. Zhang, Estimation of heterogeneous permeability using pressure derivative data through an inversion neural network inspired by the Fast Marching Method, In GEOENERGY SCIENCE AND ENGINEERING Vol. 228 (2023).
[30] Fathi, E., Carr, T. R., Adenan, M. F., Panetta, B., Kumar, A., & Carney, B. J. (2022). High-quality fracture network mapping using high frequency logging while drilling (LWD) data: MSEEL case study. In MACHINE LEARNING WITH APPLICATIONS (Vol. 10). ELSEVIER. doi:10.1016/j.mlwa.2022.100421.
[31] M. Ntibahanana, M. Luemba, K. Tondozi, Enhancing reservoir porosity prediction from acoustic impedance and lithofacies using a weighted ensemble deep learning approach, In APPLIED COMPUTING AND GEOSCIENCES 16 (2022).
[32] A. Suzuki, K. Fukui, S. Onodera, J. Ishizaki, T. Hashida, Data-Driven Geothermal Reservoir Modeling: Estimating Permeability Distributions by Machine Learning, In GEOSCIENCES Vol. 12, Issue 3 (2022) MDPI, https://doi.org/10.3390/geosciences12030130.
[33] H. Zhang, W. Wu, DBN with IQPSO Algorithm for Permeability Prediction: A Case Study of the Lizhai Geothermal Field, Zhangye Basin (Northern China), In NATURAL RESOURCES RESEARCH (Vol. 32 (5) (2023) 1941–1957.
[34] J. Song, M. Ntibahanana, M. Luemba, K. Tondozi, G. Imani, Ensemble Deep Learning-Based Porosity Inversion From Seismic Attributes, In IEEE ACCESS 11 (2023) 8761–8772, https://doi.org/10.1109/ACCESS.2023.3239688.
[35] M. Pal, P. Makauskas, S. Malik, Upscaling Porous Media Using Neural Networks: A Deep Learning Approach to Homogenization and Averaging, In PROCESSES Vol. 11, Issue 2 (2023) MDPI, https://doi.org/10.3390/pr11020601.
[36] Zou, C., Zhao, L., Xu, M., Chen, Y., & Geng, J. (2021). Porosity Prediction With Uncertainty Quantification From Multiple Seismic Attributes Using Random Forest. In JOURNAL OF GEOPHYSICAL RESEARCH-SOLID EARTH (Vol. 126, Issue 7). AMER GEOPHYSICAL UNION. doi:10.1029/2021JB021826.
[37] Yasin, Q., Ding, Y., Du, Q., Thanh, H. V., & Liu, B. (2024). Fault and fracture network characterization using soft computing techniques: Application to geologically complex and deeply-buried geothermal reservoirs. In GEOMECHANICS AND GEOPHYSICS FOR GEO-ENERGY AND GEO-RESOURCES (Vol. 10, Issue 1). SPRINGER HEIDELBERG. doi:10.1007/s40948-024-00792-8.
[38] Hawkins, A. J., Fox, D. B., Koch, D. L., Becker, M. W., & Tester, J. W. (2020). Predictive Inverse Model for Advective Heat Transfer in a Short-Circuited Fracture: Dimensional Analysis, Machine Learning, and Field Demonstration. In WATER RESOURCES RESEARCH (Vol. 56, Issue 11). AMER GEOPHYSICAL UNION. doi:Li et al.
[39] Li, Y., Juliusson, E., Palsson, H., Stefansson, H., & Valfells, A. (2017). Machine learning for creation of generalized lumped parameter tank models of low temperature geothermal reservoir systems. In GEOTHERMICS (Vol. 70, pp. 62–84). PERGAMON-ELSEVIER SCIENCE LTD. doi:10.1016/j.geothermics.2017.05.009.
[40] V. Starikov, A. Shchipanov, V. Demyanov, K. Muradov, Feature extraction and pattern recognition in time-lapse pressure transient responses, In GEOENERGY SCIENCE AND ENGINEERING 242 (2024).

[41] Yan, B., Harp, D. R., Chen, B., & Pawar, R. (2022). A physics-constrained deep learning model for simulating multiphase flow in 3D heterogeneous porous media. In FUEL (Vol. 313). ELSEVIER SCI LTD. doi:10.1016/j.fuel.2021.122693.
[42] E. Maldonado-Cruz, M.J. Pyrcz, Fast evaluation of pressure and saturation predictions with a deep learning surrogate flow model, In JOURNAL OF PETROLEUM SCIENCE AND ENGINEERING 212 (2022).
[43] Dashti, A., Stadelmann, T., & Kohl, T. (2024). Machine learning for robust structural uncertainty quantification in fractured reservoirs. In GEOTHERMICS (Vol. 120). PERGAMON-ELSEVIER SCIENCE LTD. doi:10.1016/j.geothermics.2024.103012.
[44] Bassam, A., Alvarez del Castillo, A., Garcia-Valladares, O., & Santoyo, E. (2015). Determination of pressure drops in flowing geothermal wells by using artificial neural networks and wellbore simulation tools. In APPLIED THERMAL ENGINEERING (Vol. 75, Issue SI, pp. 1217–1228). PERGAMON-ELSEVIER SCIENCE LTD. doi:10.1016/j.applthermaleng.2014.05.048.
[45] Gudala, M., & Govindarajan, S. K. (2021). Numerical investigations on a geothermal reservoir using fully coupled thermo-hydro-geomechanics with integrated RSM-machine learning and ARIMA models. In GEOTHERMICS (Vol. 96). PERGAMON-ELSEVIER SCIENCE LTD. doi:10.1016/j.geothermics.2021.102174.
[46] Y. Yang, Y. Zhang, Y. Cheng, Z. Lei, X. Gao, Y. Huang, Y. Ma, Using one-dimensional convolutional neural networks and data augmentation to predict thermal production in geothermal fields, In JOURNAL OF CLEANER PRODUCTION 387 (2023), https://doi.org/10.1016/j.jclepro.2023.135879.
[47] D. Duplyakin, K.F. Beckers, D.L. Siler, M.J. Martin, H.E. Johnston, Modeling Subsurface Performance of a Geothermal Reservoir Using Machine Learning, In ENERGIES Vol. 15, Issue 3 (2022) MDPI, https://doi.org/10.3390/en15030967.
[48] J. Ullah, H. Li, H.-J. Forster, R.M. Abdalla, M. Ehsan, M. Faisal, Harvesting Earth's heat: A deep learning Odyssey for reservoir characterization and sustainable geothermal energy management, In GEOENERGY SCIENCE AND ENGINEERING Vol. 238 (2024) ELSEVIER, https://doi.org/10.1016/j.geoen.2024.212921.
[49] Jiang, A., Qin, Z., Faulder, D., Cladouhos, T. T., & Jafarpour, B. (2022). Recurrent neural networks for short-term and long-term prediction of geothermal reservoirs. In GEOTHERMICS (Vol. 104). PERGAMON-ELSEVIER SCIENCE LTD. doi:10.1016/j.geothermics.2022.102439.
[50] Singh, U. K., Tiwari, R. K., & Singh, S. B. (2013). Neural network modeling and prediction of resistivity structures using VES Schlumberger data over a geothermal area. In COMPUTERS & GEOSCIENCES (Vol. 52, pp. 246–257). PERGAMON-ELSEVIER SCIENCE LTD. doi:10.1016/j.cageo.2012.09.018.
[51] Singh, U., Tiwari, R., & Singh, S. (2005). One-dimensional inversion of geo-electrical resistivity sounding data using artificial neural networks—A case study. In COMPUTERS & GEOSCIENCES (Vol. 31, Issue 1, pp. 99–108). PERGAMON-ELSEVIER SCIENCE LTD. doi:10.1016/j.cageo.2004.09.014.
[52] S. Zhou, Y. Wei, P. Lu, G. Yu, S. Wang, J. Jiao, P. Yu, J. Zhao, A Deep Learning Gravity Inversion Method Based on a Self-Constrained Network and Its Application. In REMOTE SENSING Vol. 16, Issue 6 (2024) MDPI, https://doi.org/10.3390/rs16060995.
[53] R. Liu, S. Misra, Machine learning assisted detection and localization of mechanical discontinuity, In INTERNATIONAL JOURNAL OF FRACTURE (Vol. 236 (2) (2022) 219–234.
[54] D.L. Siler, J.D. Pepin, V.V. Vesselinov, M.K. Mudunuru, B. Ahmmed, Machine learning to identify geologic factors associated with production in geothermal fields: A case-study using 3D geologic data, Brady geothermal field, Nevada, In GEOTHERMAL ENERGY Vol. 9, Issue 1 (2021).
[55] Jiao, J., Dong, S., Zhou, S., Zeng, Z., & Lin, T. (2024). 3-D Gravity and Magnetic Joint Inversion Based on Deep Learning Combined With Measurement Data Constraint. In IEEE TRANSACTIONS ON GEOSCIENCE AND REMOTE SENSING (Vol. 62). IEEE-INST ELECTRICAL ELECTRONICS ENGINEERS INC. doi:10.1109/TGRS.2023.3339303.
[56] N. Collard, T. Faney, P.A. Teboul, P. Bachaud, M.C. Cacas-Stentz, C. Gout, Machine learning model predicting hydrothermal dolomitisation for future coupling of basin modelling and geochemical simulations, In CHEMICAL GEOLOGY 637 (2023).
[57] Pang, Y., Shi, B., Guo, X., Zhang, X., Wen, Y., Yang, G., & Sun, X. (2023). Machine learning algorithm optimization for intelligent prediction of rock thermal conductivity: A case study from a whole-cored scientific drilling borehole. In GEOTHERMICS (Vol. 111). PERGAMON-ELSEVIER SCIENCE LTD. doi:10.1016/j.geothermics.2023.102711.
[58] J. Ullah, H. Li, U. Ashraf, P. Heping, M. Ali, M. Ehsan, M. Asad, A. Anees, T. Ren, Knowledge-based machine learning for mineral classification in a complex tectonic regime of Yingxiu-Beichuan fault zone, Sichuan basin, In GEOENERGY SCIENCE AND ENGINEERING Vol. 229 (2023).
[59] R. Boiger, S.V. Churakov, I.B. Llagaria, G. Kosakowski, R. Wust, N.I. Prasianakis, Direct mineral content prediction from drill core images via transfer learning, In SWISS JOURNAL OF GEOSCIENCES Vol. 117, Issue 1 (2024), https://doi.org/10.1186/s00015-024-00458-3.
[60] Hu, K., Liu, X., Chen, Z., & Grasby, S. E. (2023). Mineralogical Characterization From Geophysical Well Logs Using a Machine Learning Approach: Case Study for the Horn River Basin, Canada. In EARTH AND SPACE SCIENCE (Vol. 10, Issue 12). AMER GEOPHYSICAL UNION. doi:10.1029/2023EA003084.
[61] Bauer, K., Munoz, G., & Moeck, I. (2012). Pattern recognition and lithological interpretation of collocated seismic and magnetotelluric models using self-organizing maps. In GEOPHYSICAL JOURNAL INTERNATIONAL (Vol. 189, Issue 2, pp. 984–998). OXFORD UNIV PRESS. doi:10.1111/j.1365-246X.2012.05402.x.
[62] Feng, R. (2020a). Lithofacies classification based on a hybrid system of artificial neural networks and hidden Markov models. In GEOPHYSICAL JOURNAL INTERNATIONAL (Vol. 221, Issue 3, pp. 1484–1498). OXFORD UNIV PRESS. doi:10.1093/gji/ggaa083.
[63] S. Chopra, R.K. Sharma, K. Bredesen, T. Ha, K.J. Marfurt, Seismic characterization of a Triassic-Jurassic deep geothermal sandstone reservoir, onshore Denmark, using unsupervised machine learning techniques, In INTERPRETATION-A JOURNAL OF SUBSURFACE CHARACTERIZATION (Vol. 9 (4) (2021), https://doi.org/10.1190/INT-2021-0091.1.
[64] Ullah, J., Li, H., Ashraf, U., Ehsan, M., & Asad, M. (2023). A multidisciplinary approach to facies evaluation at regional level using well log analysis, machine learning, and statistical methods. In GEOMECHANICS AND GEOPHYSICS FOR GEO-ENERGY AND GEO-RESOURCES (Vol. 9, Issue 1). SPRINGER HEIDELBERG. doi:10.1007/s40948-023-00689-y.
[65] G. Buono, S. Caliro, G. Macedonio, V. Allocca, F. Gamba, L. Pappalardo, Exploring microstructure and petrophysical properties of microporous volcanic rocks through 3D multiscale and super-resolution imaging, In SCIENTIFIC REPORTS Vol. 13, Issue 1 (2023), https://doi.org/10.1038/s41598-023-33687-x.
[66] Chen, Y., & Zhang, D. (2020). Physics-Constrained Deep Learning of Geomechanical Logs. In IEEE TRANSACTIONS ON GEOSCIENCE AND REMOTE SENSING (Vol. 58, Issue 8, pp. 5932–5943). IEEE-INST ELECTRICAL ELECTRONICS ENGINEERS INC. doi:10.1109/TGRS.2020.2973171.
[67] Ali, M., Zhu, P., Jiang, R., Huolin, M., Ehsan, M., Hussain, W., Zhang, H., Ashraf, U., & Ullaah, J. (2023). Reservoir characterization through comprehensive modeling of elastic logs prediction in heterogeneous rocks using unsupervised clustering and class-based ensemble machine learning. In APPLIED SOFT COMPUTING (Vol. 148). ELSEVIER. doi:10.1016/j.asoc.2023.110843.
[68] Li, H., & Misra, S. (2021). Robust machine-learning workflow for subsurface geomechanical characterization and comparison against popular empirical correlations. In EXPERT SYSTEMS WITH APPLICATIONS (Vol. 177). PERGAMON-ELSEVIER SCIENCE LTD. doi:10.1016/j.eswa.2021.114942.
[69] R. Feng, Unsupervised learning elastic rock properties from pre-stack seismic data, In JOURNAL OF PETROLEUM SCIENCE AND ENGINEERING 192 (2020).
[70] Gao, S., Xu, M., Zhao, L., Chen, Y., & Geng, J. (2023). Seismic predictions of fluids via supervised deep learning: Incorporating various class-rebalance strategies. In GEOPHYSICS (Vol. 88, Issue 4, pp. M185–M200). SOC EXPLORATION GEOPHYSICISTS - SEG. doi:10.1190/GEO2022-0363.1.
[71] Suzuki, A., Shi, S., Sakai, T., Fukui, K., Onodera, S., Ishizaki, J., & Hashida, T. (2024). Automated parameter estimation for geothermal reservoir modeling using machine learning. In RENEWABLE ENERGY (Vol. 224). PERGAMON-ELSEVIER SCIENCE LTD. doi:10.1016/j.renene.2024.120243.
[72] D. Degen, K. Veroy, M. Scheck-Wenderoth, F. Wellmann, Crustal-scale thermal models: Revisiting the influence of deep boundary conditions, In ENVIRONMENTAL EARTH SCIENCES Vol. 81, Issue 3 (2022).
[73] Y.D. Wang, T. Chung, R.T. Armstrong, P. Mostaghimi, ML-LBM: Predicting and Accelerating Steady State Flow Simulation in Porous Media with Convolutional Neural Networks, In TRANSPORT IN POROUS MEDIA Vol. 138(1 (2021) 49–75.
[74] Taherdangkoo, R., Nagel, T., Tang, A. M., Pereira, J.-M., & Butscher, C. (2022). Coupled Hydro-Mechanical Modeling of Swelling Processes in Clay-Sulfate Rocks. In ROCK MECHANICS AND ROCK ENGINEERING (Vol. 55, Issue 12, pp. 7489–7501). SPRINGER WIEN. doi:10.1007/s00603-022-03039-8.
[75] Yin, T., Li, Q., Hu, Y., Li, G., & Yu, S. (2022). Ensemble Learning-Aided Hydrothermal Coupling Investigation on Dam Impoundment Impact: A Case Study of the Xiluodu Project in China. In LITHOSPHERE (Vol. 2022, Issue SI). GEOSCIENCEWORLD. doi:discovery.
[76] G. Jin, H. Xing, R. Zhang, Z. Guo, J. Liu, Data-driven discovery of governing equations for transient heat transfer analysis, In COMPUTATIONAL GEOSCIENCES (Vol. 26 (3) (2022) 613–631.
[77] K. Bruss, R. Kim, T.A. Myers, J.-C. Su, A. Mazumdar, Localization of Thermal Wellbore Defects Using Machine Learning, In JOURNAL OF ENERGY RESOURCES TECHNOLOGY-TRANSACTIONS OF THE ASME Vol. 144, Issue 9 (2022) ASME, https://doi.org/10.1115/1.4053516.
[78] Chen, Z., Grasby, S. E., Yuan, W., & Liu, X. (2023). Ground surface temperature monitoring data analysis and applications to geothermal exploration in volcanic areas, Mount Meager, western Canada. In GEOTHERMICS (Vol. 108). PERGAMON-ELSEVIER SCIENCE LTD. doi:10.1016/j.geothermics.2022.102610.
[79] Rezaei, M., Kelishami, S. B. A., & Sangin, S. (2024). Iran's comprehensive heat flow map generated by the Random Forest method and the Sequential Gaussian Simulation. In GEOTHERMICS (Vol. 118). PERGAMON-ELSEVIER SCIENCE LTD. doi:10.1016/j.geothermics.2024.102915.
[80] Mejia-Fragoso, J. C. ; F., Manuel A. ;. Bernal-Olaya, Rocio. (2024). Predicting the geothermal gradient in Colombia: A machine learning approach. GEOTHERMICS. doi:10.1016/j.geothermics.2024.103074.
[81] W. Colgan, A. Wansing, K. Mankoff, M. Losing, J. Hopper, K. Louden, J. Ebbing, F. G. Christiansen, T. Ingeman-Nielsen, L.C. Liljedahl, J.A. MacGregor, A. Hjartarson, S. Bernstein, N.B. Karlsson, S. Fuchs, J. Hartikainen, J. Liakka, R. S. Fausto, D. Dahl-Jensen, A. Lokkegaard, Greenland Geothermal Heat Flow Database and Map (Version 1), In EARTH SYSTEM SCIENCE DATA Vol. 14(5 (2022) 2209–2238, https://doi.org/10.5194/essd-14-2209-2022.
[82] Zhang, S., & Ritzwoller, M. H. (2024). Applying machine learning to characterize and extrapolate the relationship between seismic structure and surface heat flow. In GEOPHYSICAL JOURNAL INTERNATIONAL (Vol. 238, Issue 3, pp. 1201–1222). OXFORD UNIV PRESS. doi:heat flow.
[83] J. He, K. Li, X. Wang, N. Gao, X. Mao, L. Jia, A Machine Learning Methodology for Predicting Geothermal Heat Flow in the Bohai Bay Basin, China, Natural Resources Research 31 (1) (2022) 237–260, https://doi.org/10.1007/s11053-021-10002-x.

[84] K. Ishitsuka, Y. Kobayashi, N. Watanabe, Y. Yamaya, E. Bjarkason, A. Suzuki, T. Mogi, H. Asanuma, T. Kajiwara, T. Sugimoto, R. Saito, Bayesian and Neural Network Approaches to Estimate Deep Temperature Distribution for Assessing a Supercritical Geothermal System: Evaluation Using a Numerical Model, In NATURAL RESOURCES RESEARCH Vol. 30(5 (2021) 3289–3314.
[85] J. Chen, L. Jia, J. Zhang, Y. Feng, X. Zhao, R. Tao, Super-Resolution for Land Surface Temperature Retrieval Images via Cross-Scale Diffusion Model Using Reference Images, In REMOTE SENSING Vol. 16, Issue 8 (2024) MDPI, https://doi.org/10.3390/rs16081356.
[86] A. Shahdi, S. Lee, A. Karpatne, B. Nojabaei, Exploratory analysis of machine learning methods in predicting subsurface temperature and geothermal gradient of Northeastern United States, Geotherm. Energy 9 (1) (2021) 18, https://doi.org/10.1186/s40517-021-00200-4.
[87] Loesing, M., & Ebbing, J. (2021). Predicting Geothermal Heat Flow in Antarctica With a Machine Learning Approach. In JOURNAL OF GEOPHYSICAL RESEARCH-SOLID EARTH (Vol. 126, Issue 6). AMER GEOPHYSICAL UNION. doi:10.1029/2020JB021499.
[88] S. Mirfallah Lialestani, D. Parcerisa, M. Himi, A. Abbaszadeh Shahri, Generating 3D Geothermal Maps in Catalonia, Spain Using a Hybrid Adaptive Multitask Deep Learning Procedure, Energies 15 (13) (2022) 4602, https://doi.org/10.3390/en15134602.
[89] Bai, L., Li, J., Zeng, Z., & Tao, D. (2023). Prediction of Terrestrial Heat Flow in Songliao Basin Based on Deep Neural Network. In EARTH AND SPACE SCIENCE (Vol. 10, Issue 12). AMER GEOPHYSICAL UNION. doi:10.1029/2023EA003186.
[90] F. Alqahtani, M. Ehsan, M. Abdulfarraj, E. Aboud, Z. Naseer, N.N. El-Masry, M. F. Abdelwahed, Machine Learning Techniques in Predicting Bottom Hole Temperature and Remote Sensing for Assessment of Geothermal Potential in the Kingdom of Saudi Arabia, In SUSTAINABILITY Vol. 15, Issue 17 (2023) MDPI, https://doi.org/10.3390/su151712718.
[91] M.J. Aljubran, R.N. Horne, Thermal Earth model for the conterminous United States using an interpolative physics-informed graph neural network, In GEOTHERMAL ENERGY Vol. 12, Issue 1 (2024).
[92] A. Previati, G. Crosta, On groundwater flow and shallow geothermal potential: A surrogate model for regional scale analyses, In SCIENCE OF THE TOTAL ENVIRONMENT 912 (2024).
[93] J. Moraga, H.S. Duzgun, M. Cavur, H. Soydan, The Geothermal Artificial Intelligence for geothermal exploration, Renew. Energy 192 (2022) 134–149, https://doi.org/10.1016/j.renene.2022.04.113.
[94] Cheng, X., Qiao, W., Hu, D., Qi, Z., Feng, P., & Tinti, F. (2024). Quality analysis of machine learning methods applied to the geothermal potential assessment: A case study. In ENERGY SOURCES PART A-RECOVERY UTILIZATION AND ENVIRONMENTAL EFFECTS (Vol. 46, Issue 1, pp. 854–871). TAYLOR & FRANCIS INC. doi:10.1080/15567036.2023.2291451.
[95] Yalcin, M., Sari, F., & Yildiz, A. (2023). Exploration of potential geothermal fields using MAXENT and AHP: A case study of the Buyuk Menderes Graben. In GEOTHERMICS (Vol. 114). PERGAMON-ELSEVIER SCIENCE LTD. doi:10.1016/j.geothermics.2023.102792.
[96] Mordensky, S. P., Lipor, J. J., DeAngelo, J., Burns, E. R., & Lindsey, C. R. (2023). When less is more: How increasing the complexity of machine learning strategies for geothermal energy assessments may not lead toward better estimates. In GEOTHERMICS (Vol. 110). PERGAMON-ELSEVIER SCIENCE LTD. doi:10.1016/j.geothermics.2023.102662.
[97] Smith, C. M., Faulds, J. E., Brown, S., Coolbaugh, M., DeAngelo, J., Glen, J. M., Burns, E. R., Siler, D. L., Treitel, S., Mlawsky, E., Fehler, M., Gu, C., & Ayling, B. F. (2023). Exploratory analysis of machine learning techniques in the Nevada geothermal play fairway analysis. In GEOTHERMICS (Vol. 111). PERGAMON-ELSEVIER SCIENCE LTD. doi:10.1016/j.geothermics.2023.102693.
[98] R.C. Holmes, A. Fournier, Machine Learning-Enhanced Play Fairway Analysis for Uncertainty Characterization and Decision Support in Geothermal Exploration, Energies 15 (5) (2022) 1929, https://doi.org/10.3390/en15051929.
[99] D. Assouline, N. Mohajeri, A. Gudmundsson, J.-L. Scartezzini, A machine learning approach for mapping the very shallow theoretical geothermal potential, In GEOTHERMAL ENERGY Vol. 7, Issue 1 (2019).
[100] E. Demir, M. Cavur, Y.-T. Yu, H.S. Duzgun, An Evaluation of AI Models' Performance for Three Geothermal Sites, In ENERGIES Vol. 17, Issue 13 (2024) MDPI, https://doi.org/10.3390/en17133255.
[101] Yadav, A., Yadav, K., & Sircar, A. (2021). Feedforward Neural Network for joint inversion of geophysical data to identify geothermal sweet spots in Gandhar, Gujarat, India. In ENERGY GEOSCIENCE (Vol. 2, Issue 3). KEAI PUBLISHING LTD. doi:10.1016/j.engeos.2021.01.001.
[102] Sang, X., Xue, L., & Li, X. (2021). Considering the geological significance in data preprocessing and improving the prediction accuracy of hot springs by deep learning. In OPEN GEOSCIENCES (Vol. 13, Issue 1, pp. 482–496). DE GRUYTER POLAND SP Z O O. doi:10.1515/geo-2020-0237.
[103] Ahmmed, B., & Vesselinov, V. V. (2022). Machine learning and shallow groundwater chemistry to identify geothermal prospects in the Great Basin, USA. In RENEWABLE ENERGY (Vol. 197, pp. 1034–1048). PERGAMON-ELSEVIER SCIENCE LTD. doi:10.1016/j.renene.2022.08.024.
[104] Martin-Martin, M., Bullejos, M., Cabezas, D., & Alcala, F. J. (2023). Using python libraries and k-Nearest neighbors algorithms to delineate syn-sedimentary faults in sedimentary porous media. In MARINE AND PETROLEUM GEOLOGY (Vol. 153). ELSEVIER SCI LTD. doi:10.1016/j.marpetgeo.2023.106283.
[105] Hu, Y., Wei, X., Wu, X., Sun, J., Huang, Y., & Chen, J. (2024). Three-dimensional cooperative inversion of airborne magnetic and gravity gradient data using deep-learning techniques. In GEOPHYSICS (Vol. 89, Issue 1, pp. WB67–WB79). SOC EXPLORATION GEOPHYSICISTS - SEG. doi:10.1190/GEO2023-0225.1.
[106] I. Kaftan, M. Salk, Y. Senol, Evaluation of gravity data by using artificial neural networks case study: Seferihisar geothermal area (Western Turkey), In JOURNAL OF APPLIED GEOPHYSICS (Vol. 75 (4) (2011) 711–718.
[107] Yao, Y., Zhang, X., Wang, K., Ma, Y., Li, Y., Li, J., & Xv, H. (2024). Recovering 3D Basin Basement Relief Using High-Precision Magnetic Data Through Random Forest Regression Algorithm: A Case Study of Tianzhen-Yanggao Sag in Datong Basin. In EARTH AND SPACE SCIENCE (Vol. 11, Issue 6). AMER GEOPHYSICAL UNION. doi:10.1029/2023EA003493.
[108] Y. Xiong, M. Zhu, Y. Li, K. Huang, Y. Chen, J. Liao, Recognition of Geothermal Surface Manifestations: A Comparison of Machine Learning and Deep Learning, Energies 15 (8) (2022) 2913, https://doi.org/10.3390/en15082913.
[109] M.A. Engle, C.W. Nye, G. Neupane, S.A. Quillinan, J.F. McLaughlin, T. McLing, J. A. Martin-Fernandez, Predicting Rare Earth Element Potential in Produced and Geothermal Waters of the United States via Emergent Self-Organizing Maps, In ENERGIES Vol. 15, Issue 13 (2022) MDPI, https://doi.org/10.3390/en15134555.
[110] G. Tamburello, G. Chiodini, G. Ciotoli, M. Procesi, D. Rouwet, L. Sandri, N. Carbonara, C. Masciantonio, Global thermal spring distribution and relationship to endogenous and exogenous factors, In NATURE COMMUNICATIONS Vol. 13, Issue 1 (2022), https://doi.org/10.1038/s41467-022-34115-w.
[111] Jevinani, M. R., Dehkordi, B. H., Ferguson, I. J., & Rohban, M. H. (2024). Deep learning-based 1-D magnetotelluric inversion: Performance comparison of architectures. In EARTH SCIENCE INFORMATICS (Vol. 17, Issue 2, pp. 1663–1677). SPRINGER HEIDELBERG. doi:10.1007/s12145-024-01233-6.
[112] Xu, K., Liang, S., Lu, Y., & Hu, Z. (2024). Magnetotelluric Data Inversion Based on Deep Learning With the Self-Attention Mechanism. In IEEE TRANSACTIONS ON GEOSCIENCE AND REMOTE SENSING (Vol. 62). IEEE-INST ELECTRICAL ELECTRONICS ENGINEERS INC. doi:10.1109/TGRS.2024.3411062.
[113] Rezvanbehbahani, S., Stearns, L. A., Kadivar, A., Walker, J. D., & van der Veen, C. J. (2017). Predicting the Geothermal Heat Flux in Greenland: A Machine Learning Approach. In GEOPHYSICAL RESEARCH LETTERS (Vol. 44, Issue 24, pp. 12271–12279). AMER GEOPHYSICAL UNION. doi:10.1002/2017GL075661.
[114] He, R., Jia, L., & Zhang, J. (2023). An automatic extraction method for geothermal radiation sources based on an LST retrieval algorithm and semantic network. In NATURAL GAS INDUSTRY B (Vol. 10, Issue 5, pp. 419–435). KEAI PUBLISHING LTD. doi:10.1016/j.ngib.2023.09.003.
[115] Ouzzaouit, L. A., EL Ouassif, B., Idri, A., Qarbous, A., Barich, A., Weisenberger, T. B., & Boudad, L. (2023). Geothermal flow in Northern Morocco: A machine learning approach. In JOURNAL OF AFRICAN EARTH SCIENCES (Vol. 205). PERGAMON-ELSEVIER SCIENCE LTD. doi:10.1016/j.jafrearsci.2023.104995.
[116] Vesselinov, V. V., Ahmmed, B., Mudunuru, M. K., Pepin, J. D., Burns, E. R., Siler, D. L., Karra, S., & Middleton, R. S. (2022). Discovering hidden geothermal signatures using non-negative matrix factorization with customized k-means clustering. In GEOTHERMICS (Vol. 106). PERGAMON-ELSEVIER SCIENCE LTD. doi:10.1016/j.geothermics.2022.102576.
[117] G. Santamaría-Bonfil, E. Santoyo, L. Díaz-González, G. Arroyo-Figueroa, Equivalent imputation methodology for handling missing data in compositional geochemical databases of geothermal fluids, Geothermics 104 (2022) 102440, https://doi.org/10.1016/j.geothermics.2022.102440.
[118] C. Li, Y. Zhang, X. Ren, Modeling Hourly Soil Temperature Using Deep BiLSTM Neural Network, In ALGORITHMS Vol. 13, Issue 7 (2020) MDPI, https://doi.org/10.3390/a13070173.
[119] M.K. Mudunuru, B. Ahmmed, E. Rau, V.V. Vesselinov, S. Karra, Machine Learning for Geothermal Resource Exploration in the Tularosa Basin, New Mexico. Energies 16 (7) (2023) 3098, https://doi.org/10.3390/en16073098.
[120] Z. Xue, K. Zhang, C. Zhang, H. Ma, Z. Chen, Comparative data-driven enhanced geothermal systems forecasting models: A case study of Qiabuqia field in China, Energy 280 (2023) 128255, https://doi.org/10.1016/j.energy.2023.128255.
[121] Podlasek, S., Jankowski, M., Balazy, P., Lalik, K., & Figaj, R. (2024). Application of ANN control algorithm for optimizing performance of a hybrid ORC power plant. In ENERGY (Vol. 306). PERGAMON-ELSEVIER SCIENCE LTD. doi:10.1016/j.energy.2024.132082.
[122] Langiu, M., Dahmen, M., & Mitsos, A. (2022). Simultaneous optimization of design and operation of an air-cooled geothermal ORC under consideration of multiple operating points. In COMPUTERS & CHEMICAL ENGINEERING (Vol. 161). PERGAMON-ELSEVIER SCIENCE LTD. doi:10.1016/j.compchemeng.2022.107745.
[123] T. Hai, M.A. Ali, R. Chaturvedi, S.F. Almojil, A.I. Almohana, A.F. Alali, K. T. Almoalimi, F.Q.A. Alyousuf, M.A. Shamseldin, A low-temperature driven organic Rankine cycle for waste heat recovery from a geothermal driven Kalina cycle: 4E analysis and optimization based on artificial intelligence, In SUSTAINABLE ENERGY TECHNOLOGIES AND ASSESSMENTS Vol. 55 (2023).
[124] Khanmohammadi, S., Musharavati, F., & Tariq, R. (2022). A framework of data modeling and artificial intelligence for environmental-friendly energy system: Application of Kalina cycle improved with fuel cell and thermoelectric module. In PROCESS SAFETY AND ENVIRONMENTAL PROTECTION (Vol. 164, pp. 499–516). ELSEVIER. doi:10.1016/j.psep.2022.06.029.
[125] Abrasaldo, P. M. B., Zarrouk, S. J., & Kempa-Liehr, A. W. (2023). Characterising and predicting low discharge pressure events in less permeable geothermal production wells. In GEOTHERMICS (Vol. 112). PERGAMON-ELSEVIER SCIENCE LTD. doi:10.1016/j.geothermics.2023.102756.
[126] Huster, W. R., Schweidtmann, A. M., & Mitsos, A. (2020). Globally optimal working fluid mixture composition for geothermal power cycles. In ENERGY (Vol. 212). PERGAMON-ELSEVIER SCIENCE LTD. doi:10.1016/j.energy.2020.118731.
[127] Ding, S., Zhang, H., Tao, Z., & Li, R. (2022). Integrating data decomposition and machine learning methods: An empirical proposition and analysis for renewable

energy generation forecasting. In EXPERT SYSTEMS WITH APPLICATIONS (Vol. 204). PERGAMON-ELSEVIER SCIENCE LTD. doi:10.1016/j.eswa.2022.117635.
[128] Yilmaz, C., Koyuncu, I., Alcin, M., & Tuna, M. (2019). Artificial Neural Networks based thermodynamic and economic analysis of a hydrogen production system assisted by geothermal energy on Field Programmable Gate Array. In INTERNATIONAL JOURNAL OF HYDROGEN ENERGY (Vol. 44, Issue 33, pp. 17443–17459). PERGAMON-ELSEVIER SCIENCE LTD. doi:10.1016/j.ijhydene.2019.05.049.
[129] Li, S., Leng, Y., Chaturvedi, R., Dutta, A. K., Abdullaeva, B. S., & Fouad, Y. (2024). Sustainable freshwater/energy supply through geothermal-centered layout tailored with humidification-dehumidification desalination unit; Optimized by regression machine learning techniques. In ENERGY (Vol. 303). PERGAMON-ELSEVIER SCIENCE LTD. doi:10.1016/j.energy.2024.131919.
[130] Yang, R., Wang, Y., Song, G., & Shi, Y. (2023). Fracturing and thermal extraction optimization methods in enhanced geothermal systems. In ADVANCES IN GEO-ENERGY RESEARCH (Vol. 9, Issue 2, pp. 136–140). Yandy Scientific Press. doi:10.46690/ager.2023.08.07.
[131] W. Zhang, J. Li, CPINNs: A coupled physics-informed neural networks for the closed-loop geothermal system, In COMPUTERS & MATHEMATICS WITH APPLICATIONS Vol. 132 (2023) 161–179.
[132] Chen, G., Jiao, J. J., Jiang, C., & Luo, X. (2024). Surrogate-assisted level-based learning evolutionary search for geothermal heat extraction optimization. In RENEWABLE & SUSTAINABLE ENERGY REVIEWS (Vol. 189, Issue B). PERGAMON-ELSEVIER SCIENCE LTD. doi:10.1016/j.rser.2023.113860.
[133] Akin, S., Kok, M. V., & Uraz, I. (2010). Optimization of well placement geothermal reservoirs using artificial intelligence. In COMPUTERS & GEOSCIENCES (Vol. 36, Issue 6, pp. 776–785). PERGAMON-ELSEVIER SCIENCE LTD. doi:10.1016/j.cageo.2009.11.006.
[134] Yang, W., Xiao, C., & Liang, X. (2024). Assessment of regional-scale geothermal production based on a hybrid deep learning model: A case study of the southern Songliao Basin, China. In RENEWABLE ENERGY (Vol. 223). PERGAMON-ELSEVIER SCIENCE LTD. doi:10.1016/j.renene.2024.120062.
[135] Wang, N., Chang, H., Kong, X.-Z., & Zhang, D. (2023). Deep learning based closed-loop well control optimization of geothermal reservoir with uncertain permeability. In RENEWABLE ENERGY (Vol. 211, pp. 379–394). PERGAMON-ELSEVIER SCIENCE LTD. doi:10.1016/j.renene.2023.04.088.
[136] Jiang, A., Qin, Z., Faulder, D., Cladouhos, T. T., & Jafarpour, B. (2023). A multiscale recurrent neural network model for predicting energy production from geothermal reservoirs. In GEOTHERMICS (Vol. 110). PERGAMON-ELSEVIER SCIENCE LTD. doi:10.1016/j.geothermics.2022.102643.
[137] Zulkarnain, Surjandari, I., Bramasta, R. R., & Laoh, E. (2019). Fault Detection System Using Machine Learning on Geothermal Power Plant. In 2019 16TH INTERNATIONAL CONFERENCE ON SERVICE SYSTEMS AND SERVICE MANAGEMENT (ICSSSM2019). IEEE..
[138] Abrasaldo, P. M. B., Zarrouk, S. J., Mudie, A., Cen, J., Siega, C., & Kempa-Liehr, A. W. (2024). Detection of abnormal operation in geothermal binary plant feed pumps using time-series analytics. In EXPERT SYSTEMS WITH APPLICATIONS (Vol. 247). PERGAMON-ELSEVIER SCIENCE LTD. doi:10.1016/j.eswa.2024.123305.
[139] Matsuzaki, H., Maruyama, T., Yoshida, A., & Amano, Y. (2023). Examination of wellhead valves operation using a machine learning model to predict steam enthalpy time-series. In 2023 62ND ANNUAL CONFERENCE OF THE SOCIETY OF INSTRUMENT AND CONTROL ENGINEERS, SICE (pp. 1493–1498). IEEE. doi:10.23919/SICE59929.2023.10354183.
[140] Cetin, M., Urkan, O. D., Hekim, M., & Cetin, E. (2024). Power generation prediction of a geothermal-thermoelectric hybrid system using intelligent models. In GEOTHERMICS (Vol. 118). PERGAMON-ELSEVIER SCIENCE LTD. doi:10.1016/j.geothermics.2023.102911.
[141] Bourhis, P., Cousin, B., Loria, A. F. R., & Laloui, L. (2021). Machine learning enhancement of thermal response tests for geothermal potential evaluations at site and regional scales. In GEOTHERMICS (Vol. 95). PERGAMON-ELSEVIER SCIENCE LTD. doi:10.1016/j.geothermics.2021.102132.
[142] Sias, Q. A., Lim, S., Gantassi, R., & Choi, Y. (2023). Implementation of Single and Multi Linear Regression for Prediction of Energy Consumption based on Previous Data of Energy Production. In 2023 INTERNATIONAL CONFERENCE ON ARTIFICIAL IN[TEL]LIGENCE IN INFORMATION AND COMMUNICATION, ICAIIC (pp. 830–832). IEEE. doi:10.1109/ICAIIC57133.2023.10066989.
[143] Xiao, C., Zhang, S., Hu, Y., Gu, X., Ma, X., Zhou, T., & Jin, J. (2024). Robust optimization of geoenergy production using data-driven deep recurrent auto-encoder and fully-connected neural network proxy. In EXPERT SYSTEMS WITH APPLICATIONS (Vol. 242). PERGAMON-ELSEVIER SCIENCE LTD. doi:10.1016/j.eswa.2023.122797.
[144] M. Picozzi, A.G. Iaccarino, Forecasting the Preparatory Phase of Induced Earthquakes by Recurrent Neural Network, In FORECASTING (Vol. 3 (1) (2021), https://doi.org/10.3390/forecast3010002.
[145] C.-C. Chien, W.F. Jenkins II, P. Gerstoft, M. Zumberge, R. Mellors, Automatic classification with an autoencoder of seismic signals on a distributed acoustic sensing cable, In COMPUTERS AND GEOTECHNICS 155 (2023), https://doi.org/10.1016/j.compgeo.2022.105223.
[146] Herrmann, M., Kraft, T., Tormann, T., Scarabello, L., & Wiemer, S. (2019). A Consistent High-Resolution Catalog of Induced Seismicity in Basel Based on Matched Filter Detection and Tailored Post-Processing. In JOURNAL OF GEOPHYSICAL RESEARCH-SOLID EARTH (Vol. 124, Issue 8, pp. 8449–8477). AMER GEOPHYSICAL UNION. doi:10.1029/2019JB017468.
[147] Gauntlett, M., Hudson, T., Kendall, J.-M., Rawlinson, N., Blundy, J., Lapins, S., Goitom, B., Hammond, J., Oppenheimer, C., & Ogubazghi, G. (2023). Seismic Tomography of Nabro Caldera, Eritrea: Insights Into the Magmatic and Hydrothermal Systems of a Recently Erupted Volcano. In JOURNAL OF GEOPHYSICAL RESEARCH-SOLID EARTH (Vol. 128, Issue 5). AMER GEOPHYSICAL UNION. doi:high-r.
[148] Cheng, F., Xia, J., Ajo-Franklin, J. B., Behm, M., Zhou, C., Dai, T., Xi, C., Pang, J., & Zhou, C. (2021). High-Resolution Ambient Noise Imaging of Geothermal Reservoir Using 3C Dense Seismic Nodal Array and Ultra-Short Observation. In JOURNAL OF GEOPHYSICAL RESEARCH-SOLID EARTH (Vol. 126, Issue 8). AMER GEOPHYSICAL UNION. doi:10.1029/2021JB021827.
[149] X. Yin, C. Jiang, F. Yin, H. Zhai, Y. Zheng, H. Wu, X. Niu, Y. Zhang, C. Jiang, J. Li, Assessment and optimization of maximum magnitude forecasting models for induced seismicity in enhanced geothermal systems: The Gonghe EGS project in Qinghai, China, In TECTONOPHYSICS 886 (2024).
[150] Prezioso, E., Sharma, N., Piccialli, F., & Convertito, V. (2022). A data-driven artificial neural network model for the prediction of ground motion from induced seismicity: The case of The Geysers geothermal field. In FRONTIERS IN EARTH SCIENCE (Vol. 10). FRONTIERS MEDIA SA. doi:10.3389/feart.2022.917608.
[151] B.K. Holtzman, A. Pate, J. Paisley, F. Waldhauser, D. Repetto, Machine learning reveals cyclic changes in seismic source spectra in Geysers geothermal field, In SCIENCE ADVANCES Vol. 4, Issue 5 (2018), https://doi.org/10.1126/sciadv.aao2929.
[152] Tary, J. B., van der Baan, M., Sutherland, B., & Eaton, D. W. (2014). Characteristics of fluid-induced resonances observed during microseismic monitoring. In JOURNAL OF GEOPHYSICAL RESEARCH-SOLID EARTH (Vol. 119, Issue 11, pp. 8207–8222). AMER GEOPHYSICAL UNION. doi:10.1002/2014JB011263.
[153] Jreij, S. F., Trainor-Guitton, W. J., Morphew, M., & Ning, I. L. C. (2021). The Value of Information From Horizontal Distributed Acoustic Sensing Compared to Multicomponent Geophones Via Machine Learning. In JOURNAL OF ENERGY RESOURCES TECHNOLOGY-TRANSACTIONS OF THE ASME (Vol. 143, Issue 1). ASME. doi:10.1115/1.4048051.
[154] Lou, Y., Wang, Y., Chen, Y., Liu, N., & Ling, D. (2024). Automatic Seismic Fault Interpretation With the Aid of Data-, Physics-, and Math-Assisted Synthetic Data Generation. In IEEE TRANSACTIONS ON GEOSCIENCE AND REMOTE SENSING (Vol. 62). IEEE-INST ELECTRICAL ELECTRONICS ENGINEERS INC. doi:10.1109/TGRS.2024.3402739.
[155] K. Gao, L. Huang, T. Cladouhos, Seismic Characterization of the Blue Mountain Geothermal Field, In ENERGIES Vol. 16, Issue 15 (2023) MDPI, https://doi.org/10.3390/en16155822.
[156] J. Yazbeck, J.B. Rundle, A Fusion of Geothermal and InSAR Data with Machine Learning for Enhanced Deformation Forecasting at the Geysers, In LAND Vol. 12, Issue 11 (2023) MDPI, https://doi.org/10.3390/land12111977.
[157] Nooshiri, N., Bean, C. J., Dahm, T., Grigoli, F., Kristjansdottir, S., Obermann, A., & Wiemer, S. (2022). A multibranch, multitarget neural network for rapid point-source inversion in a microseismic environment: Examples from the Hengill Geothermal Field, Iceland. In GEOPHYSICAL JOURNAL INTERNATIONAL (Vol. 229, Issue 2, pp. 999–1016). OXFORD UNIV PRESS. doi:10.1093/gji/ggab511.
[158] Okamoto, K., Mukuhira, Y., Darisma, D., Asanuma, H., & Moriya, H. (2024). Machine learning automatic picker for geothermal microseismicity analysis for practical procedure to reveal fine reservoir structures. In GEOTHERMICS (Vol. 116). PERGAMON-ELSEVIER SCIENCE LTD. doi:compar.
[159] Diaz, M., Kim, K. Y., Lee, J., & Shin, H.-S. (2020). Prediction of rate of penetration with data from adjacent well using artificial neural network. In P. Long & N. Dung (Eds.), GEOTECHNICS FOR SUSTAINABLE INFRASTRUCTURE DEVELOPMENT (Vol. 62, pp. 517–522). SPRINGER-VERLAG SINGAPORE PTE LTD. doi:10.1007/978-981-15-2184-3_68.
[160] Yehia, T., Gasser, M., Ebaid, H., Meehan, N., & Okoroafor, E. R. (2024). Comparative analysis of machine learning techniques for predicting drilling rate of penetration (ROP) in geothermal wells: A case study of FORGE site. In GEOTHERMICS (Vol. 121). PERGAMON-ELSEVIER SCIENCE LTD. doi:10.1016/j.geothermics.2024.103028.
[161] Feng, Z., Gani, H., Damayanti, A. D., & Gani, H. (2023). An explainable ensemble machine learning model to elucidate the influential drilling parameters based on rate of penetration prediction. In GEOENERGY SCIENCE AND ENGINEERING (Vol. 231, Issue A). ELSEVIER. doi:10.1016/j.geoen.2023.212231.
[162] M.A. Ben Aoun, T. Madarasz, Applying Machine Learning to Predict the Rate of Penetration for Geothermal Drilling Located in the Utah FORGE Site, In ENERGIES Vol. 15, Issue 12 (2022) MDPI, https://doi.org/10.3390/en15124288.
[163] Seo, W., Lee, G. W., Kim, K. Y., & Yun, T. S. (2024). Predicting rate of penetration (ROP) based on a deep learning approach: A case study of an enhanced geothermal system in Pohang, South Korea. In EARTH SCIENCE INFORMATICS (Vol. 17, Issue 1, pp. 813–824). SPRINGER HEIDELBERG. doi:10.1007/s12145-023-01149-7.
[164] Laureano-Cruces, A., & Espinosa-Paredes, G. (2005). Behavioral design to model a reactive decision of an expert in geothermal wells. In INTERNATIONAL JOURNAL OF APPROXIMATE REASONING (Vol. 39, Issue 1, pp. 1–28). ELSEVIER SCIENCE INC. doi:10.1016/j.ijar.2004.08.002.
[165] Wang, R., Kuru, E., Yan, Y., Yang, X., & Yan, X. (2022). Sensitivity analysis of factors controlling the cement hot spot temperature and the corresponding well depth using a combined CFD simulation and machine learning approach. In JOURNAL OF PETROLEUM SCIENCE AND ENGINEERING (Vol. 208, Issue D). ELSEVIER. doi:10.1016/j.petrol.2021.109617.
[166] M.S. Khaled, N. Wang, P. Ashok, E. van Oort, K. Wisian, Real-time prediction of bottom-hole circulating temperature in geothermal wells using machine learning models, In GEOENERGY SCIENCE AND ENGINEERING 238 (2024).

[167] A. Abdollahian, H. Wang, H. Liu, X. Zheng, Transfer learning for acoustic cement bond evaluation: An image classification approach using acoustic variable Density log, In GEOENERGY SCIENCE AND ENGINEERING 239 (2024).
[168] Kiran, R., Dansena, P., Salehi, S., & Rajak, V. K. (2022). Application of machine learning and well log attributes in geothermal drilling. In GEOTHERMICS (Vol. 101). PERGAMON-ELSEVIER SCIENCE LTD. doi:10.1016/j.geothermics.2022.102355.
[169] K. Chhantyal, H. Viumdal, S. Mylvaganam, Soft Sensing of Non-Newtonian Fluid Flow in Open Venturi Channel Using an Array of Ultrasonic Level SensorsAI Models and Their Validations, In SENSORS Vol. 17, Issue 11 (2017) MDPI, https://doi.org/10.3390/s17112458.
[170] Ling, W., Abed, A. M., Farouk, N., Fouad, Y., Abduvalieva, D., Islam, S., AL Garalleh, H., & Alrawashdehj, A. I. (2024). Modeling of geothermal tailored CCHP system with heat recovery centered thermal design/analysis; ANN-based optimization and economic study. In CASE STUDIES IN THERMAL ENGINEERING (Vol. 59). ELSEVIER. doi:10.1016/j.csite.2024.104511.
[171] Nourpour, M., & Manesh, M. H. K. (2023). Availability and 6E assessment and optimal design of a novel cogeneration system based on integrated turbo compressor station—SOFC-solar-geothermal-steam and organic Rankine cycles with machine learning. In RENEWABLE ENERGY (Vol. 215). PERGAMON-ELSEVIER SCIENCE LTD. doi:10.1016/j.renene.2023.118908.
[172] K. Almutairi, Environmentally friendly utilization of LNG regasification process and geothermal-based dual-loop power cycle for desalinated water and hydrogen production, In DESALINATION 564 (2023).
[173] Barogh, A. R. H., & Moghimi, M. (2024). Deep neural network optimization of a continuous solar-geothermal-driven plant with integrated thermal and mechanical energy storage: Incorporating bypass mechanism. In ENERGY (Vol. 303). PERGAMON-ELSEVIER SCIENCE LTD. doi:10.1016/j.energy.2024.131885.
[174] A. Khosravi, S. Syri, Modeling of geothermal power system equipped with absorption refrigeration and solar energy using multilayer perceptron neural network optimized with imperialist competitive algorithm, In JOURNAL OF CLEANER PRODUCTION 276 (2020), https://doi.org/10.1016/j.jclepro.2020.124216.
[175] Jakhar, S., Paliwal, M. K., & Kumar, M. (2023). Machine learning predictive models for optimal design of photovoltaic/thermal collector with nanofluids based geothermal cooling. In ENVIRONMENTAL PROGRESS & SUSTAINABLE ENERGY (Vol. 42, Issue 5). WILEY. doi:10.1002/ep.14131.
[176] H.-S. Mun, M.A. Dilawar, S. Mahfuz, K.M.B. Ampode, V. Chem, Y.-H. Kim, J.-P. Moon, C.-J. Yang, Effects of a Combined Geothermal and Solar Heating System as a Renewable Energy Source in a Pig House and Estimation of Energy Consumption Using Artificial Intelligence-Based Prediction Model, In ANIMALS Vol. 12, Issue 20 (2022) MDPI, https://doi.org/10.3390/ani12202860.
[177] Milicevic, D. B., Andelkovic, L. N., Mitic, M. P., Purenovic, J. M., & Purenovic, M. M. (2018). Modelling of hydrochemical and hydromechanical parameters' synergism in the process of solid deposit creation in geothermal and other hard waters. In JOURNAL OF THE SERBIAN CHEMICAL SOCIETY (Vol. 83, Issue 5, pp. 625–640). SERBIAN CHEMICAL SOC. doi:10.2298/JSC170731015M.
[178] F.S.T. Haklidir, M. Haklidir, Prediction of geothermal originated boron contamination by deep learning approach: At Western Anatolia Geothermal Systems in Turkey, In ENVIRONMENTAL EARTH SCIENCES Vol. 79, Issue 8 (2020).
[179] Giannoulis, M., Pailot-Bonnetat, S., Barra, V., & Harris, A. (2024). External factors driving surface temperature changes above geothermal systems: Answers from deep learning. In FRONTIERS IN EARTH SCIENCE (Vol. 12). FRONTIERS MEDIA SA. doi:10.3389/feart.2024.1372621.
[180] M. Li, S. Huang, M. Dong, Y. Xu, T. Hao, X. Wu, Y. Deng, Prediction of marine heat flow based on the random forest method and geological and geophysical features, In MARINE GEOPHYSICAL RESEARCH Vol. 42, Issue 3 (2021).
[181] Bohane, P., Gohil, T. B., & Srivastav, A. K. (2024). Machine learning-based predictive approach for pitting and uniform corrosion in geothermal energy systems. In ELECTROCHIMICA ACTA (Vol. 504). PERGAMON-ELSEVIER SCIENCE LTD. doi:10.1016/j.electacta.2024.144884.
[182] T. Clemens, M.-M. Chiotoroiu, A. Corso, M. Zechner, M.J. Kochenderfer, Artificial Intelligence-Centric Low-Enthalpy Geothermal Field Development Planning, In ENERGIES Vol. 17, Issue 8 (2024) MDPI, https://doi.org/10.3390/en17081887.
[183] Zeng, H., Abedin, M. Z., Zhou, X., & Lu, R. (2024). Measuring the extreme linkages and time-frequency co-movements among artificial intelligence and clean energy indices. In INTERNATIONAL REVIEW OF FINANCIAL ANALYSIS (Vol. 92). ELSEVIER SCIENCE INC. doi:10.1016/j.irfa.2024.103073.
[184] Ramachandran, S., Bhogilla, S. S., & Vijayan, P. K. (2024). Techno-economic analysis and optimization of a binary geothermal combined district heat and power plant for Puga Valley, India. In RENEWABLE ENERGY (Vol. 234). PERGAMON-ELSEVIER SCIENCE LTD. doi:10.1016/j.renene.2024.121223.